



Title	Enhancing lipid production in a novel thermotolerant strain L1-1 isolated from an oleaginous <i>Rhodotorula toruloides</i> DMKU3-TK16 yeast by adaptive evolution toward biodiesel generation
Author(s)	吳, 志展
Citation	大阪大学, 2021, 博士論文
Version Type	VoR
URL	https://doi.org/10.18910/85366
rights	
Note	

The University of Osaka Institutional Knowledge Archive : OUKA

<https://ir.library.osaka-u.ac.jp/>

The University of Osaka

Doctoral Dissertation

**Enhancing lipid production in a novel thermotolerant strain
L1-1 isolated from an oleaginous *Rhodotorula toluroides*
DMKU3-TK16 yeast by adaptive evolution
toward biodiesel generation**

Wu Chih-Chan

July 2021

Laboratory of Applied Microbiology
International Center for Biotechnology

Department of Biotechnology
Graduate School of Engineering
Osaka University

Table of Contents

ABSTRACT	2
GRAPHICAL OVERVIEW	4
LIST OF ABBREVIATIONS	5
CHAPTER 1 General introduction	7
1.1 Background: urgent demands for renewable lipids for biodiesel	7
1.2 Current issues: plant oil as a dominant feedstock for renewable lipids	8
1.3 Alternative and promising feedstocks: oleaginous yeast-derived lipids	9
1.4 Prospects of oleaginous yeast <i>Rhodotorula toruloides</i>	10
1.5 Objectives: Isolation of a robust thermotolerant strain from <i>R. toruloides</i> for enhanced lipid production under stress conditions.....	12
CHAPTER 2 Isolation of a thermotolerant strain from <i>R. toruloides</i> for lipid production at high temperatures	14
2.1 Background: Lack of a thermotolerant <i>R. toruloides</i> strain confines the application of <i>R. toruloides</i> in industrial-scale fermentation	14
2.2 Objectives: Isolation of a robust thermotolerant strain in <i>R. toruloides</i>	15
2.3 Results: Isolated thermotolerant L1-1 is a potential strain for lipid production at high temperatures	15
2.4 Discussion.....	25
2.5 Summary: A potential thermotolerant strain L1-1 for OA-rich lipid production at high temperatures	25
CHAPTER 3 Multiple-stress tolerances in thermotolerant <i>R. toruloides</i> L1-1	30
3.1 Background: Multiple-stress tolerant strains are competitive and desired for industrial applications	30
3.2 Objectives: Characterization of stress response and lipid production of L1-1 under various stress conditions.....	31
3.3 Results: Thermotolerant L1-1 displayed multiple-stress tolerances and had enhanced lipid production under oxidative stresses (ethanol and H ₂ O ₂).....	31
3.4 Discussion.....	49

3.5 Summary: Oxidative stresses (ethanol and H ₂ O ₂) induced lipid production in multiple-stress tolerant strain L1-1.....	46
CHAPTER 4 Enhancing L1-1's lipid production of by overexpression of fatty acid desaturase genes	50
4.1 Background: Metabolic engineering in <i>R. toruloides</i> to enhance lipid production ...	50
4.2 Objectives: Enhancing lipid production of L1-1 by overexpressing fatty acid desaturases.....	50
4.3 Results: Overexpression of <i>RtFAD2</i> and co-expression of <i>RtFAD1</i> and <i>RtFAD2</i> enhanced lipid production in <i>R. toruloides</i>	51
4.4 Discussion.....	77
CHAPTER 5 General conclusions and discussion.....	78
5.1 Summary of the work	78
5.2 Suggestions and future works	80
5.3 Future perspectives	82
6. MATERIALS AND METHODS.....	83
6.1 Strains and culture medium	83
6.2 Isolation of thermotolerant mutants from <i>R. toruloides</i> DMKU3-TK16.....	84
6.3 Spot assay	84
6.4 Cell growth analysis in liquid medium.....	85
6.5 Measurement of intracellular ROS	85
6.6 Cell wall lytic enzyme susceptibility	86
6.7 Lipid production	86
6.8 Analysis of fatty acid composition	88
6.9 Lipid staining.....	89
6.10 Bioinformatics analysis.....	89
6.11 Plasmid construction.....	90
6.12 Functional expression in <i>S. cerevisiae</i>	92
6.13 Yeast transformation.....	93
6.14 Real-time PCR analysis	93

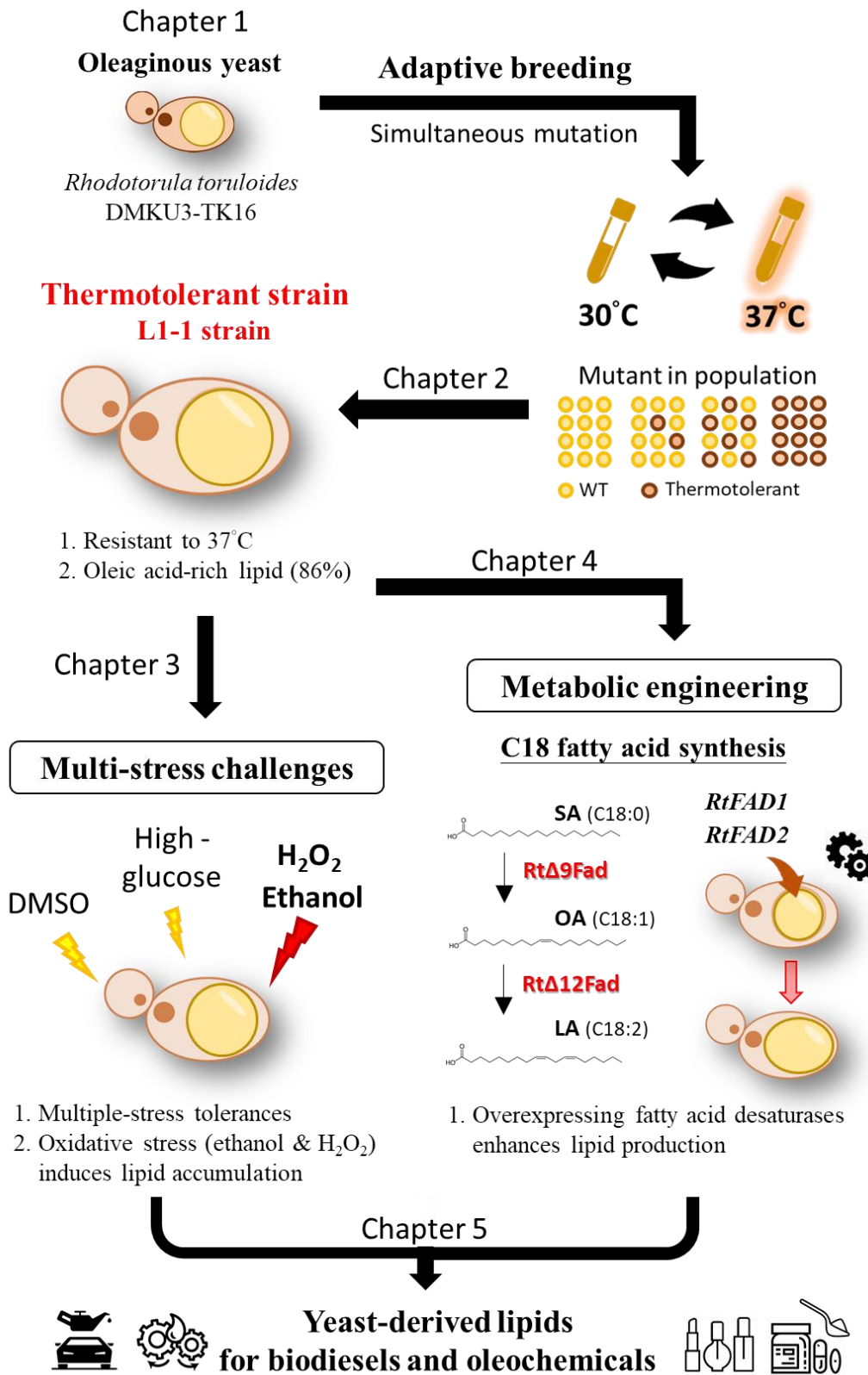
7. REFERENCES	97
8. ACKNOWLEDGEMENTS	108
9. RESEARCH ACHIEVEMENTS	109
9.1 Publications.....	109
9.2 Conferences	109

ABSTRACT

Biodiesel is a renewable, biodegradable and a promising substitute for the conventional fossil fuels used in our daily lives. Recently, yeast-derived lipids produced from oleaginous yeast *Rhodotorula toruloides* have drawn much attention and are now considered attractive alternatives to the dominant feedstocks of plant-derived oils presently used in biodiesel industries. However, the lack of a robust strain that can produce lipids under the multiple stresses that occur during industrial-scale fermentation limits the usefulness of *R. toruloides* for mass lipid production. To produce lipids that are economically competitive with conventional plant-derived oils, it is essential to enhance lipid production and robustness for practical fermentation in industrial-scale production. In this work, I chose oleaginous yeast *R. toruloides* DMKU3-TK16 (TK16) as a platform for microbial lipid production because this strain natively produces lipids at high content levels (nearly 70% of dry biomass) under optimized conditions. To further explore the tolerances against various physical and chemical stresses that may occur during fermentation processes, first I successfully isolated a novel thermotolerant strain, L1-1, from TK16 by adaptive breeding at 37°C. L1-1 produced more lipids, and those lipids had high oleic acid content (86%) at 37°C, which is desirable in feedstock for biodiesel industries. Additionally, this thermotolerant L1-1 exhibited multiple-stress tolerances as well as enhanced lipid production under oxidative stresses induced by ethanol and H₂O₂. Lastly, I also aimed to enhance lipid productivity in the L1-1 strain by overexpressing two native *R. toruloides* genes, *RtFAD1* and *RtFAD2*, encoding C18 fatty acid desaturases. In summary, in this dissertation I isolated L1-1, a novel thermotolerant strain showing multiple-stress tolerances, and improved its lipid-producing ability by manipulating the C18 fatty acid desaturase pathway in order to further explore the competitiveness of

L1-1 as a promising platform for biodiesel production.

GRAPHICAL OVERVIEW



LIST OF ABBREVIATIONS

AA: amino acid

ALA: α -linoleic acid

Ble: bleomycin resistant gene

cDNA: complementary DNA

CDS coding sequence

CWI: cell wall integrity

DCFH-DA: 2', 7' – dichlorodihydrofluorescein diacetate

DCW: dry cell weight

DMSO: dimethyl sulfoxide

DNA: deoxyribonucleic acid

EDTA: ethylene diaminetetra acetic acid

FA: fatty acid

FAD: fatty acid desaturase

FAEE: fatty acid ethyl ester

FAME: fatty acid methyl ester

FID: flame-ionization detection

GC: gas chromatography

GPD: glyceraldehyde-3-phosphate dehydrogenase

Hyg: hygromycin resistant gene

LA: linoleic acid

MA: myristic acid

MAPK: mitogen-activated protein kinase

NaCl: sodium chloride

OA: oleic acid

PA: palmitic acid

PBS: phosphate-buffered saline

PCR: polymerase chain reaction

POA: palmitoleic acid

RNA: ribonucleic acid

ROS: reactive oxygen species

RPM: revolutions per minute

SA: stearic acid

SCD: stearyl-CoA desaturase

SD¹: synthetic defined

SD²: standard deviation

SFA: saturated fatty acid

SPM: stokes per minute

TAG: triacylglycerol

Tris-HCl: Tris (hydroxymethyl) aminomethane hydrochloride

UFA: unsaturated fatty acid

YM: yeast-malt extract

YPD: yeast extract peptone dextrose

CHAPTER 1

General introduction

1.1 Background: Urgent demands for renewable lipids for biodiesel

Demand for fossil fuels has been increasing vastly in recent decades. World fossil fuel production rose to 50,938 terawatt hours (TWh) in 2017 from 18,231 TWh in 1965 (BP's Statistical Review of World Energy 2019). In recent years, concerns over the sustainability and renewability of fossil oils for energy have been increasing due to the decline of the earth's petroleum reserves. The world reserves of petroleum are predicted to be exhausted in 2030 (BP's Statistical Review of World Energy 2019). As a consequence, global crude oil prices have increased drastically, from 20.67 U.S. dollars per barrel (1998) to 71.67 U.S. dollars per barrel (2018) (BP's Statistical Review of World Energy 2019). Also, fossil fuels impact the environment by causing air pollution and greenhouse effects through excessive emission of carbon dioxide CO₂, hydrocarbons (HC), nitrogen oxides (NO_x) (x = 1, 2), and sulfur oxides (SO_x) (x = 2, 3) (Lapuerta *et al.* 2008). Therefore, many countries have implemented policies to decrease the emissions of pollutant gases by increasing the production and utilization of biofuels while reducing the use of conventional fossil fuels (e.g. Energy Independence and Security Act of 2007) (Vicente *et al.*, 2009). This fact has encouraged research toward the development of new alternatives for producing biofuels, with a major interest in transportation fuels.

Renewable biodiesel is perceived as a sustainable and renewable energy to replace conventional fossil diesel. Currently, biodiesel is converted primarily from renewable plant oils, animal fats, and cooking wastes (Vicente *et al.*, 2009). Biodiesel made from palm oil has demonstrated a 73% reduction in HC emissions and a 46% reduction in CO emission in diesel engine operation. Therefore, biodiesel is proposed to be an

environmentally friendly fuel.

1.2 Current issues: Plant oil as a dominant feedstock for renewable lipid

The main feedstocks for biodiesel production are neutral lipids (triacylglycerols, TAGs) from plant oils, animal fats, waste cooking oils, and certain microbial lipids (Ma and Liu 2019; Selvaraj *et al.* 2019). A triacylglycerol contains three acyl-chains attached to a glycerol backbone. Presently, refined lipids from feedstocks are not utilizable for engine combustion owing to their lower volatility and higher viscosity, density, and molecular weight compared to fossil diesel (Makareviciene *et al.* 2020). To overcome the operational problems, transesterification has been employed to produce biodiesel. Transesterification is carried out by mixing TAGs, alcohols (ethanols or methanols), and catalysts (strong acids or bases) under heat treatments. In the transesterification reaction, the alcohols (methanol or ethanol) are used as acyl receptors to generate the end products of fatty acid methyl esters (FAMES) or fatty acid ethyl esters (FAEEs) with crude glycerols (Hassan and Kalam 2013). The end products of a mixture of raw biodiesel and raw glycerol finally undergo a cleaning step with water to generate refined biodiesel (Tan *et al.* 2019; Shomal *et al.* 2019).

Presently, biodiesel is produced primarily by the transesterification of vegetable oils. In the United States, it is produced primarily from soybeans. It is estimated that, in order to meet all demand for transport fuels in the United States, 0.53 billion m³ of biodiesel would need to be produced (Bhatia 2014). However, plant-based oils cannot realistically meet the demand for biodiesel due to their long growth cycles and vast acreage requirements. Moreover, the production yields of plant-based feedstocks are heavily restricted, geographically and seasonally, crop-producing areas (Arous *et al.* 2019). Therefore, an alternative source for biodiesel production will be indispensable.

1.3 Alternative and promising feedstocks: Oleaginous yeast-derived lipids

Due to the limitations of the plant-based production system, much attention has been paid to the development of microbial lipids. Compared with plant-based oil production, microbial cells have much more competitive features, such as short production cycles and less dependence on large venues, seasons, or climates; they are also easy to scale up (Patel *et al.* 2020). So far, it has been found that several oleaginous microorganisms, such as algae, yeasts, bacteria, and fungi, accumulate lipids to more than 20% of dry cellular weight (DCW) under optimized culture conditions (Patel *et al.* 2020). Therefore, microbial lipids are perceived as potential and alternative feedstocks to replace currently used plant oils.

However, not all oleaginous microbes are suitable as feedstocks for biodiesel production due to the qualities of their lipids. Most oleaginous bacteria produce TAGs together with complex polyesters like polyhydroxyalkanoates (PHAs). This means it is difficult to extract and separate TAGs and complex polyesters from oleaginous bacteria (Indest *et al.* 2016; Mahan *et al.* 2017). Additionally, although several autotrophic microalgae can produce lipid content to nearly 50% of DCW (Chen and Jiang 2017), the lipid production of microalgae depends mainly on the climate, sunlight, and largeness of venue (Aratboni *et al.* 2019). These drawbacks confine the development of microalgae-based biodiesel production. On the other hand, the lipids produced by microalgae and fungi usually contain high amounts of very-long-chain fatty acids (over 20 carbons) and polyunsaturated fatty acids, which are not ideal feedstocks for biodiesel production because of their high ignition temperatures and instability of oxidation during long-term storage (Patel *et al.* 2020). During long-term storage, polyunsaturated fatty acids are prone to auto-oxidation, which then causes acidification and polymerization, further leading to gel formation and damage to vehicle engines (Rizwanul Fattah *et al.* 2014). Recently, oleaginous yeasts are considered emerging

platforms for lipid production because of their outstanding lipogenicity and ability to utilize a wide range of carbon sources and industrial wastes (Kaminen *et al.* 2020; Vasconcelos *et al.* 2019; Lamers *et al.* 2016). The reported genera of oleaginous yeasts include *Rhodotorula*, *Rhodospiridium*, *Yarrowia*, *Candida*, *Cryptococcus*, *Trichosporon*, and *Lipomyces* (Sreeharsha and Mohan 2020). These yeasts are well known to be able to convert carbon flux into TAGs under nitrogen-limited conditions (Spagnuolo *et al.* 2019). Typically, the lipid contents among these oleaginous yeasts range from 20% to 70% of DCW depending on the species and culture conditions (Karamerou and Webb 2019). Moreover, the majority of fatty acids from yeast cells are similar to plant-derived oils (mainly C16 and C18 fatty acids), which means the current biodiesel production processes based on plant oils can be applied to yeast-derived lipids (Christophe *et al.* 2012; Liu *et al.* 2020). Recent attempts to produce low-cost yeast lipids have succeeded by using cheap materials in oleaginous yeasts (Polburee and Savitree 2020; Soccol *et al.* 2017). Therefore, oleaginous yeasts have high potential to become alternative platforms to replace plant-derived oils used in biodiesel industries.

1.4 Prospects of oleaginous yeast *Rhodotorula toruloides*

Rhodotorula toruloides (formerly *Rhodospiridium toruloides*), an oleaginous yeast, belongs to the subphylum Pucciniomycotina in phylum Basidiomycota, and it is known to be an outstanding producer of microbial-derived lipids and carotenoids. *R. toruloides* naturally accumulates a large amount of lipids by utilizing a broad range of sugars and cheap industrial substrates such as glucose (hexose), xylose, and arabinose (pentoses), acetic acid, crude glycerol, and biomass hydrolysates (Wiebe *et al.* 2012; Uprety *et al.* 2017; Huang *et al.* 2013; Papanikolaou *et al.* 2017; Fei *et al.* 2016). In addition, this strain can assimilate pentoses and hexoses, such as glucose, xylose, and arabinose, simultaneously to produce lipid. Although this strain displayed reduced lipid

production in cultures containing both pentoses and hexoses, it may have the potential to utilize biomass hydrolysates including pentoses and hexoses as cheap carbon sources (Wiebe *et al.* 2012). After lipid extraction and purification to remove unfavorable compounds, the purified lipids derived from *R. toruloides* could be used as a feedstock for biodiesel (Dong *et al.* 2016). One recent report successfully produced economically competitive biodiesel (US\$ 0.76/L) in *R. toruloides* compared to the standard biodiesel made from soybean (US\$ 0.81/L) by using pilot-scale fermentation with sugarcane juice and urea as a medium (Soccol *et al.* 2017).

Furthermore, several sets of biomolecular tools for genetic engineering have been established, such as transformation systems and gene expression and disruption systems, and these techniques have bolstered the engineering capacity to improve lipid productivity in *R. toruloides* (Park *et al.* 2018). Within the past 10 years, the genome sequences of several *R. toruloides* strains, such as MTCC457, NP11, and IFO0880, have also been reported and widely used as gene information for the design of different metabolic engineering strategies (Kumar *et al.* 2012; Zhu *et al.* 2012; Dinh *et al.* 2019).

Other than these standard strains, *R. toruloides* DMKU3-TK16 (TK16), isolated from a soil sample in Thailand, can accumulate high lipid amounts up to 71.3% of DCW under nitrogen-limited conditions. Because of TK16's high lipid production ability, it is believed to be a potential platform for microbial lipid production (Kraisintu *et al.* 2010). Aside from its excellent lipid production ability, the lipid produced by TK16 contains high amounts of oleic acid (OA) (40-60% of total lipids) (Kraisintu *et al.*, 2010; Wu *et al.*, 2018). OA-rich lipid is an ideal feedstock for biodiesel production owing to its oxidative stability and proper flow fluidity at low temperatures during long-term storage. Therefore, this strain is a promising producer of desirable lipids for biodiesel manufacturing.

1.5 Objectives: Isolation of a robust thermotolerant strain from *R. toruloides* for enhanced lipid production under stress conditions

During industrial fermentation, temperature increases in the fermenter result from the metabolic activities of cultured microorganisms and ambient temperatures. However, the increased temperatures in the fermenter cannot be efficiently dispersed due to the limited specific surface area of the fermenter vessel, particularly at larger scales (Qazizada 2016). Therefore, a cooling system is needed in most industrial fermentation processes (Abdel-Banat *et al.*, 2009). However, a cooling system consumes a lot of energy, which further increases the production cost. As a result, thermotolerant strains are frequently used to the heat problem. Although the oleaginous yeast *R. toruloides* has promising potential for lipid production toward economically competitive biodiesels, there is no report of a thermotolerant strain in the *Rhotorula* genus. A robust thermotolerant strain will be needed for the practical production of large-scale fermenters in the future. Thermotolerant strains offer advantage such as avoiding the costs of cooling systems and reducing contamination by other microorganisms. Therefore, the main objective of this thesis is to isolate a thermotolerant strain from TK16 and to further enhance the lipid production of the isolated strain by stress exposure and metabolic engineering strategies for biodiesel generation. In this dissertation, I first aimed to isolate a thermotolerant L1-1 strain from the parental strain TK16 by adaptive breeding at 37°C, and then analyzed the strain's thermotolerance, lipid production, and fatty acid composition under heat stress (Chapter 2). I then explored the strain's multiple-stress tolerances and lipid-producing abilities by assessing the phenotypes and lipid production under various stress conditions (Chapter 3). Finally, I tried to increase the strain's lipid production by overexpressing

two native genes encoding fatty acid desaturases involving in C18 fatty acid desaturation (Chapter 4).

CHAPTER 2

Isolation of a thermotolerant strain from *R. toruloides* for lipid production at high temperatures

2.1 Background: Lack of a thermotolerant *R. toruloides* strain confines the application of *R. toruloides* in industrial-scale fermentation

The optimal temperatures for most industrial microorganisms range from 25°C to 37°C (Abdel-Banat *et al.* 2010). Controlling temperatures to within an optimal growth range is required during fermentation processes where microorganisms produce heat during the process through metabolic activities, or where ambient heat is input from the environment. Without a cooling system, the fermentation process eventually induces thermal stress in cells, reducing growth and production yield. Therefore, a cooling system is indispensable in most industrial fermentation processes (Abdel-Banat *et al.* 2010). However, the high energy input required for the fermentation system increases the production cost during the fermentation process, especially in the summer or in tropical areas. Hence, thermotolerant strains are frequently employed. For example, thermotolerant strains of the genus *Kluyveromyces* were used for ethanol production over 40°C (Anderson *et al.* 1986; Banat *et al.* 1992). In another example, Wallace-Salinas and Gorwa-Grauslund (2013) successfully improved the thermotolerance of one industrial *S. cerevisiae* strain, Ethanol Red, to produce ethanol by applying a long-term adaptation strategy. These cases showed that thermotolerant strains are favorable for industrial fermentation at higher temperatures.

The optimal lipid-producing temperature of 30°C was widely used in most scientific reports on *R. toruloides*. Although there has been no report of thermotolerant *Rhodotorula* strains, the urgent need for a robust *Rhodotorula* strain has been discussed for future application in industries (Qi *et al.* 2014; Uprety *et al.* 2017; Díaz *et al.*, 2018).

Toward expanding the competitiveness of *R. toruloides* and the possibility of practically using it in industrial-scale production, a thermotolerant *R. toruloides* strain will be indispensable.

2.2 Objectives: Isolation of a robust thermotolerant strain in *R. toruloides*

Thermotolerant yeasts offer potential advantages in the industries by reducing cooling costs during the fermentation process, thereby making the process economically competitive to other platforms. Thus the aim of this chapter is to isolate a thermotolerant from the high lipid producing yeast TK16 by adaptive breeding strategy. Moreover, the lipid productivity and fatty acid profile of produced lipids would be examined. Although there is no report of isolating thermotolerant strains from *Rhodotorula* yeasts, several successful reports have been published in *S. cerevisiae*. Satomura *et al.* (2013) isolated one thermotolerant strain from *S. cerevisiae* by breeding with stepwise adaptation which possessed faster growth than wild-type at 39°C. Caspeta *et al.* (2015) also isolated 7 thermotolerant strains from *S. cerevisiae*, which displayed improved growth at 40°C, by adaptive breeding. These studies showed adaptive breeding could be one feasible strategy to obtain a thermotolerant strain from *R. toruloides*.

2.3 Results: Isolated thermotolerant L1-1 is a potential strain for lipid production at high temperatures

2.3.1 Assessment of the effects of temperatures on the growth of the wild-type

***Rhodotorula toruloides* DMKU3-TK16**

To examine the effects of temperatures on the growth of TK16, the spot assay was performed. The temperatures ranging from 30°C, 32°C, 34°C, 36°C and 38°C were being testified. Based on the results of spot assay in Fig. 2.3.1, cells incubated at 30°C

and 32°C showed normal growth, and cell grown at 34°C exhibited suppressed growth. Contracting with cells grown at 30°C, cell grown over 36°C showed strongly reduced growth. These results indicated that temperatures over 36°C could strongly suppress the growth of TK16.

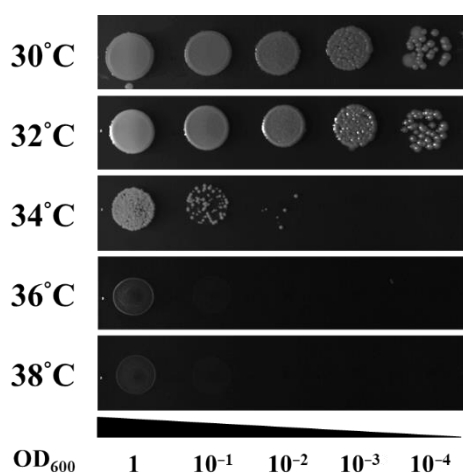


Fig. 2.3.1 Spot assay of TK16 at various temperatures. Cells with an OD₆₀₀ of 1.0 were adjusted into OD₆₀₀ of 1, 10⁻¹, 10⁻², 10⁻³ and 10⁻⁴. The diluted culture were spotted on YM plate. Cells were incubated at various temperatures for 2–5 days.

2.3.2 Isolation of a thermotolerant L1-1 from TK16 by adaptive breeding

To isolate a thermotolerant from TK16, a breeding strategy was applied. The wild-type TK16 was used as the parental strain. According to the previous results of spot assay, TK16 could not grow over 36°C, hence the selective temperature of the adaptive strategy was chosen to be 37°C. Firstly, the wild-type TK16 was cultured at 37°C and recovered at 30°C repeatedly with a simultaneous mutation rate (Fig. 2.3.2A). During the repeats of the selective procedures, the population of the thermotolerant mutants would become dominant in the mixed cultures. Finally, the stable mutants were examined on YM plates at 37°C. After 41 cycles of the selections, a stable thermotolerant strain L1-1 was successfully obtained. Based on the growth phenotype on YM plates at 37°C, L1-1 could form colonies at 37°C in comparison to wild-type TK16 which could not form colonies at 37°C (Fig. 2.3.2B). These results indicated that one thermotolerant candidate L1-1 was successfully isolated.

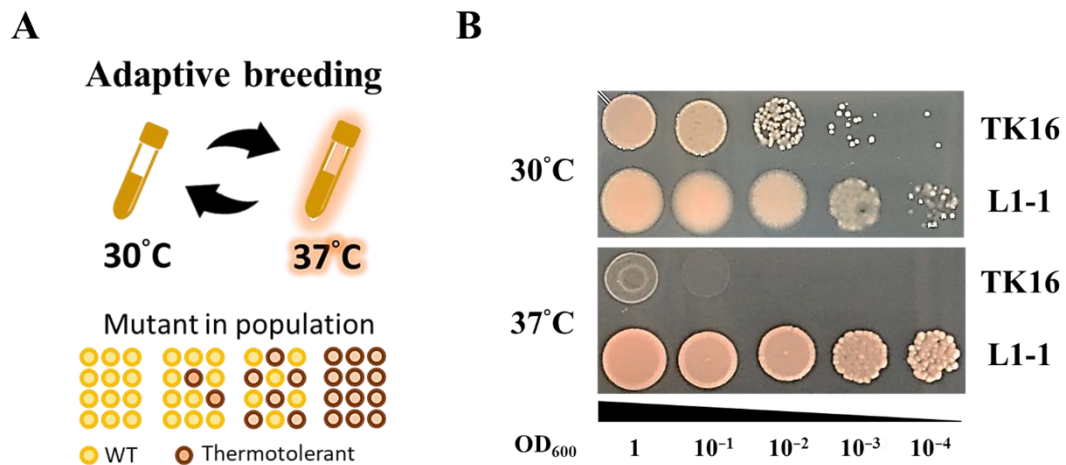


Fig. 2.3.2 Spot assay of parental TK16 and thermotolerant L1-1. Cells with an OD₆₀₀ of 1.0 were adjusted into OD₆₀₀ of 1, 10⁻¹, 10⁻², 10⁻³ and 10⁻⁴. The diluted cultures were spotted on the YM plate. The spotted cells were incubated at 30°C and 37°C for 2 days and 5 days, respectively.

2.3.3 Growth performance of thermotolerance L1-1 in liquid broth

To examine if the thermotolerant L1-1 could maintain its growth in liquid medium, L1-1 was grown in YM broth at 37°C. The OD₆₀₀ of L1-1 were measured at each time point. The results (Fig. 2.3.3) indicated that L1-1 cultivated at 30°C had a similar growth pattern with the parental TK16. However, compared to the results at 37°C (Fig. 2.3.3), L1-1 exhibited better growth than parental TK16. The OD₆₀₀ of L1-1 could reach 6.33 ± 0.23 after a 28-h cultivation while the OD₆₀₀ of wild-type was 0.85 ± 0.20 . These results clearly demonstrated that L1-1 possessed improved thermotolerance and growth at 37°C. These results also confirmed that 37°C reduced the growth of TK16 in liquid medium.

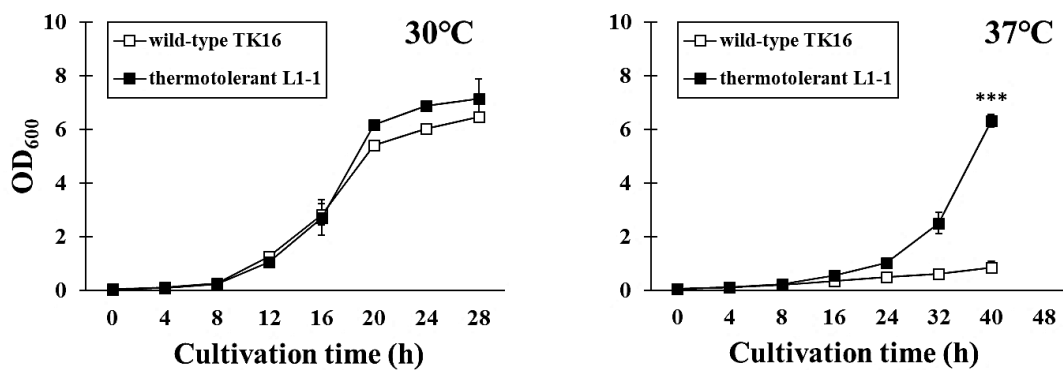


Fig. 2.3.3 Growth curve of thermotolerant L1-1 in liquid medium. Growth curves of yeast strains in the YM medium at 30°C and 37°C were measured by OD₆₀₀. White boxes indicate wild-type TK16, and black boxes indicate thermotolerant L1-1. The error bars are shown as \pm standard error mean (SEM) based on three independent measurements. *** $p < 0.001$ were determined by Student's *t*-test.

2.3.4 Cell morphology of L1-1 grown in liquid medium

To further confirm the suppression effect of high temperatures on cell shape, the cell morphology of wild-type TK16 and L1-1 grown at 37°C were examined under a bright-field microscope. The cell morphology of TK16 and L1-1 cultivated at 30°C in liquid YM medium had no difference in cell shape (Fig. 2.3.4). However, the cell morphology of TK16 grown at 37°C showed abnormally elongated shape and enlarged cell size. Compared to the cell morphology of TK16 at 37°C, the cell morphology of L1-1 was as same as those grown at 30°C. Accordingly, the L1-1 maintained the cell morphology at 37°C in YM medium.

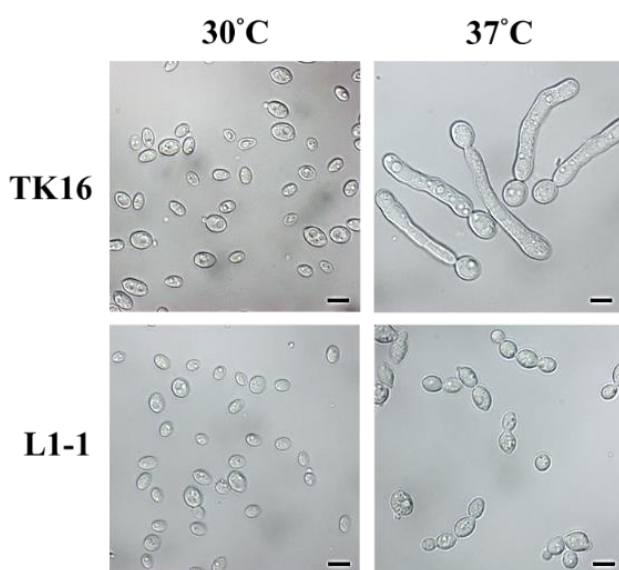
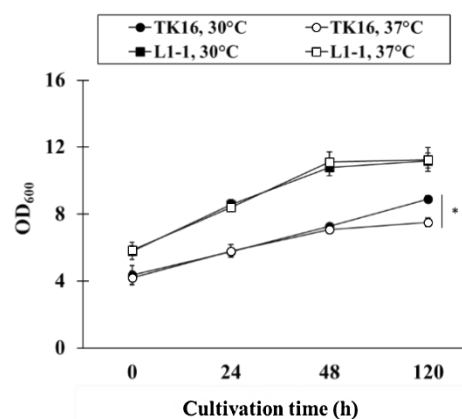


Fig. 2.3.4 Cell morphology of thermotolerant L1-1. TK16 and L1-1 were grown in the 25 mL of YM medium at 30°C and 37°C. The cell morphology was observed by a light microscope. Scale bars are shown in 5 μm .

2.3.5 Growth performance of L1-1 in nitrogen-limited medium (lipid producing conditions)

The final goal of this study is to isolate a thermotolerant strain to produce lipid at high temperatures. Therefore, the lipid production of the thermotolerant L1-1 was investigated in the nitrogen-limited medium. Although nitrogen-limited media could be used for inducing lipid accumulation in cells, recent studies also demonstrated that high-glucose concentration in media could also impose hyperosmotic stress on yeast cells. To evaluate the growth of the L1-1 in nitrogen-limited medium, I observed the cell growth under nitrogen-limited conditions at 30°C and 37°C for a 120-h cultivation. The results indicated that L1-1 still could maintain the OD_{600} at 37°C as the same level at 30°C under nitrogen-limited condition, and generate higher OD_{600} than the TK16 at 37°C (Fig. 2.3.5).

Fig. 2.3.5 Growth performance of the thermotolerant L1-1 strain in nitrogen-limited medium. Cells were grown in nitrogen-limited medium at 30°C or 37°C. Growth curves of the wild-type and L1-1 were measured by OD₆₀₀. Error bars: SEM based on three independent measurements. * $p < 0.05$ by Student's *t*-test.



2.3.6 Lipid production of thermotolerant L1-1 at 37°C

To evaluate the lipid production of L1-1 at 37°C, I measured the DCW, lipid content, and titer. Lipid content indicates the percentage of total lipids in the dry biomass, and lipid titer indicates the total lipid amount in culture media. According to the results (Fig. 2.3.6A), the DCW of wild-type TK16 at 37°C was significantly reduced, but L1-1 produced similar level of DCW to that produced at 30°C. These results demonstrated L1-1 could maintain its biomass in nitrogen-limited condition at 37°C. Additionally, L1-1 also had increased lipid content and lipid titer at 37°C ($13.42 \pm 0.04\%$ of DCW and 1.71 ± 0.06 mg/mL) (Fig. 2.3.6B and C). Notably, the lipid production of L1-1 was further enhanced at 37°C. Conversely, the 37°C decreased the lipid production of wild-type TK16. Taken these data together (Fig. 2.3.6), the isolated thermotolerant L1-1 displayed improved the lipid production at 37°C.

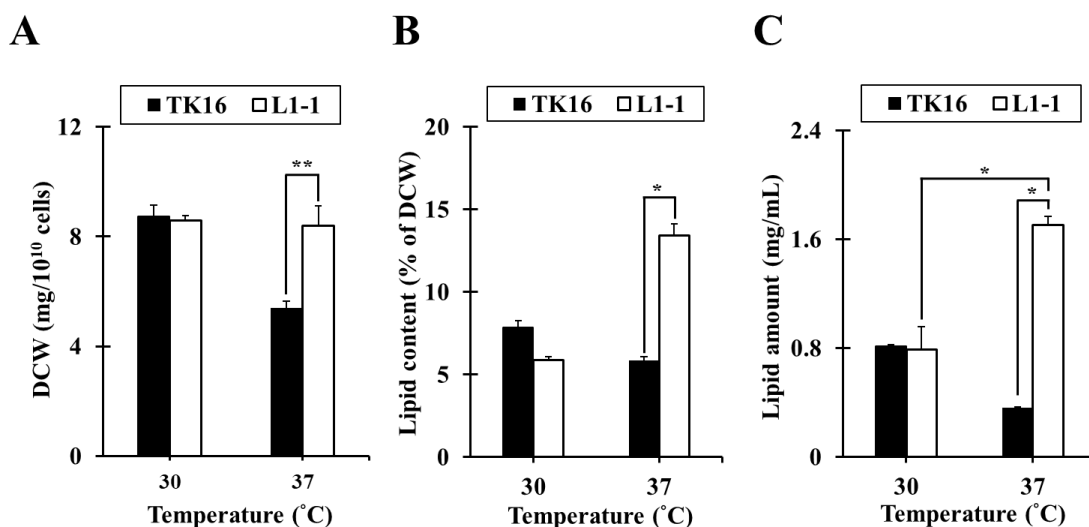


Fig. 2.3.6 Dry biomass and lipid production of L1-1. Yeast cells were cultured at 30°C or 37°C for 120 h in nitrogen-limited conditions. A: Dry biomass. B: Lipid content. C: Lipid titer. Error bars: SEM based on three independent measurements. * $p < 0.05$ and ** $p < 0.01$ by Student's t -test.

2.3.7 Cell morphology of thermotolerant L1-1 strain in nitrogen-limited medium

Thermal and osmotic stresses could lead to the morphological alterations of *S. cerevisiae* and *Schizosaccharomyces pombe* by affecting the cell surface (Adya *et al.* 2006). To confirm if thermotolerant L1-1 could maintain its cell shape under thermal stress and high-osmotic stress of nitrogen-limited medium, I examined the cell morphology of L1-1 cells at the end-point of lipid production at 37°C. The wild-type TK16 showed morphological defects at 37°C, whereas the thermotolerant L1-1 exhibited normal cell shape at 37°C (Fig. 2.3.7). These results indicated thermotolerant L1-1 also had better resistances against the hyperosmotic pressure than the TK16 at 37°C.

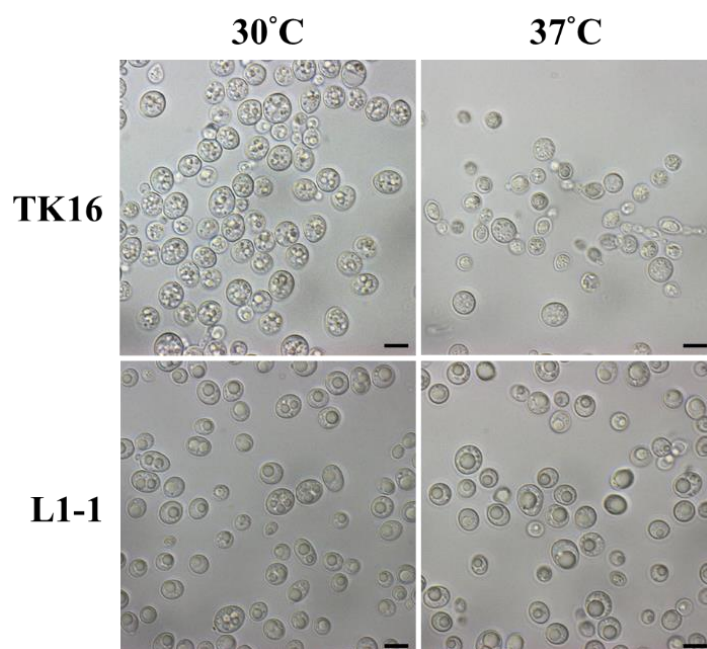


Fig. 2.3.7 Cell morphology of the wild-type TK16 and thermotolerant L1-1 grown at 30°C or 37°C in nitrogen-limited medium for 120 h. Scale bars: 5 μ m.

2.3.8 Fatty acid composition and titer of thermotolerant L1-1

Lipids rich in monounsaturated fatty acids, such as palmitoleic acid (PA, C16:1) and oleic acid (OA, C18:1), are ideal feedstocks for biodiesel production because of their oxidative stability and proper fluidity at low temperatures (Joshi *et al.* 2007; Knothe 2005; Verma *et al.* 2006). To determine the fatty acid profile of L1-11 for biodiesel production, I analyzed the lipids of L1-1. The results revealed that the produced lipids of L1-1 at 37°C consisted mainly of PA (7.5%), stearic acids (SA, C18:0) (4.1%), and OA (86%). Compared with the OA content of wild-type TK16 at 37°C (60%), the thermotolerant L1-1 had a much higher amount of OA (86%) (Table 2.3.8A). Furthermore, L1-1 grown at 37°C accumulated a greater OA titer compared to wild-type TK16 at 37°C (1,400 μ g/mL versus 78.50 μ g/mL) (Table 2.3.8B). These results demonstrated that L1-1 could produce high content and titer of OA at 37°C as an ideal feedstock for biodiesel.

Table 2.3.8A Fatty acid profile of the wild-type TK16 and thermotolerant L1-1 in nitrogen-limited medium. Yeast cells were grown in the nitrogen-limited medium at 30°C or 37°C for 120 h. The relative fatty acid profile is shown as a percentage (%) of total fatty acid. Myristic acid (MA, C14:0); Palmitic acid (PA, C16:0); Palmitoleic acid (POA, C16:1); Stearic acid (SA, C18:0); Oleic acid (OA, C18:1); Linoleic acid (LA, C18:2); α -linolenic acid (ALA, C18:3).

Strains	Temperature (°C)	Relative fatty acid composition (%)						
		C14:0	C16:0	C16:1	C18:0	C18:1	C18:2	C18:3
Wild-type	30	0.4	16.1	0.3	17.0	59.7	6.1	0.3
	37	1.5	22.3	0.4	16.6	57.5	1.6	0.0
L1-1	30	0.2	13.2	0.2	13.4	42.5	26.6	3.9
	37	0.5	7.5	0.6	4.1	86.0	1.4	0.0

Table 2.3.8B Fatty acid titer of the wild-type TK16 and thermotolerant L1-1 in nitrogen-limited medium. The titer of fatty acid is shown as the fatty acid weight (μg) per liquid culture (mL). Myristic acid (MA, C14:0); Palmitic acid (PA, C16:0); Palmitoleic acid (POA, C16:1); Stearic acid (SA, C18:0); Oleic acid (OA, C18:1); Linoleic acid (LA, C18:2); α -linolenic acid (ALA, C18:3).

Strains	Temperature ($^{\circ}\text{C}$)	Fatty acid titer ($\mu\text{g}/\text{mL}$)						
		C14:0	C16:0	C16:1	C18:0	C18:1	C18:2	C18:3
Wild-type	30	1.200	24.20	0.700	21.10	88.00	10.80	0.200
	37	1.500	28.30	0.600	19.60	78.50	2.400	0.000
L1-1	30	1.100	25.70	0.300	19.60	77.10	42.20	5.700
	37	8.000	110.7	18.40	56.80	1400	26.10	0.000

2.4 Discussion

2.4.1 Effects of high temperatures on the growth of wild-type TK16 and thermotolerant L1-1

The normal growth condition of TK16 is 28°C (Kraisintu *et al.* 2010), and the results of a spot dilution assay (Fig. 2.3.1) indicated that TK16 could not grow above 36°C. Reduced growth and an abnormal growth shape of TK16 were also observed during cultivation in the YM liquid culture at 37°C (Fig. 2.3.4). These results demonstrated that increased temperatures influenced the growth of the wild-type TK16. For industrial fermentation, thermotolerant strains have several important advantages, one of which is to lower the cost of cooling to optimal temperatures in large fermenters (Abdel-Banat *et al.* 2010). To explore the thermotolerance of the original TK16, I aimed to isolate a novel thermotolerant strain by adaptive breeding. In this chapter, I isolated thermotolerant strain L1-1, which showed better growth performance in YM broth at 37°C compared to the wild-type TK16, which could not grow well at this temperature ($OD_{600} < 1.0$) (Fig. 2.3.3). In addition, I observed that higher temperature damaged the morphology of the wild-type TK16 cultivated in YM broth at 37°C. In contrast, the L1-1 strain at 37°C showed only the normal cell shape (Fig. 2.3.4). The defective cell shape of TK16 may have been caused by the increased sensitivity toward osmotic pressure at 37°C or by a defect in cell division. Therefore, L1-1 may possess improved tolerance against osmotic pressure. These results implied that the isolated L1-1 not only has enhanced thermotolerance but also better resistance to osmotic stress at 37°C.

2.4.2 Increased lipid production resulted from an increased amount of OA in the thermotolerant L1-1

The performance of lipid production in thermotolerant L1-1 was further induced

at 37°C (Fig. 2.3.7). The large amount of induced lipids came mainly from the increased amount of OA (Table 2.3.8B). In yeast and fungi, $\Delta 9$ -desaturase ($\Delta 9$ -Fad) introduces a double bond at the position of C9 of SA to synthesize OA, and the OA would be further used as a substrate for LA synthesis. In *S. cerevisiae*, Gonzalez and Martin (1996) demonstrated that LA may serve as a regulator to control $\Delta 9$ -FAD (*ScOLE1*) expression by rapidly degrading the mRNA with a 5'-exoribonuclease (encoded by the *XRNI*). Research into *S. cerevisiae* implied that intracellular LA might serve as feedback inhibition to control the $\Delta 9$ -FAD expression levels and eventually control the intracellular levels of OA. Based on our data (Fig. 2.3.8A), the cultivation temperature of 37°C would greatly decrease the LA content in cells. Therefore, the increased OA amount in the thermotolerant L1-1 may result from the decrease in LA, which could not suppress the expression of $\Delta 9$ -FAD in L1-1, in turn leading to the increase in the amount of OA.

2.4.4 Increased OA along with decreased LA and ALA content may be linked to enhanced thermotolerance in thermotolerant L1-1

Swan and Watson (1999) reported a $\Delta 9$ -FAD defective mutant in *S. cerevisiae* that could not synthesize OA and become sensitive to high temperatures, and the supplementation with OA recovered its heat tolerance. Furthermore, a study of the dimorphic fungus *Histoplasma capsulatum* also demonstrated that cells supplemented with OA (C18:1) were less sensitive to increased temperatures and drastically decreased their expression levels of heat shock genes involved in heat stress responses (Maresca *et al.* 1992). These results implied that OA may be involved in the thermotolerance of yeast and fungi. Although how OA affects the heat-shock response in yeast is unknown, Glatz *et al.* (2016) provided evidence that small heatshock proteins (Hsp15.8 and Hsp16) directly interact with membrane lipids in *S. pombe*, and they suggested that the cell

membrane lipid might be involved in the signal transduction of the heatshock response.

Previous studies have revealed that microbial cells change their membrane properties in order to adapt to various temperatures (Beney *et al.* 2001). The fluidity of membrane properties could be altered by the components of fatty acids attached to phospholipids. The elevated content of unsaturation in membrane fatty acids would increase membrane fluidity (Quinn *et al.* 1989). Under high temperatures, the fluidity of the membrane would be increased. To sustain membrane integrity in microbial cells, the ratio of unsaturated fatty acid would be strictly regulated. One report (Swan and Watson, 1999) suggested that yeast cells enriched with ALA were more sensitive to heat owing to membrane damage associated with the increased membrane fluidity. Therefore, the decreased contents of LA and ALA found in TK16 and L1-1 may be considered as mechanisms by which cells sustain membrane rigidity in response to heat stress. Although the correlation between the enhanced thermotolerance of L1-1 and increased OA is still not clear, the increased OA along with the decreased LA and ALA in L1-1 may be attributable to the thermotolerance of L1-1.

2.4.5 High OA content in L1-1 at 37°C

OA-rich oils and lipids are preferable feedstocks for biodiesel production due to their stability in long-term storage. To produce OA-rich oils and lipids for biodiesel production, several efforts have been made in plant and yeast. Recently, standard biodiesel is made from soybean oils. The OA content of *Glycine max* (soybean) is around 25% of total lipid (Thapa *et al.* 2016). One trial increased OA content to 40% by selecting the $\Delta 12\text{-fad}$ mutant in *Glycine max* which could not produce LA. In addition, recent research in the oleaginous yeast *Yarrowia lipolytica* also successfully enhanced the OA content from 58% to 90% of total lipid by overexpressing $\Delta 9\text{-FAD}$ and disrupting $\Delta 12\text{-FAD}$ (Tsakraklides *et al.* 2018). In this chapter, the thermotolerant

L1-1 produced 86% OA of total lipid at 37°C. The OA content of L1-1 exceeded the record for soybean and is comparable to the record for an engineered *Y. lipolytica* strain. Therefore, the L1-1 strain could be a potential platform to produce high-OA lipid for biodiesel production.

2.4.6 Comparison of lipid production with other microbial strains at high temperatures

Although there is no report on lipid production of *R. toruloides* at high temperatures, one report on another oleaginous yeast, *Y. lipolytica*, showed that three *Y. lipolytica* strains accumulated 10% to 25% lipid content at 35°C (Hackenschmidt *et al.* 2019). In that report, which was published after my publication in 2017, the engineered strain H222pox1-6 and nonengineered strain 1889 accumulated 25% lipid content in cells, and another strain, 63, produced only 10% lipid content. Those data implied that different strains may have different thermotolerances to heat and different lipid-producing abilities under heat stress. Furthermore, genetic engineering may help us to improve the lipid production of yeast strains to produce more lipids under heat stress. In this chapter, the thermotolerant L1-1 produced lipid content of $13.42 \pm 0.04\%$ and lipid titer of 1.71 ± 0.06 g/L at 37°C. In the future, other genetic engineering strategies, such as the disruption of the fatty acid degradation pathway, may be employed to enhance lipid production in the L1-1 strain.

2.4.7 Future perspectives

Thermotolerant L1-1 is the first reported thermotolerant strain in *R. toruloides* yeast, and it exhibited improved performance of lipid production and enhanced thermotolerance at 37°C. Therefore, L1-1 have a promising potential for lipid production at high temperatures which could reduce the production cost from

temperature maintenance. Aside from improved thermotolerance, L1-1 was also able to produce high content of OA (86%) in total lipids, which are favorable feedstocks for biodiesel industries. Furthermore, *R. toruloides* have also been receiving much interest in the production of high-valuable oleochemicals, such as polyunsaturated fatty acids (PUFAs) which could be used in the food industries due to their health benefits. The current sources of PUFAs are from fish oils, which has significant concerns in terms of over-fishing and ocean pollutions. Hence harnessing *R. toruloides* as a new platform for generating PUFAs is also appealing (Athenaki *et al.* 2018; Papanikolaou and Aggelis 2011; Bellou *et al.* 2016). In this chapter, I showed that an increased culture temperature affected the composition of the mono-unsaturated of C18 fatty acids, which may serve as the building blocks for PUFA synthesis in yeast cells. The information gained in this chapter could thus assist in the design of a rational fermentation strategy and further metabolic engineering for PUFA production in *R. toruloides*.

2.5 Summary: a potential thermotolerant strain, L1-1, for OA-rich lipid production at high temperatures

The results of this chapter revealed that the thermotolerant L1-1, isolated from *R. toruloides* DMKU3-TK16, has the potential to be an alternative lipid producer for biodiesel production at higher temperatures. L1-1 exhibited improved growth performance and lipid productivity versus the wild type at 37°C. The fatty acid profiles of L1-1 revealed that its OA (C18:1) content, which was 86%, was much higher than that of the wild type when both were cultured at 37°C. Besides, the results of the alteration of fatty acid composition at high temperature also provided information regarding how *R. toruloides* DMKU3-TK16 adapts and responds to high temperature. L1-1 responded to heat by increasing the OA content (C18:1) while decreasing the contents of LA (C18:2) and ALA (C18:3) at 37°C.

CHAPTER 3

Multiple-stress tolerances in thermotolerant *R. toruloides* L1-1

3.1 Background: Multiple-stress tolerant strains are competitive and desired for industrial applications

Yeast cells encounter chemical and physical stresses such as heat, osmotic pressure, and inhibitory compounds during fermentation (Auesukaree 2017; Guan *et al.* 2017; Gibson *et al.* 2007). Thermal stress generated during fermentation results in protein denaturation and cell membrane disorder (Los and Murata 2004). Moreover, industrial media with high concentrations of glucose, sorbitol, and NaCl increase hyperosmolarity, leading to a loss of intracellular water, shrinkage of cells, and cytoskeletal collapse, eventually inducing mitochondrial dysfunction (Hohmann 2002). Highly permeable compounds such as ethanol, H₂O₂, and DMSO, generated from the decomposition of media or from the metabolism of yeast cells, also act on the mitochondrial membrane and lead to leakage of reactive oxygen species (ROS) from the electron transport chain (Anness 1980; Lahtvee *et al.* 2016; Sadowska-Bartosz *et al.* 2013). These stress factors reduce production yield by interrupting the intracellular physiology. Therefore, yeast strains showing resistance to multiple stresses are desirable for practical industrial applications. Studies of *S. cerevisiae* have described strains displaying multiple-stress resistance. Mutant strains isolated by an adaptive strategy in laboratory environments exhibited enhanced tolerances to various stresses (Cakar *et al.* 2005; Caspeta and Nielsen 2015). Although many multiple-stress-tolerant strains have been reported in model yeast *S. cerevisiae*, multiple-stress-tolerant strains of *R. toruloides* have not yet been reported. Consequently, to broaden the advantages and competitiveness of *R. toruloides* thermotolerant L1-1, it is necessary to determine

whether this strain could be resistant to other stresses.

3.2 Objectives: Characterization of stress response and lipid production of L1-1 under various stress conditions

In Chapter 2, thermotolerant strain L1-1 was successfully isolated from *R. toruloides* DMKU3-TK16 by an adaptive breeding strategy, and this strain previously displayed greater thermotolerance to parental strain TK16 (Wu *et al.* 2018). Accordingly, I speculated that this strain may also possess enhanced tolerances to other stresses. In the present chapter, I investigated the the multi-stress tolerances of L1-1 and aimed to elucidate the cell responses corresponding to enhanced stress resistance. Finally, I examined the lipid-producing ability of the thermotolerant strain under various stress conditions.

3.3 Results: Thermotolerant L1-1 displayed multiple-stress tolerances and had enhanced lipid production under oxidative stresses (ethanol and H₂O₂)

3.3.1 Growth responses of L1-1 against various stresses

To investigate the resistance of L1-1 under the stresses which may occur during fermentation, the growth of L1-1 on YM agar plates containing 30 g/L ethanol, 1.5 mM H₂O₂, 250 g/L glucose, and 40 g/L DMSO was assessed. According to the results of the spot assay (Fig. 3.3.1), the L1-1 strain not only displayed better thermotolerance than the wild-type but also showed obvious tolerances to 30 g/L ethanol, 1.5 mM H₂O₂ and 40 g/L DMSO. There was no significant difference between the growth of the wild-type TK16 and L1-1 strains under the osmotic stresses (250 g/L glucose, 180 g/L sorbitol, and 60 g/L NaCl). Ethanol, H₂O₂, and DMSO have all been shown to increase intracellular ROS levels, resulting in oxidative stresses, in the model *Saccharomyces* yeasts (Lahtvee *et al.* 2016; Pedroso *et al.* 2009; Anness 1980). Ethanol and H₂O₂

primarily impact the cellular membranes by increasing the fluidity and permeability and thereby disrupting the normal membrane structures. Penetration of ethanol and H₂O₂ acting on mitochondria causes mitochondria dysfunction and further induces oxidative stress (Lahtvee *et al.* 2016; Pedroso *et al.* 2009). DMSO, a polar solvent and cell perturbant generated from the decomposition of methionine into S-methyl methionine in malt-based media or metabolism of yeasts (Anness 1980), caused the disruption of mitochondria by cell membrane thinning, increased the fluidity of the membrane's hydrophobic core, and elevated the ROS levels (Sadowska-Bartosz *et al.* 2013). Based on these discoveries in *Saccharomyces* yeasts, I speculated that the improved tolerance to ethanol, H₂O₂ and DMSO found in the thermotolerant L1-1 might be linked to the enhanced resistance against oxidative stress.

Agitation affects the physiological activity of the cells and alter their abilities to tolerate stressors (Pina *et al.* 2004). To further confirm the stress tolerances of L1-1 in agitated liquid medium, the maximum specific growth rate and maximum cell density of cells grown in agitated YM broth containing 30 g/L ethanol, 4 mM H₂O₂, 250 g/L glucose, and 40 g/L DMSO were quantitated. The thermotolerant strain exhibited faster growth and higher cell density under the thermal (37°C) and oxidative (ethanol and H₂O₂) stress conditions than the wild-type strain (Table 3.3.1). These growth results corresponded to the spot assay results under the thermal and oxidative stress conditions. Moreover, the L1-1 strain showed a higher maximum cell density when cultured in YM broth containing 250 g/L glucose, although the L1-1 strain did not show a similar performance on the YM agar plate containing the same concentration of glucose. It is also worth noting that the wild-type strain could grow in liquid broth containing a higher concentration of H₂O₂ (4 mM) than the concentration of H₂O₂ (1.5 mM) present on the agar plate. Combining the results of the spot assay and the growth performance in liquid culture, the thermotolerant L1-1 exhibited greater tolerance to multiple

stressors—i.e., heat stress (37°C), oxidative stress (ethanol, H₂O₂, and DMSO) and osmotic stress (glucose)—than the original strain.

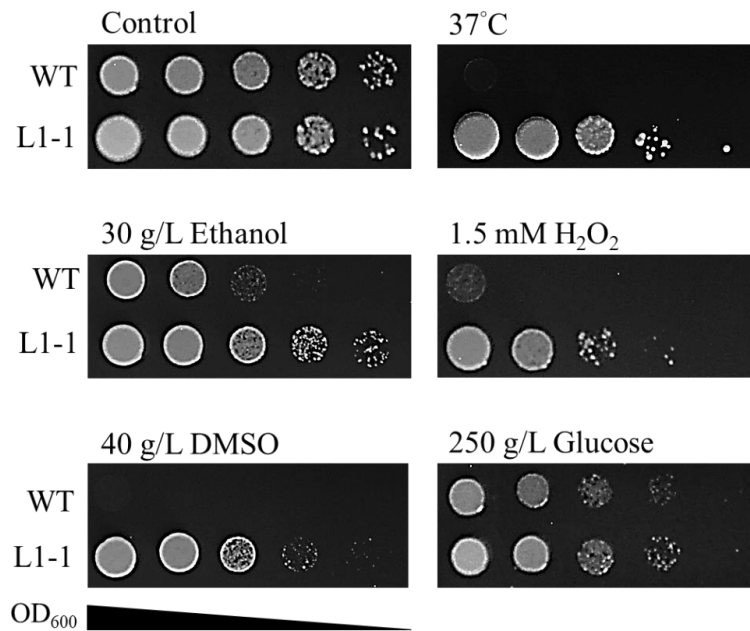


Fig. 3.3.1 Spot dilution assay of the thermotolerant strain and wild-type. The cells were spotted and grown to YM plates or YM plates containing 30 g/L ethanol, 1.5 mM H₂O₂, 250 g/L glucose, or 40 g/L DMSO. Plates were incubated at 30°C for 2–4 days.

Table 3.3.1 Growth response of thermotolerant and wild-type strains under stress conditions. The cells were inoculated in 5 mL of YM medium or YM medium with 30 g/L ethanol, 4 mM H₂O₂, 320 g/L glucose, or 40 g/L DMSO to an OD₆₀₀ of 0.1. The cultures were cultivated at 30°C or 37°C. The value of OD₆₀₀ was measured at 3-h intervals until the growth reached the maximum OD₆₀₀. The maximum specific growth rate (μ) was determined. Error bars: SD of the mean based on three independent measurements. *P* values were determined by Student's *t*-test. "ns" represents no significant difference. **p*<0.05; ***p*<0.01; ****p*<0.001; *****p*<0.0001. The standard deviation of each data point was based on three independent measurements.

Conditions	Maximum specific growth rate (μ , h ⁻¹)			Maximum cell density (OD ₆₀₀)		
	WT	L1-1	<i>P</i> -value	WT	L1-1	<i>P</i> -value
YM	0.06 ± 0.01	0.16 ± 0.02	*	6.04 ± 0.07	7.75 ± 0.12	***
37°C	0.02 ± 0.00	0.08 ± 0.01	**	0.37 ± 0.35	5.94 ± 0.33	****
Ethanol	0.05 ± 0.02	0.14 ± 0.03	*	2.72 ± 0.68	6.43 ± 0.23	**
H ₂ O ₂	0.02 ± 0.00	0.25 ± 0.02	*	0.13 ± 0.00	6.18 ± 0.38	**
Glucose	0.13 ± 0.01	0.13 ± 0.00	ns	4.86 ± 0.48	7.33 ± 0.26	*
DMSO	0.07 ± 0.02	0.10 ± 0.03	ns	3.24 ± 0.10	6.50 ± 0.22	***

3.3.2 Cell wall lytic enzyme sensitivity of the L1-1 strain

The yeast cell wall plays a vital role as the primary line against external stresses and is critical for supporting the cell structure. To cope with external damages which can compromise it, the cell wall must exhibit high strength under stress conditions; this quality is indispensable for cell survival. Cell wall stress signals are transmitted through the cell wall integrity (CWI)-mitogen-activated protein kinase (MAPK) cascade to activate the expression of a set of genes involved in cell wall biogenesis when cell wall is disrupted, hence contributing to thickening and condensing at the affected portions of the cell wall (Levin 2011). Generally, the yeast cell wall is composed of chitins, glucans, mannans, and glycoproteins (Klis *et al.* 2006). To assess whether the thermotolerant L1-1 maintains a more rigid cell wall against various stresses than the wild-type, I examined the susceptibility of thermotolerant cells to the cell wall lytic enzyme Uzukizyme under various conditions. Uzukizyme is a fungal cell wall lysis enzyme from the *Trichoderma* sp. (OMI 5074) and is mainly consist of β -1,3-glucanase, chitinase, and protease activities. The results of the cell wall lytic enzyme treatment (Fig. 3.3.2) demonstrated that, the thermotolerant L1-1 had better resistance to the cell wall lytic enzyme while growing under thermal stress (37°C), oxidative stresses (30 g/L ethanol and 4 mM H₂O₂), high osmotic stress (250 g/L glucose) and exposure to a cell wall and membrane-disturbing agent (40 g/L DMSO). These findings demonstrated that the L1-1 strain possessed a rigid cell wall to defend itself against each of the external stresses studied in Fig 3.3.1. Moreover, under 250 g/L glucose stress, the resistance to Uzukizyme of L1-1 was enhanced in comparison to that of L1-1 cells grown under the control condition (Fig. 3.3.2A). The results also suggested that high glucose in medium might contribute to a rigid cell wall in *R. toruloides*.

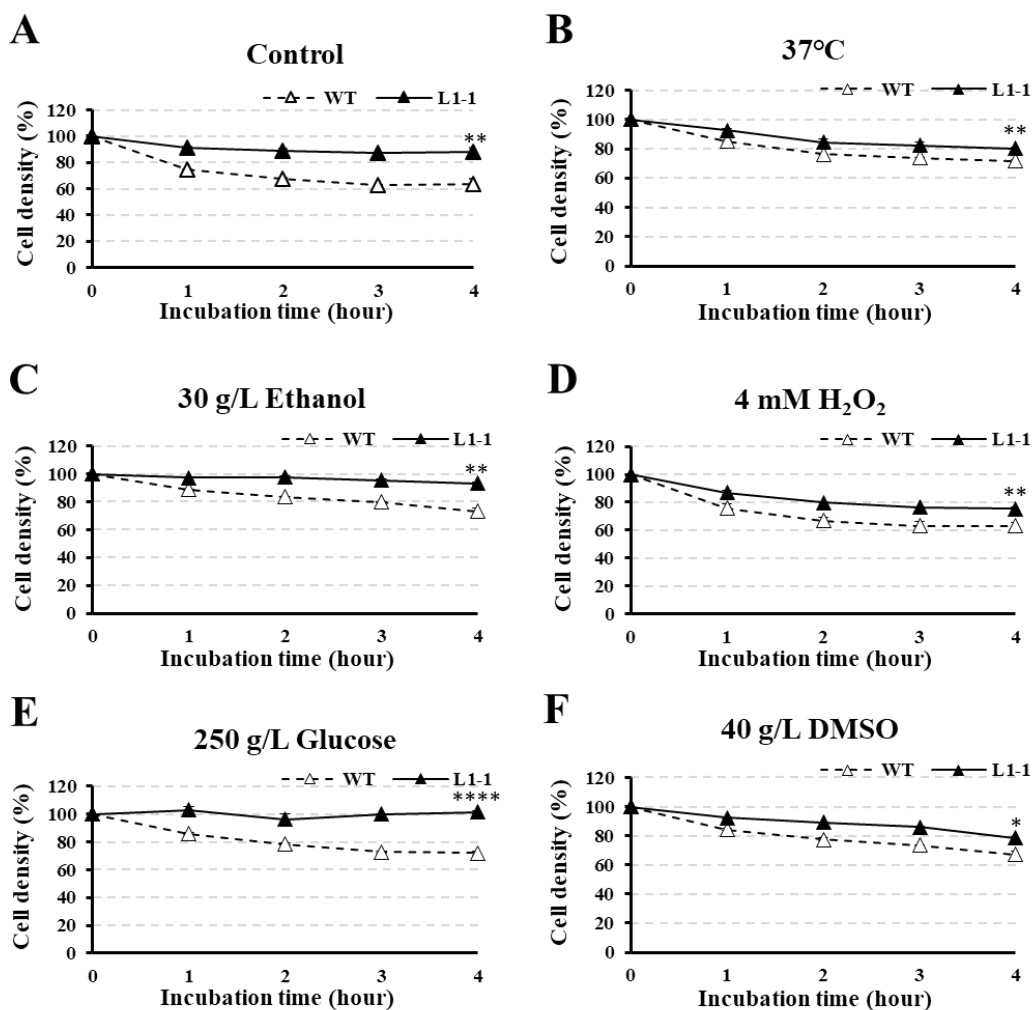


Fig. 3.3.2 Cell wall rigidity under various stress conditions. The cells cultivated under various stress condition (A: YM, control; B: 37°C; C: 30 g/L ethanol; D: 4 mM H₂O₂; E: 250 g/L glucose; F: 40 g/L DMSO) in the tubes at 30°C or 37°C were collected and treated with Uzukizyme. The cell density is shown as the ratio of OD₆₀₀ compared to that at time zero. Error bars: standard error of the mean based on three independent measurements. The *p* values were determined by Student's *t*-test. **p*<0.05; ***p*<0.01; *****p*<0.0001. The SD of each data point was based on three independent measurements.

3.3.3 Alteration of cell membrane properties in response to environmental stresses

Stresses have been shown to alter the composition of lipids in cell membrane, which are participated in the physical functions of microbial cells (Stanley *et al.* 2010; Bravim *et al.* 2010; de Freitas *et al.* 2012). Alterations of membrane lipid composition change the physical cell surface properties, including phase transition temperature and

viscosity (Bloom *et al.* 1991). A higher ratio of unsaturated fatty acids in the cell membrane lipid matrix has been correlated with an increment of the membrane fluidity under various stresses such as temperature, salt, and pressure (Bravim *et al.* 2010; de Freitas *et al.* 2012). To determine whether unsaturated fatty acids contributed to the stress resistance in the thermotolerant L1-1 strain, I analyzed the membrane fatty acid compositions of the cells grown under various stress conditions in YM broth. Based on the fatty acid profile results (Table 3.3.3), the percentage of unsaturated fatty acids in membrane lipids growing under heat stress ($82.0 \pm 1.2\%$) and DMSO-induced stress ($85.4 \pm 0.8\%$) was higher than in the wild-type TK16 ($67.3 \pm 1.0\%$ in heat stress, $p < 0.0001$; $76.1 \pm 2.2\%$ in DMSO-induced stress, $p < 0.05$) (Table 3.3.3). Moreover, there was no difference in unsaturated fatty acid content between the wild-type TK16 and thermotolerant strain L1-1 under the conditions of oxidative stress, or hyperosmotic stress induced by 250 g/L glucose. These results implied that the changes in unsaturated content in the cells were not a major cause of the multiple-stress tolerance. Although the regulation of unsaturated fatty acid has been shown to involve in oxidative and osmotic stress tolerances in yeasts (Navarro-Tapia *et al.* 2018; Vázquez *et al.* 2019), the data (Table 3.3.3) indicated that the proportions of unsaturated fatty acid were only slightly decreased in L1-1 cells, while they were much decreased in TK-16 exposed to heat stress. Therefore, I concluded that altering the fatty acid profiles of cell membrane was not the main reason contributing to the enhanced stress tolerances against oxidative stresses (ethanol and H₂O₂) and hyperosmotic stress (glucose) in L1-1.

Table 3.3.3 Membrane fatty acid profile under stress conditions.

The thermotolerant strain and wild-type cells were grown in 5 mL of YM medium or YM medium with 30 g/L ethanol, 4 mM H₂O₂, 250 g/L glucose, or 40 g/L DMSO at 30°C or 37°C. The relative fatty acid composition is shown as a percentage (%) of total fatty acids. C14:0: myristic acid; C16:0: palmitic acid; C16:1 palmitoleic acid; C18:0: stearic acid; C18:1: oleic acid; C18:2: linoleic acid; C18:3: α -linolenic acid; FA: fatty acid; SFA: saturated fatty acid; UFA: unsaturated fatty acid. The standard deviation of each data point was based on three independent measurements.

Growth condition	Strain	% of total FA								SFA (%)	UFA (%)
		SFA			UFA						
		C14:0	C16:0	C18:0	C16:1	C18:1	C18:2	C18:3			
Control	WT	2.3 ± 0.9	15.1 ± 1.1	2.2 ± 0.1	4.5 ± 1.5	61.2 ± 5.4	11.9 ± 5.0	2.7 ± 0.8	19.7 ± 2.2	80.3 ± 0.2	
	L1-1	0.8 ± 0.2	8.0 ± 0.2	1.5 ± 1.0	0.6 ± 0.4	63.1 ± 1.2	22.0 ± 1.2	4.0 ± 0.8	10.3 ± 1.3	89.7 ± 0.8	
37°C	WT	2.1 ± 0.3	24.1 ± 0.5	6.5 ± 0.9	8.6 ± 0.8	52.7 ± 0.7	5.7 ± 0.9	0.4 ± 0.2	32.7 ± 1.7	67.3 ± 1.0	
	L1-1	1.0 ± 0.7	14.6 ± 0.7	2.4 ± 0.7	1.0 ± 0.5	75.3 ± 2.0	5.2 ± 1.9	0.5 ± 0.4	18.0 ± 2.1	82.0 ± 1.2	
Ethanol	WT	1.4 ± 1.4	15.6 ± 4.8	8.4 ± 6.0	3.2 ± 0.3	58.8 ± 7.9	11.7 ± 1.7	0.9 ± 0.2	25.4 ± 12.3	74.6 ± 9.5	
	L1-1	2.0 ± 0.9	14.6 ± 0.2	3.5 ± 0.5	2.5 ± 0.8	63.3 ± 4.9	13.3 ± 2.9	1.0 ± 0.1	20.0 ± 1.6	80.0 ± 1.2	
H ₂ O ₂	WT	1.5 ± 1.4	15.0 ± 5.0	4.2 ± 2.3	16.0 ± 5.0	51.4 ± 12.9	17.7 ± 4.1	8.6 ± 2.5	20.8 ± 8.7	79.2 ± 8.1	
	L1-1	1.1 ± 0.6	9.4 ± 1.7	2.4 ± 1.8	1.1 ± 0.9	48.5 ± 12.8	28.8 ± 6.5	8.7 ± 3.0	12.9 ± 4.1	87.1 ± 3.1	
DMSO	WT	0.9 ± 0.5	19.0 ± 2.2	4.0 ± 0.5	2.8 ± 2.1	44.4 ± 1.9	24.0 ± 1.7	4.9 ± 0.5	23.9 ± 3.1	76.1 ± 2.2	
	L1-1	0.6 ± 0.4	12.1 ± 0.6	1.9 ± 0.0	2.0 ± 2.4	52.1 ± 4.5	26.9 ± 5.7	4.4 ± 0.4	14.6 ± 1.0	85.4 ± 0.8	
Glucose	WT	0.5 ± 0.1	9.6 ± 2.1	1.2 ± 0.6	2.9 ± 3.4	79.8 ± 5.0	5.0 ± 4.0	1.0 ± 0.8	11.3 ± 2.7	88.7 ± 2.2	
	L1-1	0.5 ± 0.3	10.3 ± 0.5	0.6 ± 0.0	1.3 ± 1.3	70.8 ± 8.6	14.7 ± 8.7	1.8 ± 1.3	11.4 ± 0.8	88.6 ± 0.3	

3.3.4 Intracellular ROS levels of thermotolerant L1-1 under various environmental stresses

Thermal, oxidative, high-osmotic and DMSO-induced stresses might induce an elevation of intracellular ROS content in yeast cells, which in turn causes cell damages. These environmental factors have been known to induce intracellular reactive oxygen species (ROS), such as $\bullet\text{O}^{2-}$, $\bullet\text{OH}$ and H_2O_2 , by causing the dysfunction of mitochondria and leakage of proton and electron from electron transport chain. Hence, reducing ROS generation and maintaining a non-toxic steady-state of intracellular ROS level is a critical mechanism to reduce cell damage after stress exposure (Kitichantaropas *et al.* 2016; Herrero *et al.* 2008). Heat, ethanol, H_2O_2 , DMSO, and high-concentration of glucose have been proved to the trigger intracellular ROS accumulations (Zhang *et al.* 2015; Semchyshyn and Lozinska 2012; Pérez-Gallardo *et al.* 2013; Pastor *et al.* 2009). Therefore, I surmised that the thermotolerant L1-1 might have an improved ability to maintain ROS homeostasis compared to the original strain under not only thermal stress but also other stress conditions. To investigate the ability of the thermotolerant strain to maintain ROS homeostasis, the ROS levels were determined under different stress conditions. The results indicated that the thermotolerant L1-1 strain maintained the lower ROS levels under almost all the stress conditions (heat, ethanol, H_2O_2 and DMSO) except glucose (Fig. 3.3.4). Accordingly, these results indicated that the thermotolerant L1-1 strain had greater redox homeostasis under stress conditions, and the abilities to maintain ROS homeostasis appeared to be the major mechanism contributing to the multiple-stress tolerances. The ROS levels of the wild-type TK16 and thermotolerant L1-1 strains cultivated with 250 g/L glucose were also not significantly different (Fig. 3.3.4). Consequently, I surmised that there were other cell responses that promoted the enhanced growth of the thermotolerant strain under glucose-induced stress in liquid broth.

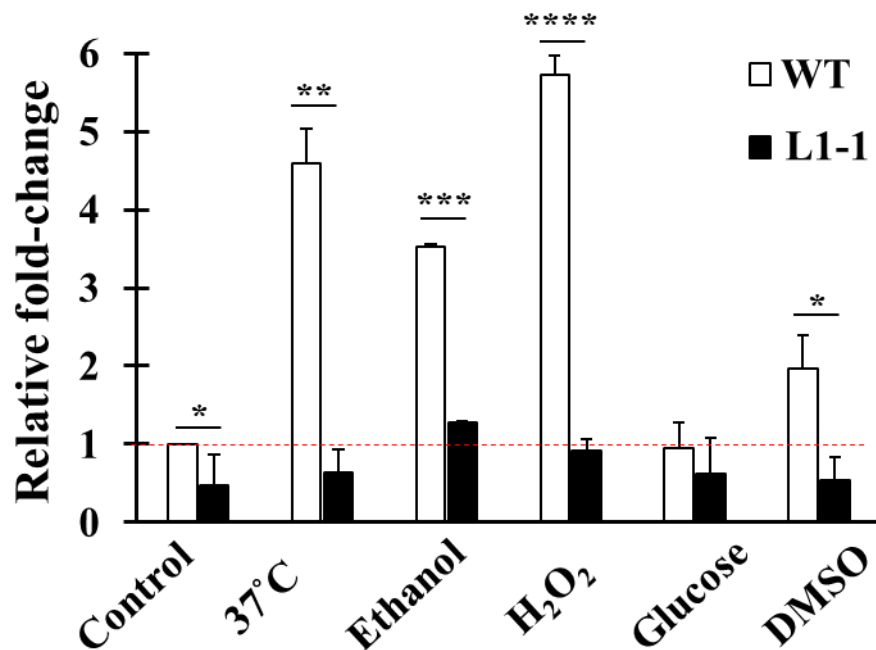


Fig. 3.3.4 Intracellular ROS levels under various stress conditions. The cells were cultivated under various stress conditions (YM, control; 37°C; 30 g/L ethanol; 4 mM H₂O₂; 250 g/L glucose; 40 g/L DMSO) in the tubes at 30°C or 37°C. The log-phase cells were collected and treated with 50 μM DCFH-DA to determine the intracellular ROS levels. The ROS levels were evaluated by measuring the absorbance at 500 nm. The relative ROS level represents the ratio of the ROS level to that of the wild-type grown at 30°C in YM medium. Error bars: standard error of the mean based on three independent measurements. The *p* values were determined by Student's *t*-test. **p*<0.05; ***p*<0.01; ****p*<0.001; *****p*<0.0001. The standard deviation of each data point was based on three independent measurements.

3.3.5 Lipid production of thermotolerant L1-1 under single-stress conditions in nitrogen-limited broth

3.3.5.1 Biomass, lipid content and lipid titer of L1-1 under various single-stress conditions

Although the thermotolerant L1-1 displayed resistances to various stresses under the aforementioned conditions, the lipid-producing ability under these stresses remained unknown. To further investigate the production of the thermotolerant L1-1 under those stress conditions, the L1-1 cells were grown in the nitrogen-limited broth

with different stress-inducing reagents for 120 h. Compared to the dry biomass produced by the wild-type under the stress conditions, the thermotolerant L1-1 generated a significantly higher dry biomass level at each of 37°C ($p < 0.01$), 4 mM H₂O₂ ($p < 0.05$) and 4% (w/w) DMSO ($p < 0.01$) (Fig. 3.3.5.1A). Additionally, the dry biomass data of the thermotolerant L1-1 cultivated at 30°C and 37°C in the standard nitrogen-limited medium and cultivated in the standard medium with 4 mM H₂O₂ were not significantly different. These results demonstrated that the thermotolerant L1-1 could withstand the stresses induced by heat and 4 mM H₂O₂ in nitrogen-limited broth and maintain its biomass.

Based on the results of lipid content (Fig. 3.3.5.1B), there was no significant difference between the wild-type TK16 and the L1-1 strain cultivated under the stresses induced by 4 mM H₂O₂, 40 g/L DMSO and 320 g/L glucose ($p > 0.05$). On the other hand, the L1-1 accumulated higher lipid content than the wild-type TK16 under the stress conditions induced by 37°C and 30 g/L ethanol ($p < 0.05$; $p < 0.0001$). Notably, the lipid content of the thermotolerant L1-1 under 30 g/L ethanol-stress significantly increased to $37.1 \pm 0.6\%$ of dry biomass in comparison to that at 30°C ($12.2 \pm 0.9\%$ of dry biomass, $p < 0.001$). Based on the lipid-titer data, there were no significant differences in lipid production between the thermotolerant and wild-type strains under exposure to 40 g/L DMSO and 320 g/L glucose. However, when compared to the lipid titer of the wild-type strain under the conditions of 37°C, 4 mM H₂O₂, or 30 g/L ethanol (0.3 ± 0.0 ; 0.3 ± 0.2 ; 0.3 ± 0.0 g/L), the thermotolerant L1-1 strain produced a greater amount of lipid than the wild-type (1.4 ± 0.0 g/L, $p < 0.001$; 1.4 ± 0.4 g/L, $p < 0.05$; 2.5 ± 0.6 g/L, $p < 0.05$) (Fig. 3.3.5.1C). The thermotolerant L1-1 cells produced the greatest amount of lipid (2.5 ± 0.6 g/L) under ethanol-induced stress, based on the results of the lipid-production analysis under single-stress conditions.

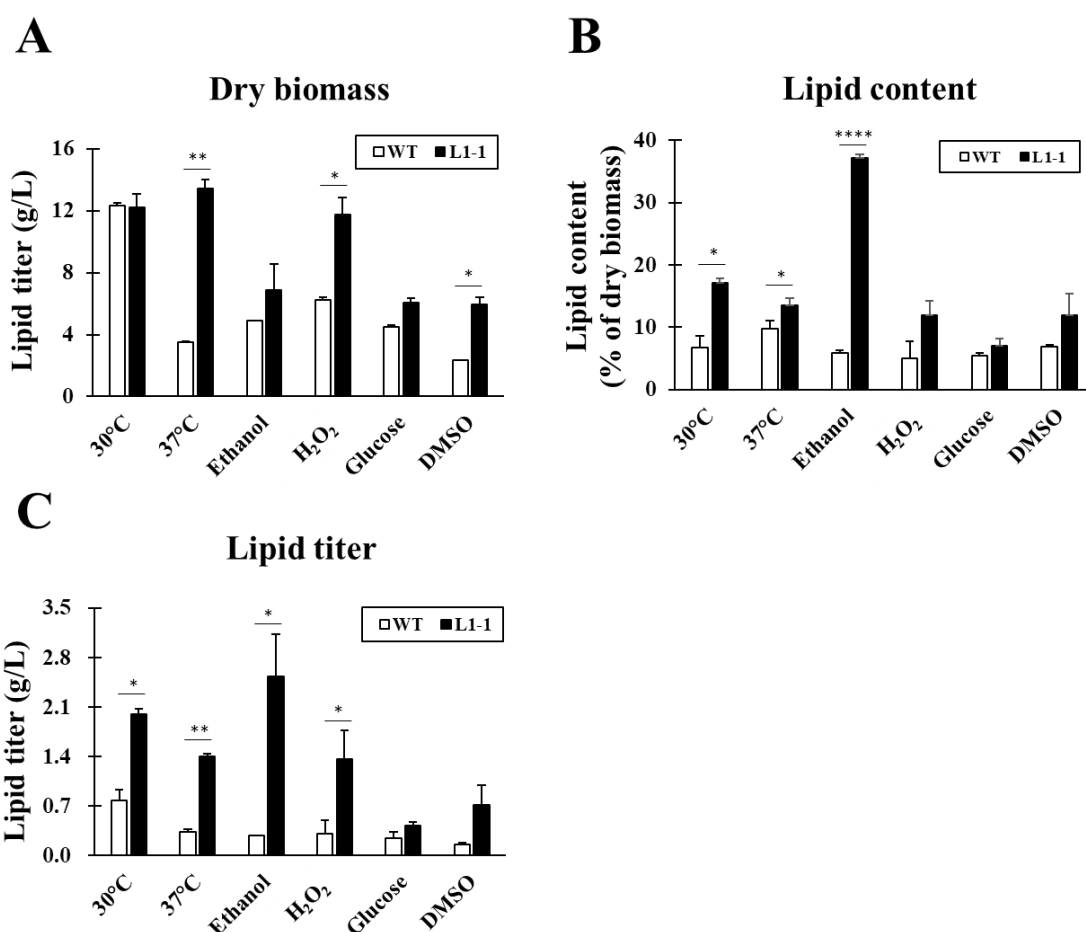


Fig. 3.3.5.1 Lipid production under single-stress conditions. The cells were cultivated under various single-stress conditions (30°C, non-stress control; 37°C; 4 mM H₂O₂; 40 g/L DMSO; 30 g/L ethanol; 320 g/L glucose) in the nitrogen-limited broth at 30°C or 37°C for 120 h. Dry biomass (A) was shown in gram per liter of culture liquid, lipid content (B) was shown in a percentage of dry biomass, and lipid titer (C) was presented in gram per liter of culture liquid. The SD of each data point was based on three independent measurements. The *p* values were determined by Student's *t*-test. **p*<0.05; ***p*<0.01; *****p*<0.0001.

3.3.5.2 Lipid droplets of L1-1 under ethanol-induced stress condition

Examining the lipid droplets in the thermotolerant L1-1 at 120 h under non-stress conditions by Sudan IV, the size of lipid droplets were larger than that in the L1-1 cultivated under non-stress condition (Fig. 3.3.5.2). Under ethanol stress, the size of lipid droplets increased to $58.1 \pm 3.3\%$, while the size of droplets shrunk from $21.5 \pm$

2.6% in the absence of stress to $13.7 \pm 7.0\%$ at 120 h under ethanol stress (Fig. 3.3.5.2). These semi-quantitative data from microscopic images indicated that the thermotolerant L1-1 could tolerate 30 g/L ethanol and generated a larger size of lipid droplets. Collectively, these findings demonstrated that ethanol-induced stress elevate lipid production in the nitrogen-limited broth.

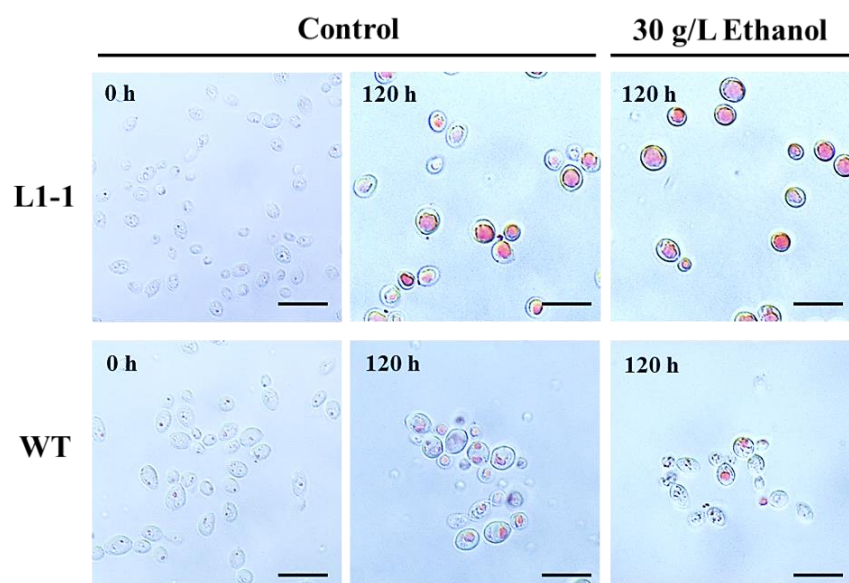


Fig. 3.3.5.2 Lipid staining of L1-1 under ethanol-induced stress conditions. The cells were cultivated under various single-stress conditions (YM, control; 30 g/L ethanol) in the nitrogen-limited broth at 30°C for 120 h. The grown cells were harvested at 0 and 120 h for lipid staining. Red color indicates the stained neutral lipids. Scale bar: 10 μm . WT, wild-type.

3.3.6 Lipid staining of thermotolerant L1-1 under dual-stress conditions

3.3.6.1 Lipid droplets of L1-1 under various ethanol-induced stress conditions

To further investigate whether ethanol stress could further increase the lipid productivity of the thermotolerant L1-1 under other stresses, the lipid-producing ability of thermotolerant L1-1 cells grown under ethanol combined with other stresses were assessed. The cells of the wild-type TK16 and the thermotolerant L1-1 strain grown under dual stresses (30 g/L ethanol at 37°C, E+37°C; 30 g/L ethanol and 4 mM H₂O₂,

E+H; 30 g/L ethanol with 40 g/L DMSO, E+D; 30 g/L ethanol with 320 g/L glucose, E+G) in the nitrogen-limited broth were harvested and stained by Sudan IV for the observation of lipid droplets. Under bright-field microscopic observation, the thermotolerant L1-1 at 120 h possessed clear lipid droplets in cells under all the stress conditions, with the size of the lipid droplets accounting for $14.3 \pm 3.1\%$ of the total cell size at E+37°C, $55.2 \pm 3.5\%$ at E+H, $30.9 \pm 3.6\%$ at E+D and $42.1 \pm 7.1\%$ at E+G (Fig. 3.3.6.1). These results indicated that the thermotolerant L1-1 could accumulate lipids under most of the dual stresses including ethanol. On the other hand, the wild-type TK16 only formed obvious lipid droplets under the conditions of ethanol combined with glucose (E+G: $18.1 \pm 5.2\%$) (Fig. 3.3.6.1). The data indicated that ethanol combined with H₂O₂ or DMSO affected the lipid accumulation of the wild-type TK16 rather than the thermotolerant L1-1 strain.

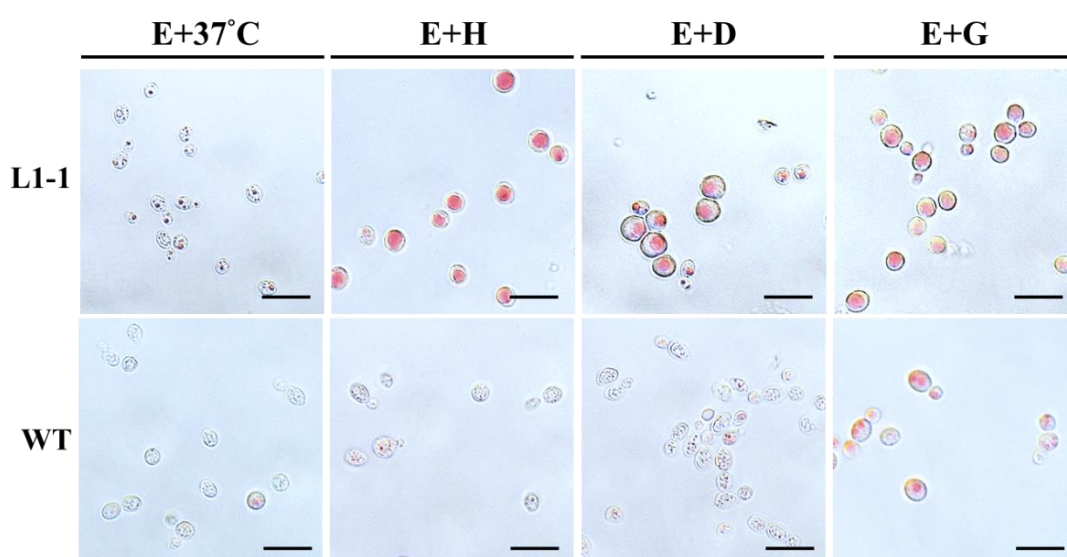


Fig. 3.3.6.1 Lipid staining of L1-1 under dual-stress conditions. The cells were cultivated under dual stress (E+37°C: 30 g/L at 37°C; E+H: 30 g/L with 4 mM H₂O₂; E+D: 30 g/L with 40 g/L DMSO; E+G: 30 g/L with 320 g/L glucose) in the nitrogen-limited broth at 30°C or 37°C with reciprocal shaking at 220 spm for 120 h. The grown cells were harvested for lipid staining and fatty acid quantification by GC-FID. Observation of intracellular neutral lipids in the wild-type and thermotolerant L1-1 under dual stress conditions in nitrogen-limited broth by microscopy. The neutral lipids were

stained by Sudan IV, and the cell images were observed at 120 h from a bright-field scope. Red color indicates the stained neutral lipids. Scale bar: 10 μm . WT, wild type.

3.3.6.2 Biomass, lipid content and lipid titer of L1-1 under dual-stress conditions.

To quantitatively evaluate the lipid production of the thermotolerant L1-1 under dual stresses in the nitrogen-broth, the yeast cells were cultivated under dual-stress conditions in the nitrogen-limited conditions with ethanol combining other stress inducers. Comparing with the wild-type TK16, the thermotolerant L1-1 displayed higher cell mass than the wild-type under the E+H and E+G stresses. Moreover, the dry biomass of thermotolerant L1-1 produced under E+H stress was significantly greater than that of cells grown under the non-stress condition (30°C) (16.2 ± 0.2 vs. 12.2 ± 0.9 g/L; $p < 0.01$) (Fig. 3.3.6.2). The data demonstrated that E+H stress increased the biomass amount in cells.

The lipid content results showed that the thermotolerant L1-1 possessed higher lipid content than the wild-type TK16 under all the dual stresses (Fig. 3.3.6.2). Combining the results of lipid content of the thermotolerant L1-1 under single stresses and dual stresses (Fig. 3.3.5.1 and Fig. 3.3.6.2), I found that the thermotolerant L1-1 accumulated greater lipid content under the stress conditions combined with ethanol than under any of the individual single-stresses. This phenomenon confirmed that the ethanol stress could induce the lipid accumulation in cells. Examining the lipid titer of the thermotolerant L1-1 under dual stresses, it can be seen that the thermotolerant L1-1 showed a significantly higher lipid titer than the wild-type under all stress conditions except E+37°C (Fig. 3.3.6.2). The highest lipid titer of the thermotolerant L1-1 was observed under the E+H condition, which reached 3.0 ± 0.2 g/L. Although the lipid content of the thermotolerant L1-1 under the E+H condition was significantly lower than that under ethanol stress alone ($18.4 \pm 1.1\%$ vs. $37.1 \pm 0.6\%$; $p < 0.05$), the lipid

titer of the thermotolerant L1-1 cells was not significantly different between the culture under ethanol stress and that under the E+H condition (2.5 ± 0.9 g/L vs. 3.0 ± 0.2 g/L; $p>0.05$) (Fig. 3.3.5.1 and 3.3.6.2) because of the higher dry biomass produced by the thermotolerant L1-1 cells under E+H stress in comparison to that generated under ethanol stress alone (16.1 ± 0.2 g/L vs. 6.9 ± 1.7 g/L; $p<0.05$).

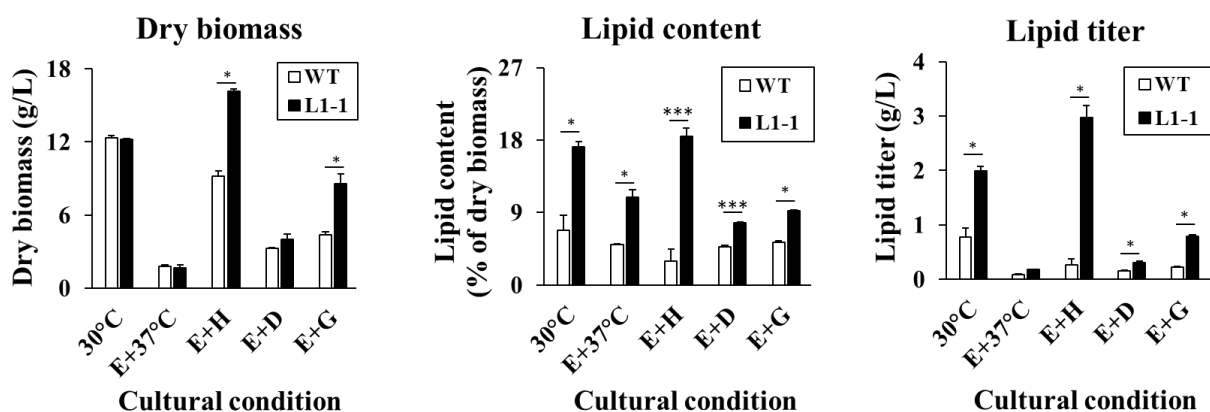


Fig. 3.3.6.2 Lipid production under dual-stress conditions. The cells were cultivated under dual stress (E+37°C: 30 g/L at 37°C; E+H: 30 g/L with 4 mM H₂O₂; E+D: 30 g/L with 40 g/L DMSO; E+G: 30 g/L with 320 g/L glucose) in the nitrogen-limited broth at 30°C or 37°C for 120 h. Dry biomass was presented in gram per liter of culture liquid, lipid content was present in a percentage of dry biomass, and lipid titer was presented in gram per liter of culture liquid. The SD of each data point was based on three independent measurements. The p values were determined by Student's t -test. * $p<0.05$; *** $p<0.001$.

3.4 Discussion

3.4.1 Maintaining ROS levels under stress conditions contributing to multiple-stress tolerances in thermotolerant L1-1

Heat, ethanol, H₂O₂, and DMSO have all been shown to increase intracellular ROS levels, resulting in oxidative stresses, in model *Saccharomyces* yeasts (Lahtvee *et al.* 2016; Pedroso *et al.* 2009; Anness 1980; Kitichantaropas *et al.* 2016; Herrero *et al.* 2008). Hence, reducing ROS accumulation and maintaining a nontoxic steady-state

level of ROS are important physical responses to reduce cell damage after stress exposure (Kitichantaropas *et al.* 2016; Herrero *et al.* 2008). In this chapter, the thermotolerant L1-1 exhibited greater tolerances to not only 37°C but also ethanol, H₂O₂, and DMSO compared to the wild-type TK16 (Fig. 3.3.1 and Table 3.3.1). By assessing cell wall rigidity, alterations of fatty acids in cell membranes, and the intracellular ROS levels of the L1-1 strain under the various stress conditions, I concluded that maintaining intracellular ROS levels was the main contributor to the enhancement of stress tolerances to heat (37°C), ethanol, H₂O₂, and DMSO (Fig. 3.3.4). These data also suggested that isolation of the thermotolerant L1-1 from heat stress might enhance its ability to maintain ROS levels at a nontoxic state, thus resistance to thermal (37°C), oxidative (ethanol and H₂O₂), and DMSO-induced stresses.

3.4.2 Oxidative stresses induce L1-1 to produce lipid

According to the lipid production data in this chapter, oxidative stress induced by ethanol significantly induced lipid production by L1-1 to nearly 40% of DCW, and ethanol combined with H₂O₂ further increased lipid titer up to 3 g/L from 2.5 g/L (ethanol stress only). Collectively, these findings demonstrated that various oxidative stresses elevated lipid production in the nitrogen-limited broth.

Guo *et al.* (2019) isolated two *R. toruloides* strains (R-ZL2 and R-ZY13), displaying enhanced lipid production compared to the original strain, from osmotic stress (LiCl) and oxidative stress (ethanol-H₂O₂) by UV mutagenesis. Compared to the R-ZL2 mutant isolated from osmotic stress, the R-ZY13 mutant isolated from oxidative stress displayed higher expression levels of *FAS1* (encoding fatty acid synthase 1), *FAS2* (encoding fatty acid synthase 2), *GPD1* (encoding glycerol-3-phosphate dehydrogenase 1), and *GUT2* (encoding glycerol-3-phosphate dehydrogenase 2). These genes are well known to involve lipid synthesis pathways and to enhance lipid production in

oleaginous yeasts (Dulermo and Nicaud 2011). Therefore, I assumed that the enhanced lipid production of L1-1 under ethanol stress may result from the aforementioned genes involved in lipid synthesis. Oxidative stress may also alter the carbon metabolic flux from glycolysis to the pentose phosphate pathway by the post-translational modification of enzymes involved in the glycolytic pathway, leading to the increase in NADPH (Shi *et al.* 2017). NADPH is the major energy source for lipid synthesis in *S. cerevisiae* (Ralser *et al.* 2009). Therefore, oxidative stress may enhance lipid accumulation by inducing NADPH generation from the pentose phosphate pathway.

Additionally, as there is no report of ethanol assimilation in *R. toruloides*, I also examined whether *R. toruloides* can assimilate ethanol as a carbon source for lipid synthesis. Zhang *et al.* (2018) reported that *R. glutinis* was able to utilize cellulosic ethanol wastewater as a substrate for lipid production. Therefore, the present findings may provide new clues for the enhancement of lipid production with an ethanol-containing medium in *Rhodotorula* yeast, which would have practical applications. In our results, the enhanced lipid production by L1-1 also implied a possibility that *Rhodotorula* yeast may assimilate ethanol as a carbon source. Although there is no direct evidence indicating that *Rhodotorula* yeast can synthesize lipid with ethanol as a carbon source, ethanol consumption by *Rhodotorula* yeast should be examined to assess this possibility.

3.4.4 Future perspectives

R. toruloides has a highly promising role for industrial applications. Unveiling the stress responses in the wild-type and thermotolerant strain will thus be important for designing a rational fermentation process and developing appropriate industrial media. Collectively, the information provided here could lead to a molecular engineering strategy to realize *R. toruloides* yeasts with multiple-stress tolerances. Such strains

would be useful in large-scale fermentation and fermentation based on industrially inhibitory components such as lignocellulosic biomass, crude glycerol and ethanol containing wastes.

3.5 Summary: Oxidative stresses (ethanol and H₂O₂) induced lipid production in multiple-stress tolerant strain L1-1

In this chapter, I demonstrated that L1-1 strain is tolerant to multiple stressors and conducted a primary phenotypic analysis of the strain by determining its end-point biomass and lipid production. I found that the strain was resistant to heat, ethanol, H₂O₂, glucose, and DMSO stressors. These results also demonstrated that the redox balance, the strengthening of the cell wall, and the composition of membrane fatty acids were all correlated with protection against various stresses. Nevertheless, redox homeostasis seems to be a major mechanism underlying the various stress tolerances of L1-1. Notably, our data also indicated that ethanol stress served to further enhance lipid production in this strain under nitrogen-limited conditions.

CHAPTER 4

Enhancing L1-1's lipid production of by overexpression of fatty acid desaturase genes

4.1 Background: Metabolic engineering in *R. toruloides* to further enhance lipid production

Although oleaginous yeasts produce more lipid than most yeasts, their yields and titers are still not enough for industrial demands (Zhang *et al.* 2016). Many efforts have been made to increase the amounts of lipids in oleaginous yeasts. Toward this end, several designs have been adapted, especially in the model yeast *Y. lipolytica* (Spagnuolo *et al.* 2019; Wong *et al.* 2019). These metabolic strategies have principally centered on increasing lipid production by overexpressing enzymes involved in the lipid synthesis pathways or by deleting those involved in lipid catabolism. For example, Zhang *et al.* (2016) doubled lipid production by overexpressing two native enzymes, acetyl-CoA carboxylase (*ACC1*) and diacylglycerol acyltransferase (*DGAT*), in *R. toruloides* strain IFO0880. In addition, Zhang *et al.* (2016) demonstrated that overexpressing native malic enzyme (*ME*) and stearoyl-CoA desaturase (*SCD*) from mammals slightly enhanced the lipid titers in IFO0880 strains (1.2-fold and 1.3-fold compared to the wild type). Tsai *et al.* (2019) also demonstrated that overexpressing a native enzyme of Δ^9 -fatty acid desaturase (*Δ^9 -FAD*) successfully quadrupled lipid production in *R. toruloides* strain NP11. Therefore, metabolic engineering is considered a promising way to enhance lipid production in *R. toruloides*.

4.2 Objectives: Enhancing lipid production in L1-1 by overexpressing fatty acid desaturases

Recent studies have revealed that overexpressing fatty acid desaturases can

effectively elevate the levels of intracellular lipids in oleaginous yeast *Y. lipolytica* (Yan *et al.* 2020). Fatty acid desaturases are membrane-bound proteins that catalyze the desaturation reaction to introduce a double bond into hydrocarbon chains of fatty acids to produce unsaturated and polyunsaturated fatty acids (Bai *et al.*, 2016; Díaz *et al.*, 2018). They act specifically on the location and stereochemistry of double bonds in the fatty acids (Fickers *et al.* 2003). For example, $\Delta 9$ -Fad is an endoplasmic reticulum-bound enzyme that catalyzes a double bond between carbons 9 and 10 of SA (C18:0) to generate OA (C18:1). $\Delta 12$ fatty acid desaturase ($\Delta 12$ -Fad) introduces a double bond between carbons 12 and 13 of OA to synthesize LA (C18:2). $\Delta 12$ -Fad primarily regulates the synthesis and content of OA (C18:1) and LA (C18:2) in yeast cells (Ledesma-Amaro and Nicaud 2015). These two fatty acid desaturases play vital roles in the unsaturation of C18 fatty acids, which are the main fatty acid components in oleaginous yeast cells. Yan *et al.* (2020) demonstrated co-overexpression of mammalian $\Delta 9$ -FAD (stearoyl-CoA desaturase, *SCD*), and native *Yl12-FAD* in model *Y. lipolytica* showed a 10% increase in lipid content. On the basis of their results, I assumed that harnessing the expression of these two Fads might further improve lipid production in L1-1. Although Tsai *et al.* (2019) functionally characterized and overexpressed *R. toruloides* $\Delta 9$ -Fad (*RtFAD1*) in *R. toruloides* strains to enhance lipid yield, the functions of *R. toruloides* $\Delta 12$ -Fad (*RtFAD2*) have remained unknown. Therefore, in this chapter I began attempting to identify and characterize the function of *RtFAD2* from *R. toruloides* NBRC8766 and to examine the effects of expressing *RtFAD2* and its co-overexpressing *RtFAD1* in L1-1.

4.3 Results: Overexpression of *RtFAD2* and its co-expression of *RtFAD1* and

RtFAD2* enhanced lipid production in *R. toruloides

4.3.1 Identification of putative *RtFAD2* in *R. toruloides* NBRC8766

4.3.1.1 Phylogenetic analysis of putative *RtFAD2* in *R. toruloides* NBRC8766

There is only one annotated putative *RtFAD2* in the open-genome database of *R. toruloides* NP11 (a haploid strain of *R. toruloides* NBRC8766) in the NCBI protein database (GenBank accession no. XP_016269356.1, Zhu *et al.* 2012). The putative coding sequence of *RtFAD2* (1,353 bp) encodes a deduced polypeptide consisting of 451 amino acids with a predicted molecular mass of 50.6 kDa. Therefore, the *RtFad2* sequence was BLAST searched against the NCBI database, and 16 homologs of $\Delta 12$ -Fad and 2 homologs of $\Delta 9$ -Fad were used for the phylogenetic tree construction (Fig. 4.3.1.1). The phylogenetic relationship illustrated the distinguishable clusters among Ascomycota, Basidiomycota and plant $\Delta 12$ -Fads and the outgroup of yeast $\Delta 9$ -Fad (Fig. 4.3.1.1). The phylogenetic tree also indicated that *RtFad2* is most close to $\Delta 12$ -Fad from *R. kratochvilovae* and *R. glutinis*.

4.3.1.2 Conserved protein region analysis of putative $\Delta 12$ -Fad in *R. toruloides* NP11

The conserved domain analysis compared the fatty acid desaturases from *M. alpina*, *Y. lipolytica*, *Trichophyton asahii*, *Ogataea parapolyomorpha*, *C. parapsilosis* and *L. starkeyi*. The deduced amino acid sequence of $\Delta 12$ -Fad demonstrated two regions of transmembrane domains are similar to conserved $\Delta 12$ -Fad-like domain (bold line) containing 4 highly conserved histidine sequences (boxed) (HXXXH, HXX(X)HH, and HXXHH) (Fig. 4.3.1.2). Accordingly, the putative *R. toruloides* $\Delta 12$ -Fad obtained from NCBI protein database was used for functional identification to produce LA in *S. cerevisiae*.

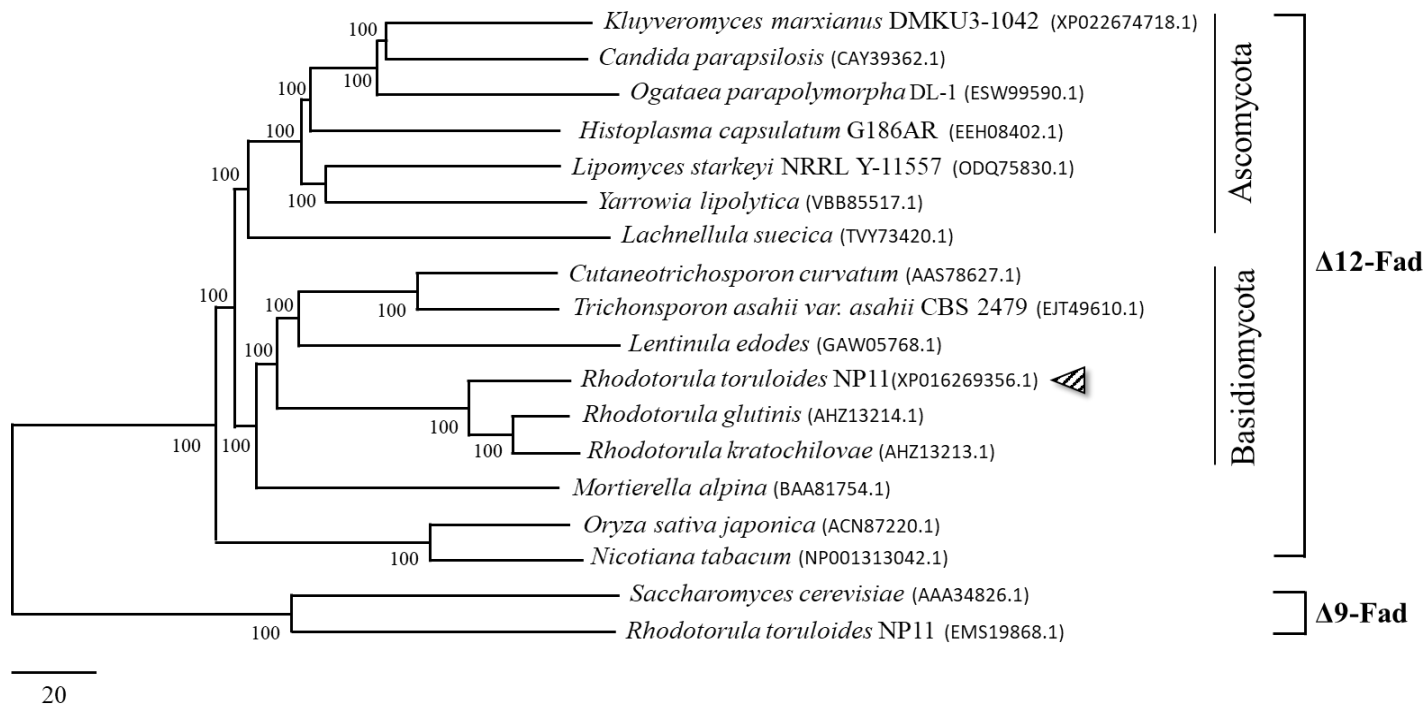


Fig. 4.3.1.1 Phylogenetic analysis of $\Delta 12$ -Fads from yeast *R. toruloides* NBRC8766. The phylogenetic tree was constructed by the characterized and deduced $\Delta 12$ -Fad protein homologs with $\Delta 9$ -Fads as an outgroup. The species' names are followed by GenBank protein accession number. Branch lengths are proportional to the phylogenetic distances. Arrow indicates the position of *RtFad2*.

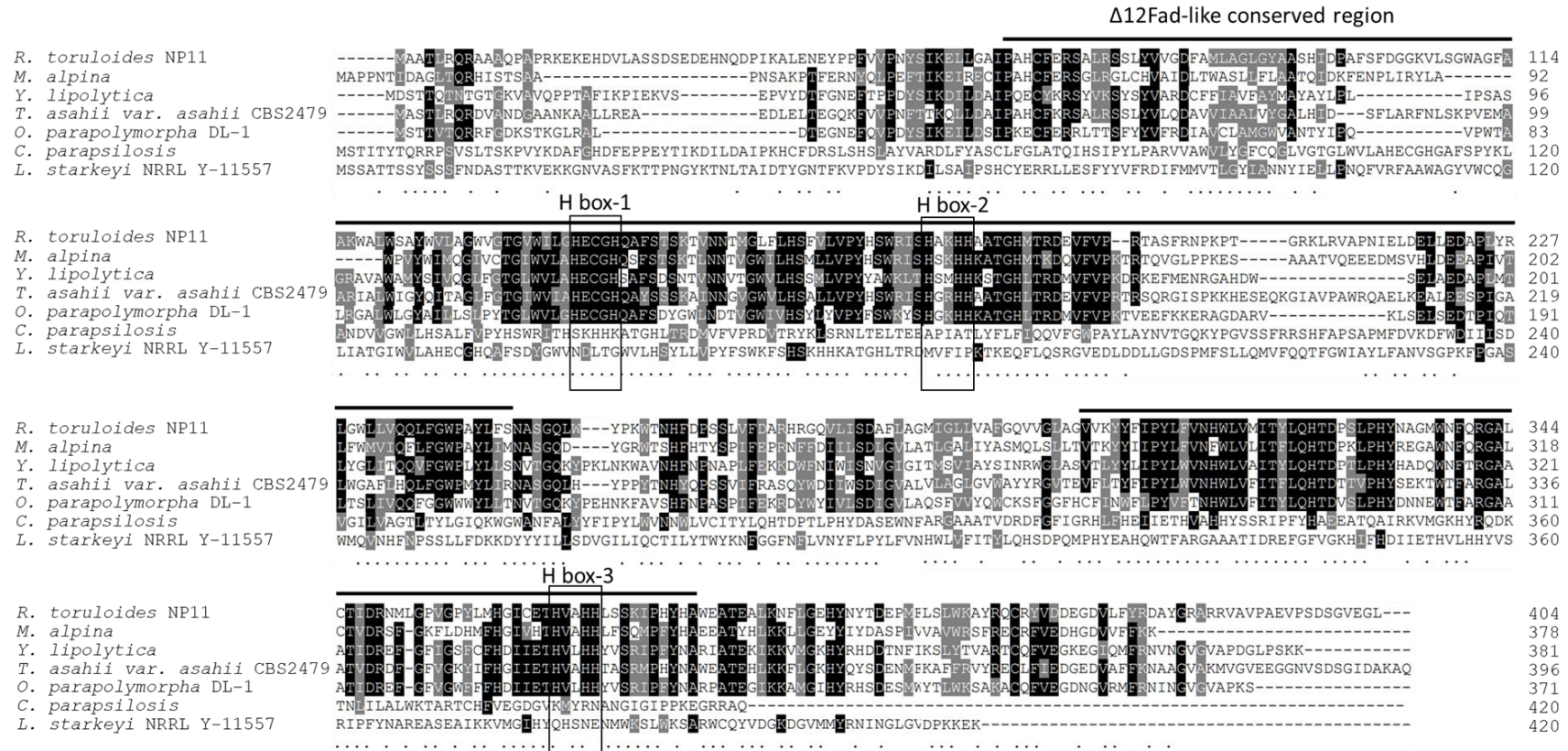


Fig. 4.3.1.2 Protein conserved domain analysis of Δ12-Fads from yeast *R. toruloides* NBRC8766. Amino acid sequence alignment of Δ12-Fad orthologs. Amino acid sequences of various species were compared using the multiple sequence alignment software T-Coffee (<http://tcoffee.org.cat>). Identical amino acid residues are labeled in black boxes, and the conservative regions are indicated in gray. The conservative histidine-rich motifs (H-box) are boxed. Putative transmembrane motifs of *RtFad2* are barred.

4.3.2 Functional analysis of *RtFad2* by using a heterologous expression system in *S. cerevisiae*

To identify the function of *RtFad2*, the protein was expressed in *S. cerevisiae*. The mainly produced fatty acids in the wild-type *S. cerevisiae* are PA (C16:0), POA (C16:1), SA (C18:0) and OA (C18:1) (Fig. 4.3.2). Linoleic acid (LA, C18:2) was not detected in control cells (Fig. 4.3.2). The results of GC-FID analysis of the total fatty acids revealed that one apparent fatty acid peak was detected (indicated by arrow), which was absent in the yeast transformed with empty vector pYES2 (Fig. 4.3.2). Comparing the retention time of commercial fatty acid standard, the apparent peak was identified as LA (C18:2). Accordingly, the results demonstrated that *RtFad2* had the enzymatic activity to produce LA from OA.

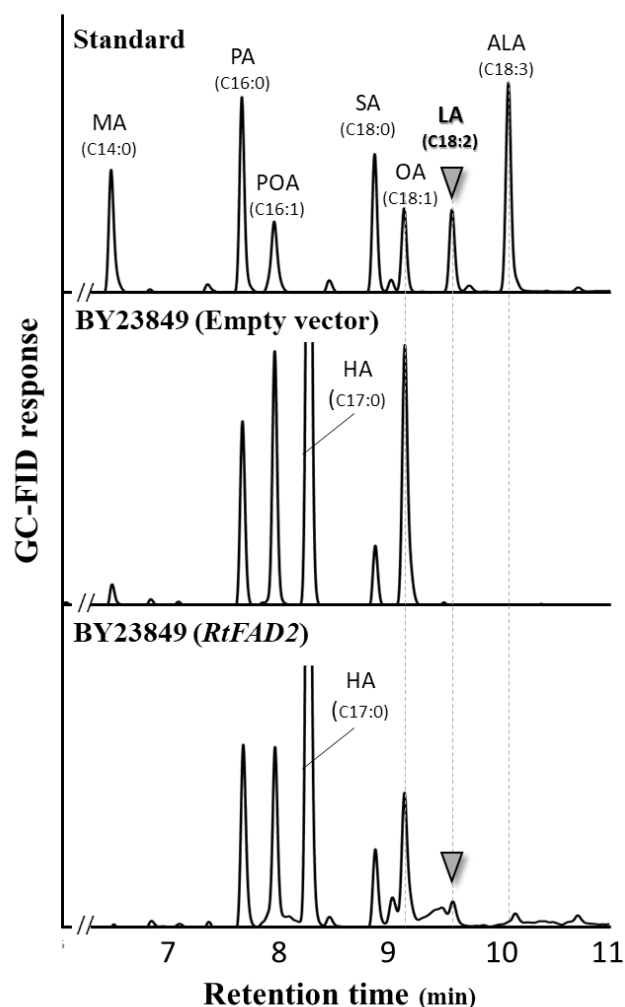


Fig. 4.3.2 Identification of linoleic acid in *S. cerevisiae* expressing *RtFAD2* by GC-FID. The peak of LA was identified by a comparison with the commercially available fatty acid methyl ester standard. Myristic acid, MA (C14:0); palmitic acid, PA (C16:0); palmitoleic acid, POA (C16:1); stearic acid, SA (C18:0); Oleic acid, OA (C18:1); linoleic acid, LA (C18:2); α -linolenic acid, ALA (C18:3).

4.3.3 Growth characteristics of *RtFAD2* and *RtFAD1+RtFAD2* overexpressing *R. toruloides* strains under nutrient conditions

4.3.3.1 Overexpression of *RtFAD2* in *R. toruloides* strains affected the cell growth

To characterize the growth effects of overexpressing *RtFAD2* in *R. toruloides*, I next introduced the genomic sequence of *RtFAD2* into two strains (TK16 and thermotolerant L1-1). The spot assay results indicated that overexpressing *RtFAD2* in

the TK and L1-1 strain displayed the defect growth at 30°C comparing to the wild-type TK16 (Fig. 4.3.3.1A). The results indicated three individual transformants of TK16 and L1-1 showed the same reduced growth comparing to the wild-type TK16 and L1-1. These results (Fig. 4.3.3.1A) demonstrated the reduced growth of transformants were resulted from the *RtFAD2* overexpression in cells rather than the effects of random insertion of introduced cassettes in the genome. The thermotolerant L1-1 strain was evolutionarily isolated from TK16 strain and considered to be more resistant to heat than TK16. To investigate whether overexpressing *RtFAD2* would affect the thermotolerance of L1-1, the L1-1 transformants were cultivated at 30°C, 33°C, 35°C and 37°C. The results indicated the thermotolerance of L1-1 transformants recovered their growth at 37°C (Fig. 4.3.3.1B). In addition, the recovery of cell growth was dependent on the increased temperatures (35°C and 37°C) (Fig. 4.3.3.1B). Accordingly, I assumed that increased temperatures decreased the enzyme activity of *RtFad2*. Although the enzyme stability of *RtFad2* has not been reported, Esteban *et al.* (2004) revealed the enzyme activity of $\Delta 12$ -Fad dropped to 40% at 40°C compared to the 100% activity at 25°C in plant *Carthamus tinctorius*. Hence, I reckoned the recovery of defected growth in the *RtFAD2* expressing L1-1 at 37°C was due to the suppression of $\Delta 12$ -Fad enzyme activity which led to the decreased LA content in cells.

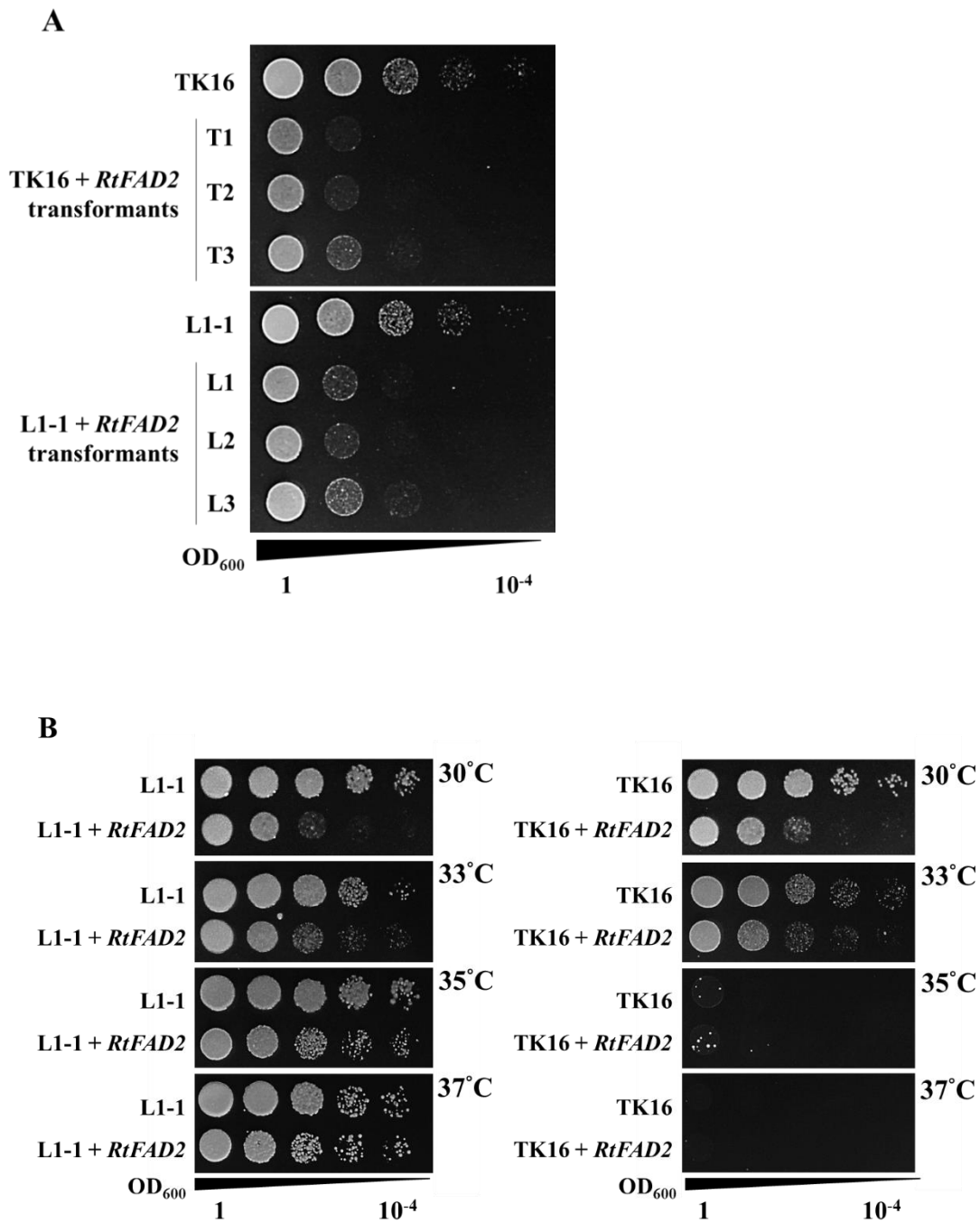


Fig.4.3.3.1 Spot assay of *R. toruloides* strains grown under various temperatures. Spot assay of *RtFAD2* overexpressing transformants in *R. toruloides* TK16 and thermotolerant L1-1. A. Three different *RtFAD2* overexpressing transformants of TK16 or L1-1 grown at 30°C. B. *RtFAD2* overexpressing transformants of TK16 and L1-1 grown under various temperatures.

4.3.3.2 Overexpressing *RtFAD2* increased LA content in cells.

Overexpression of $\Delta 12$ -Fads has been shown to increase the intracellular LA content in oleaginous yeasts (Tezaki *et al.* 2017; He *et al.* 2015; Wang *et al.* 2017). The intracellular LA also has been shown to increase the fluidity of the cell membrane and further affect the membrane integrity (Rodríguez-Vargas *et al.* 2007). Accordingly, I considered that overexpressing *RtFAD2* in the strains might lead to the increase of intracellular LA content and eventually increase the fluidity of cell membranes resulting in growth defect. Therefore, the intracellular LA contents of the *RtFAD2* overexpressing strains were measured. According to the results (Fig. 4.3.3.2), the *RtFAD2* overexpressing strains of TK16 and L1-1 had higher levels of LA contents than the wild-type TK16 and L1-1. Therefore, the results suggested the increased LA content in cells may link to the reduced growth of the *RtFAD2* transformants.

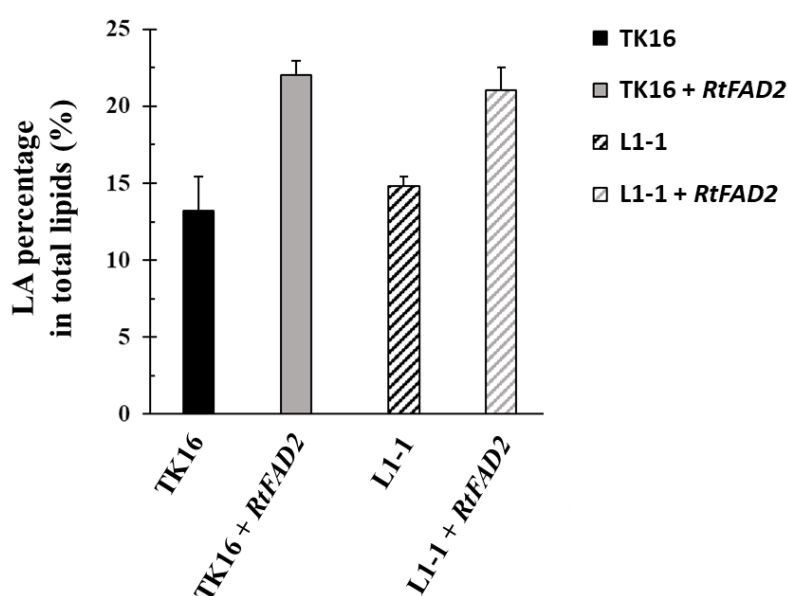


Fig.4.3.3.2 LA content of the wild-type and *RtFAD2* transformants in *R. toruloides* strains. The average and SD of each data point was based on three independent measurements.

4.3.3.3 Recovery of the growth of *RtFAD2* transformants by co-overexpressing *RtFAD1* in *R. toruloides* strains.

4.3.3.3.1 Co-overexpressing *RtFAD1* reduced intracellular LA content

Next, to recover the growth of *RtFAD2* transformants, the *RtFAD1* was co-expressed in the TK16 and L1-1. Expressing *RtFAD1* has been shown to increase the OA content in *R. toruloides* cells (Tsai *et al.* 2019). Therefore, I assumed that increased OA level may recover the cell growth by reducing the intracellular LA content during cell growth hence maintain the cell integrity in the nutrient medium. Fig. 4.3.3.3.1 indicated that co-overexpressing *RtFAD1* and *RtFAD2* reduced the intracellular LA ratio in the nutrient medium.

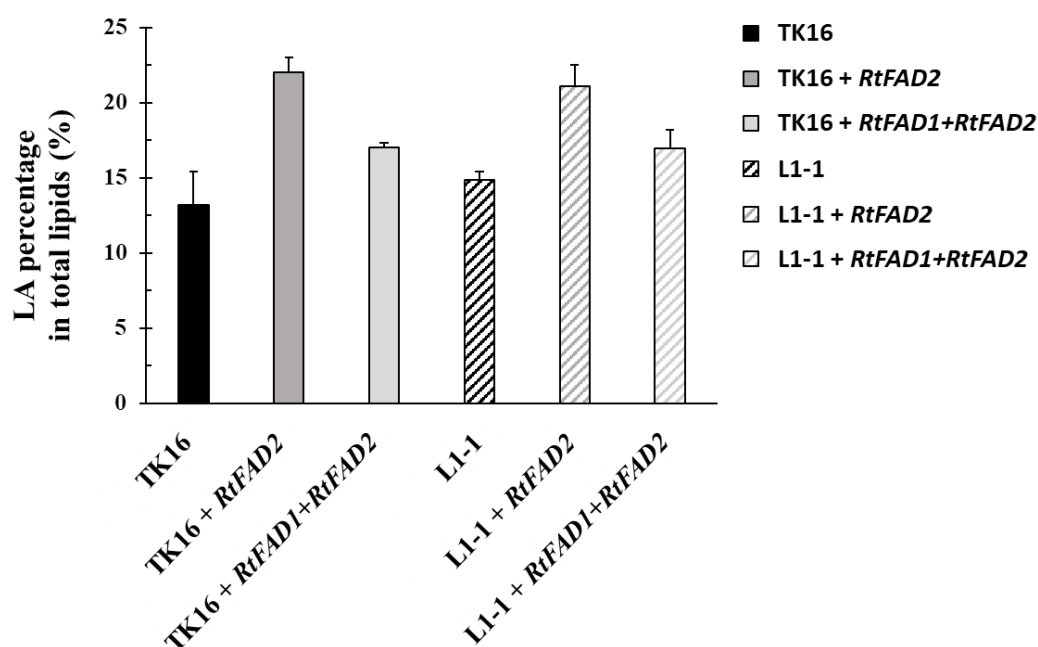


Fig. 4.3.3.3.1 LA content among *RtFAD2* and *RtFAD1+RtFAD2* strains.

4.3.3.3.2 Recovery of cell morphology by co-overexpressing *RtFAD1* in *RtFAD2* transformants

To examine the effects of co-overexpressing *RtFAD1* in *RtFAD2* strains on lipid accumulation, the transformant cells were collected from the YPD medium and stained with Sudan IV for lipid droplet examination. The results of cell morphology (Fig. 4.3.3.3A) indicated the *RtFAD1+RtFAD2* co-overexpressing strains in TK16 and L1-1

recovered the round shape of cells as same as the wild-type. On the contrary, the *RtFAD2* transformants only showed an elongated cell shape. These data suggested that reducing the LA content in cells could recover the cell morphology by changing the cell membrane fluidity in *R. toruloides*.

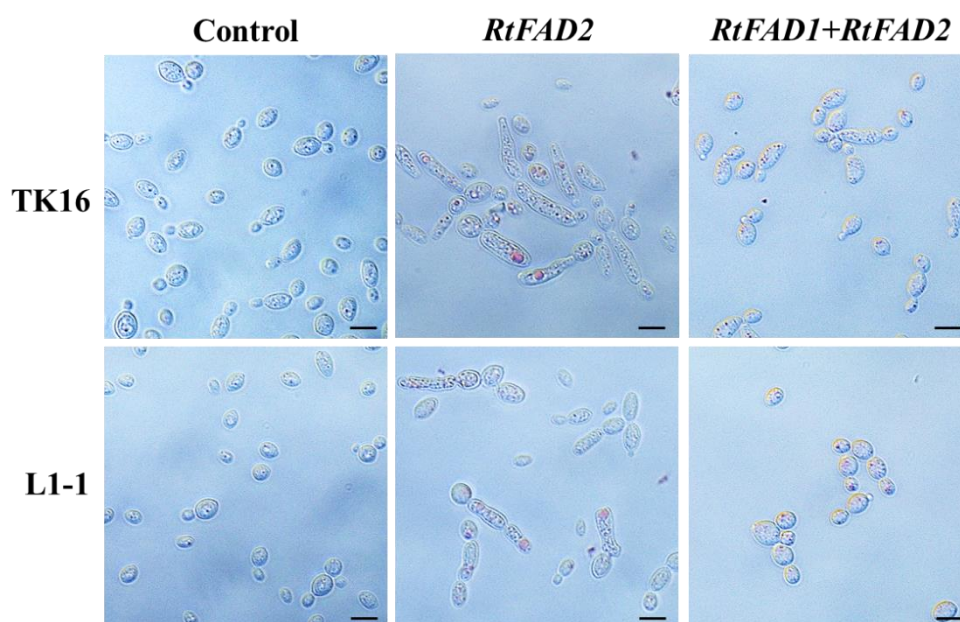


Fig.4.3.3.3.2 Cell morphology of all transformants. Scale bar: 5 μm .

4.3.3.3.3 Overexpressing *RtFAD1* in *RtFAD2* transformants recovers cell growth

Aside from the cell morphology, I next confirmed the cell growth of the co-expressing strains in the nutrient medium. All the strains were inoculated into the YPD medium and OD_{600} was measured every 6 h. The results (Fig. 4.3.3.3.3) showed that the *RtFAD1+RtFAD2* co-overexpressing strain of TK16 slightly recovered the cell growth comparing the *RtFAD2* overexpressing strain. However, the *RtFAD1+RtFAD2* co-overexpressing strain of L1-1 displayed the recovery of growth than the *RtFAD2* overexpressing strain. According to these data (Fig. 4.3.3.3.3 and Fig. 4.3.3.3.2), reducing the LA content by co-overexpressing *RtFAD1* in *RtFAD2* strains could recover the cell morphology and cell growth.

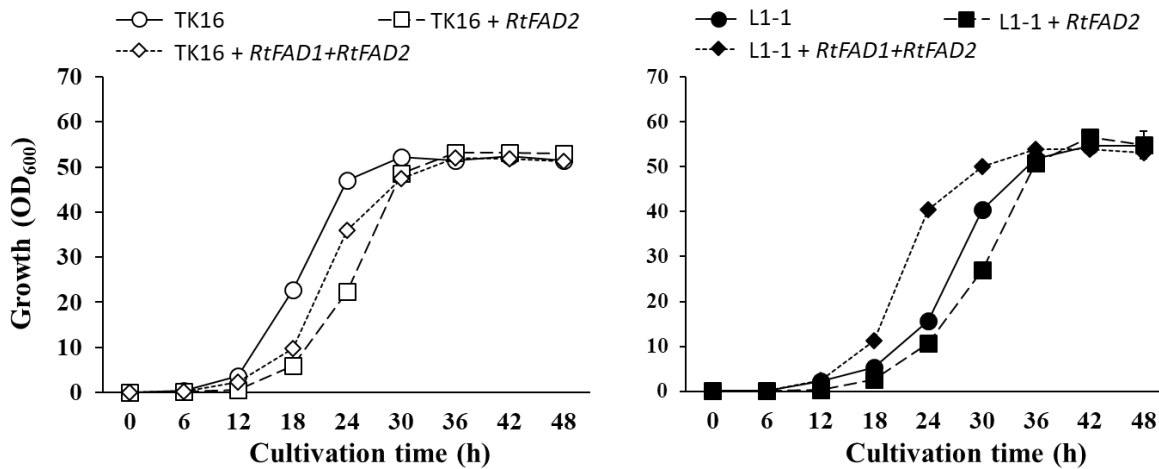


Fig. 4.3.3.3.3 Growth curve of *RtFAD2* and *RtFAD1+RtFAD2* overexpressing transformants in *R. toruloides* TK16 and thermotolerant *R. toruloides* L1-1. The cells were cultured in YPD medium at 30°C and the OD₆₀₀ values were measured at each 6 h-interval. The average and SD of each data point was based on three independent measurements.

4.3.4 Expression of *RtFAD2* and co-overexpression of *RtFAD1* and *RtFAD2* gene increased lipid production in *R. toruloides* strains

4.3.4.1 Growth of engineered strains in the nitrogen-limited medium

To investigate the effects of *RtFAD2* expression and *RtFAD1+RtFAD2* co-overexpression on lipid production in all the studied strains. According to Fig. 4.3.3.1B, the enzyme activity of *RtFad2* may be decreased by temperatures over 30°C. Hence, the 30°C was chosen for lipid production. The OD₆₀₀ and dry biomass were determined to evaluate the cell growth in the nitrogen-limited medium. The *RtFAD2* and *RtFAD1+RtFAD2* transformants of L1-1 showed lower OD₆₀₀ value (172 ± 1 , 165 ± 2) than the wild-type L1-1 (200 ± 6) at 120 h (Fig. 4.3.4.1A). However, the *RtFAD2* expressing TK16 transformants showed higher OD₆₀₀ value than the wild-type TK16 (140 ± 5 , 109 ± 6), and there was no difference of OD₆₀₀ between the wild-type TK16 and its *RtFAD1+RtFAD2* transformant (109 ± 6 , 102 ± 2) at 120 h. The TK16 and L1-1

engineered strains did not display reduced biomass comparing to their wild-types in the nitrogen-limited medium (Fig. 4.3.4.1B). These data indicated that overexpression of *RtFAD2* and co-overexpression of *RtFAD1* and *RtFAD2* did not affect the cell mass in the nitrogen-limited

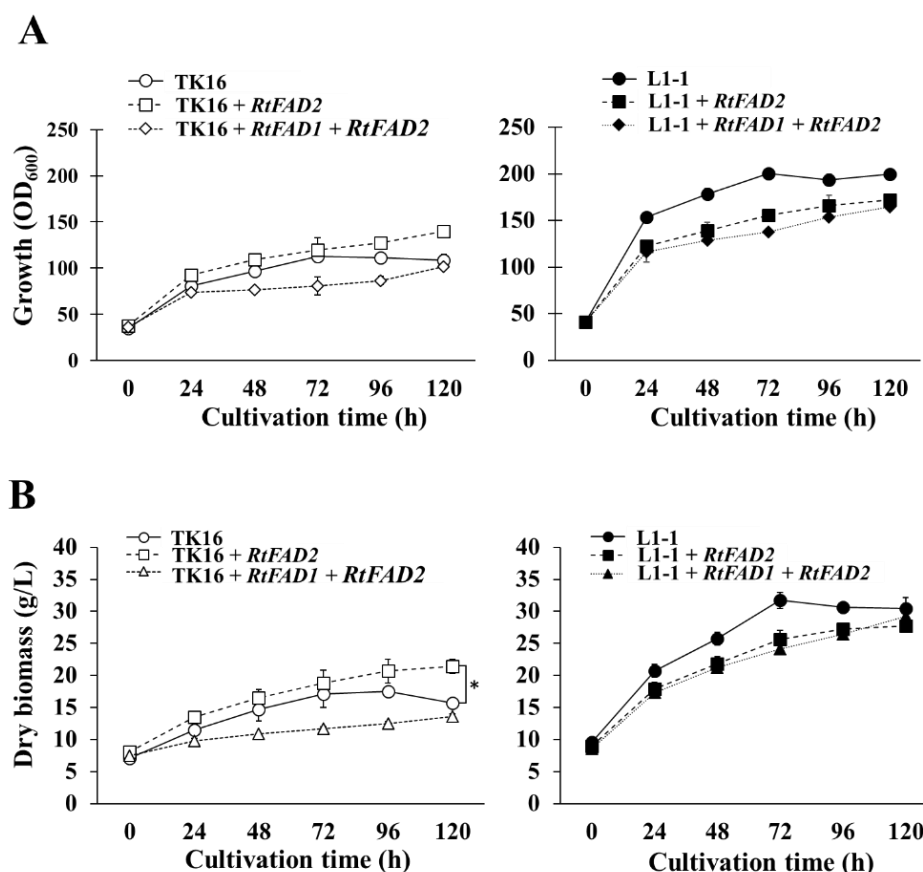


Fig. 4.3.4.1 Effects of *RtFAD2* overexpression and *RtFAD1*+*RtFAD2* co-overexpression on the growth in *R. toruloides* strains under nitrogen-limited conditions. Cell density was determined by OD₆₀₀. The dry biomass was freeze-dried and measured gravimetrically. A. Growth curve of the wild-type and all transformants. B. Dry biomass of the wild-type and all transformants. The present average and error bars were based on three independent measurements. The *p* values were determined by Student's *t*-test. **p*<0.05.

4.3.4.2 Lipid droplets of engineered strains in the nitrogen-limited medium

Next, the yeast cells were collected and stained with Sudan IV for lipid droplet examination at 0 and 120 h. After a 120-h cultivation, the cells of all strains accumulated

apparent lipid droplets. Additionally, the *RtFAD2* overexpressing and *RtFAD1+RtFAD2* co-overexpressing strains of TK16 and L1-1 displayed larger lipid droplets than the wild-type (Fig. 4.3.4.2). Therefore, these data demonstrated that the overexpression of *RtFAD2* and co-overexpression of *RtFAD1+RtFAD2* could increase lipid accumulation in *R. toruloides*.

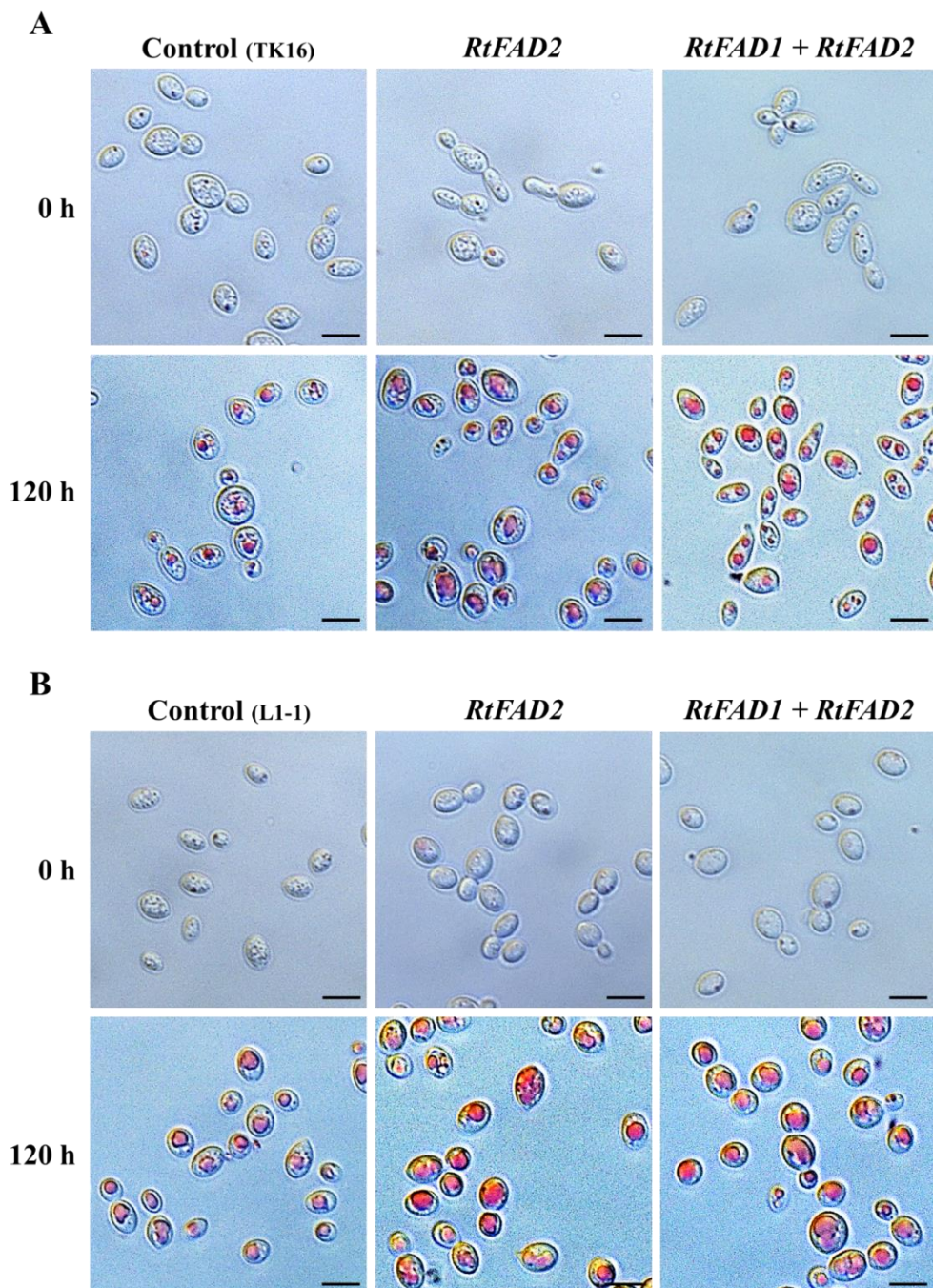


Fig. 4.3.4.2 Lipid droplets of the *R. toruloides* strains under nitrogen-limited

conditions. A and B. Observation of lipid droplet in the wild-type TK16, L1-1, and corresponding transformants. The lipid droplets were stained by Sudan IV, and the cells were observed at 0 and 120 h during the cultivation by a bright-field microscope. Scale bar: 5 μ m.

4.3.4.3 Lipid titers of the engineered strains in the nitrogen-limited medium

To evaluate the lipid production of each strain, the lipid titers were measured. The lipid titers of TK16, L1-1, and their transformants showed a stable phase from 72 h after inoculation. The *RtFAD2*-overexpressing TK16 produced the highest lipid titer (5.9 ± 0.9 g/L) among *RtFAD1+RtFAD2* and the TK16 wild-type (3.5 ± 0.2 , 2.5 ± 0.2) at 120 h. The *RtFAD2* transformant in L1-1 also generated the highest lipid titer (6.7 ± 0.7 g/L) among *RtFAD1+RtFAD2* strain and the L1-1 wild-type (6.0 ± 0.6 g/L, 4.5 ± 0.5 g/L) at 120 h. According to these data, although expressing *RtFAD2* and co-overexpressing *RtFAD1+RtFAD2* both enhanced the lipid titers, overexpressing *RtFAD2* gave the highest lipid titers in *R. toruloides* (Fig. 4.3.4.2).

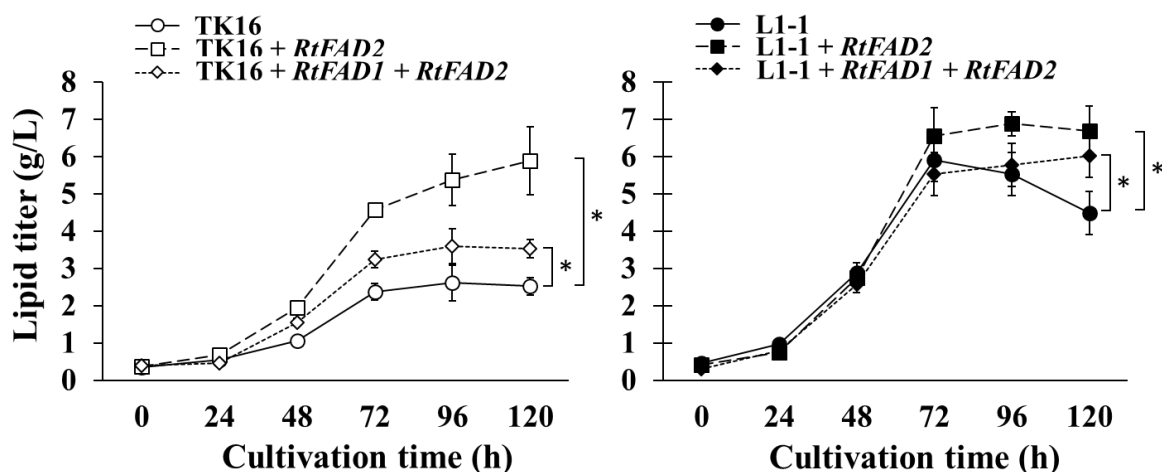


Fig. 4.3.4.3 Lipid titers of *RtFAD2* gene overexpression and *RtFAD1+RtFAD2* co-overexpression in *R. toruloides* strains under nitrogen-limited conditions. The lipid titer was presented as gram per liter of liquid culture. The present average and error bars of each data point were based on three independent measurements. The *p* values were determined by Student's *t*-test. **p*<0.05.

4.3.4.4 Lipid content of the engineered strains in the nitrogen-limited medium

Next, the lipid content of all the strains at each time point was further investigated. The *RtFAD2* overexpressing and *RtFAD1+RtFAD2* co-overexpressing strains of TK16 had similar lipid content ($27 \pm 2.8\%$ of DCW; $26.0 \pm 0.6\%$ of DCW) and were higher than that in the wild-type TK16 ($16.1 \pm 1.7\%$ of DCW) at 120 h (Fig. 4.3.4.4). The *RtFAD2* overexpressing L1-1 accumulated the highest lipid content ($24.2 \pm 2.0\%$ of DCW) than the L1-1 and *RtFAD1+RtFAD2* co-overexpressing strain ($14.8 \pm 0.8\%$, $20.4 \pm 2.0\%$ of DCW) at 120 h (Fig. 4.3.4.4). These results suggested that expressing *RtFAD2* and co-overexpressing *RtFAD1+RtFAD2* elevated the lipid accumulation in the studied strains. The *RtFAD2* overexpressing transformants of TK16 and L1-1 gave the highest lipid content ($27 \pm 2.8\%$ and $24.2 \pm 2.0\%$ of DCW).

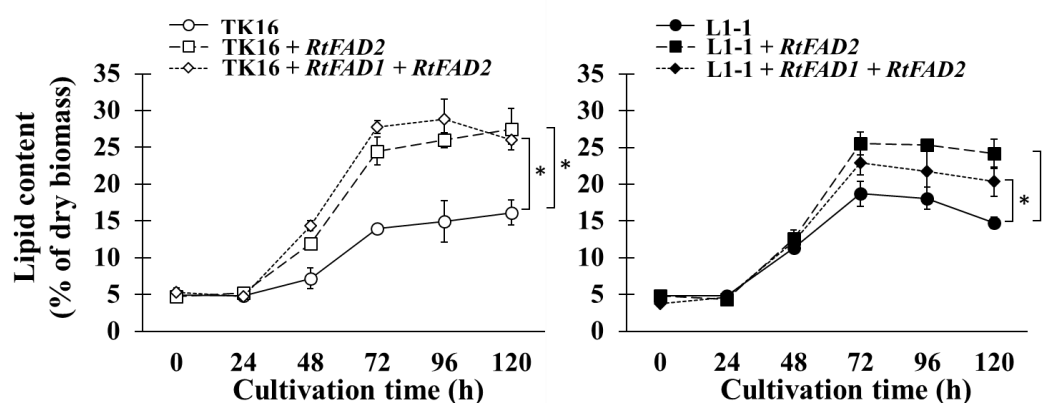


Fig. 4.3.4.4 Lipid content of *RtFAD2* gene overexpression and *RtFAD1+RtFAD2* co-expression in *R. toruloides* strains under nitrogen-limited conditions. The lipid content was presented as percent of dry biomass. The present average and error bars of each data point were based on three independent measurements. The *p* values were determined by Student's *t*-test. **p*<0.05.

4.3.5 *RtFAD2* overexpression significantly increased the LA production in *R. toruloides* strains

To assess the *RtFAD2* overexpressing and *RtFAD1+RtFAD2* co-overexpressing

effects on the fatty acid composition in total lipids in *R. toruloides*, I thus examined the fatty acid profile at the 120-h time point. The results of fatty acid analysis (Fig. 4.3.5A) revealed that the lipid produced in the *RtFAD2* overexpressing TK16 and L1-1 strains contained $28.1 \pm 0.9\%$ and $24.3 \pm 1.8\%$ LA of the total lipid which were higher than the wild-type TK16 and L1-1 ($14 \pm 2.7\%$, $18.8 \pm 1.3\%$ of total lipids) (Table 4.3.5 and Fig. 4.3.5 A). The OA contents of the *RtFAD2* overexpressing TK16 and L1-1 strains were decreased to $48.1 \pm 1.9\%$ and $47.5 \pm 1.9\%$ comparing to their corresponding wild-types (TK16, $57.2 \pm 4.7\%$; L1-1, $53.5 \pm 1.8\%$) (Table 4.3.5 and Fig. 4.3.5 A). These results indicated that the overexpression of *RtFAD2* increased the LA content by converting OA into LA.

Although co-overexpressing *RtFAD1* and *RtFAD2* in TK16 and L1-1 also contained higher LA percentage ($23.7 \pm 0.9\%$, $21.1 \pm 1.0\%$ of total lipids) than the wild-type (TK16, $14 \pm 2.7\%$; L1-1, $18.8 \pm 1.3\%$ of total lipids), the LA contents were slightly decreased in comparison to the *RtFAD2* expressing strains (TK16 + *RtFAD2*, $28.1 \pm 0.9\%$; L1-1 + *RtFAD2*; $24.3 \pm 1.8\%$) (Table 4.3.5 and Fig. 4.3.5). According to Fig. 4.3.5, the decreases of OA content with the increases of LA content in the *RtFAD1+RtFAD2* transformants were also observed in comparison to their original wild-types. *RtFAD1+RtFAD2* transformants were expected to have the higher LA content than the *RtFAD2* transformants because *RtFad1* could synthesize OA as substrate for LA synthesis by *RtFad2*. However, the data (Table 4.3.5 and Fig. 4.3.5A) demonstrated that the LA contents of *RtFAD1+RtFAD2* transformants were slightly lower than those in *RtFAD2* transformants.

The LA titers of *RtFAD2* overexpressing TK16 and L1-1 were at the same levels (1.7 ± 0.3 g/L, 1.6 ± 0.0 g/L), and 4.3-fold and 2-fold higher than those in the TK16 and L1-1 wild-type (0.4 ± 0.1 g/L, 0.8 ± 0.0 g/L). The LA titers of *RtFAD1+RtFAD2* co-overexpressing TK16 and L1-1 produced were also slightly decreased in comparison

to the *RtFAD2* overexpressing strains in TK16 and L1-1 (0.8 ± 0.0 g/L, 1.3 ± 0.3 g/L) (Fig. 4.3.5B). To sum up all the data of Table 4.3.5 and Fig. 4.3.5, overexpressing *RtFAD2* gave the best effects on enhancing LA production in this study.

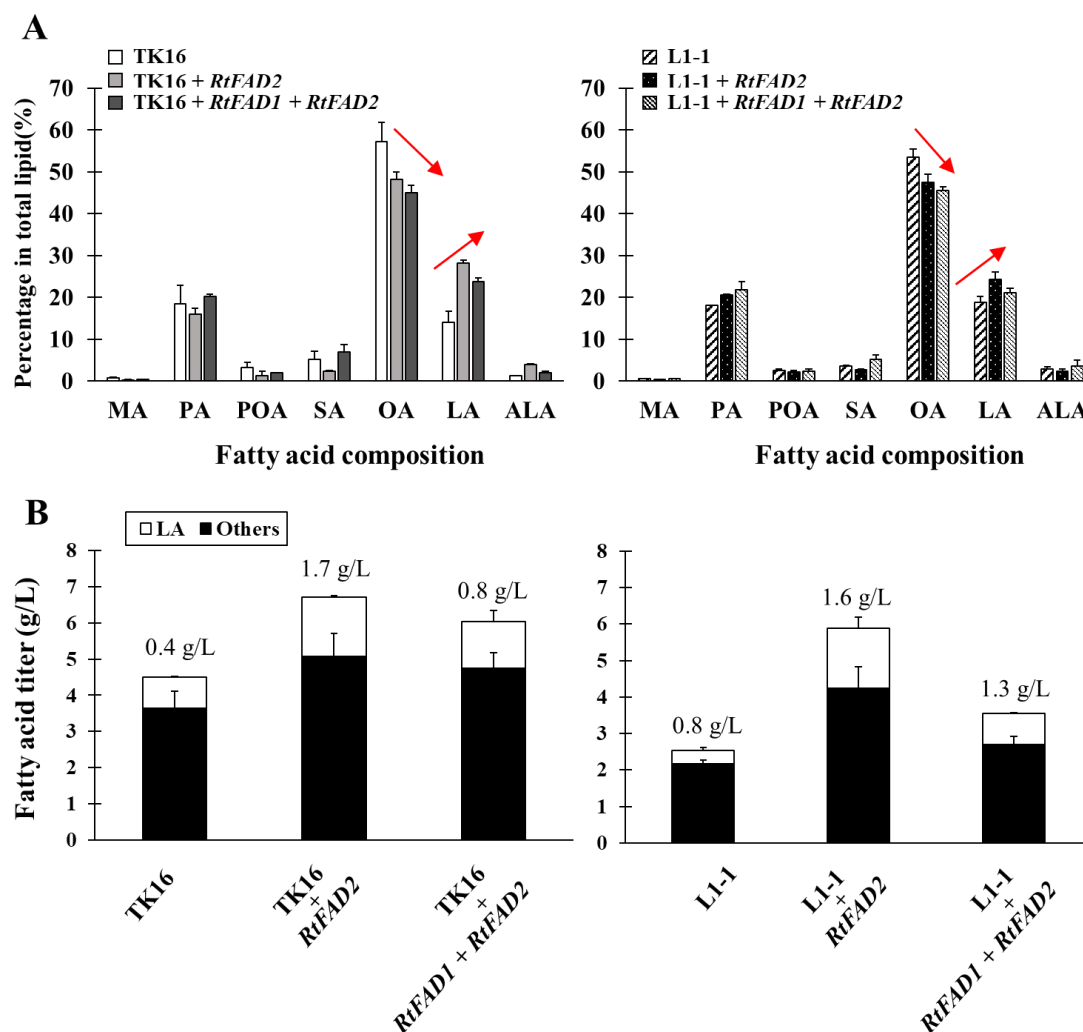


Fig. 4.3.5 Fatty acid profile and linoleic acid production in the *RtFAD2* overexpressing and *RtFAD1*+*RtFAD2* co-overexpressing transformants in *R. toruloides* strains under nitrogen-limited conditions. (A) Fatty acid composition of the wild-type TK16, L1-1 and corresponding transformants. The fatty acid composition is presented in the percentage in total lipids. Myristic acid, MA (C14:0); palmitic acid, PA (C16:0); palmitoleic acid, POA (C16:1); stearic acid, SA (C18:0); Oleic acid, OA (C18:1); linoleic acid, LA (C18:2); α -linolenic acid, ALA (C18:3). (B) LA titer in the total lipid at 120-h culture. The number with bar indicated the LA titers of each corresponding transformants. The present average and error bars were based on three independent measurements.

Table 4.3.5 Fatty acid composition of the transformants and wild-type strains after a 120 h-cultivation under nitrogen-limited conditions. The fatty acid composition is shown as a percentage (%) of total lipids. Myristic acid, MA (C14:0); palmitic acid, PA (C16:0); palmitoleic acid, POA (C16:1); stearic acid, SA (C18:0); Oleic acid, OA (C18:1); linoleic acid, LA (C18:2); α -linolenic acid, ALA (C18:3). The standard deviation of each data point was based on three independent measurements.

Strain	Fatty acid composition of total lipids (%)						
	MA	PA	POA	SA	OA	LA	ALA
TK16	0.7 \pm 0.2	18.4 \pm 4.4	3.3 \pm 1.2	5.2 \pm 2.0	57.2 \pm 4.7	14 \pm 2.7	1.2 \pm 0.0
TK16 + <i>RtFAD2</i>	0.3 \pm 0.1	15.9 \pm 1.5	1.3 \pm 1.1	2.4 \pm 0.2	48.1 \pm 1.9	28.1 \pm 0.9	3.9 \pm 0.1
TK16 + <i>RtFAD1</i> + <i>RtFAD2</i>	0.4 \pm 0.1	20.1 \pm 0.6	1.9 \pm 0.0	6.9 \pm 1.8	45.0 \pm 1.6	23.7 \pm 0.9	1.9 \pm 0.4
L1-1	0.5 \pm 0.0	18.1 \pm 0.1	2.6 \pm 0.2	3.5 \pm 0.3	53.5 \pm 1.8	18.8 \pm 1.3	2.9 \pm 0.5
L1-1 + <i>RtFAD2</i>	0.3 \pm 0.0	20.5 \pm 0.2	2.1 \pm 0.4	2.7 \pm 0.2	47.5 \pm 1.9	24.3 \pm 1.8	2.4 \pm 0.5
L1-1 + <i>RtFAD1</i> + <i>RtFAD2</i>	0.5 \pm 0.1	21.8 \pm 2.0	2.4 \pm 0.5	5.1 \pm 1.1	45.5 \pm 1.0	21.1 \pm 1.0	3.5 \pm 1.4

4.3.6 *RtFAD1* expression levels were suppressed in the *RtFAD1*+*RtFAD2* co-expressing transformants

I expected the co-expressing *RtFAD1* with *RtFAD2* would further enhance the LA production by elevating the precursor OA in cells. However, the co-expressing transformants did not show enhanced LA production in comparison to the *RtFAD2* expressing strains. I suspected that the enhanced LA might suppress the expression of *RtFAD1*. Bossie and Martin (1989) suggested that the LA could serve as a regulator to control the $\Delta 9$ -FAD expression levels in *S. cerevisiae*. Gonzalez and Martin (1996) clearly demonstrated a supplement of LA in growth medium rapidly decreased the half-life of $\Delta 9$ -FAD (*ScOLE1*) from 10 min to 2.5 min, and a 5'-exoribonuclease encoded by the *XRNI* was required for the rapid degradation of the *ScOLE1* transcript in *S. cerevisiae*. To elucidate the mechanism, the expression levels of introduced *RtFAD1* and *RtFAD2* in the co-expressing strains were examined by real-time PCR. The results indicated the *RtFAD1* levels were significantly decreased at the 120 h comparing to those at 0 h in the nitrogen-limited medium (Fig. 4.3.6). On the contrary, the expression

levels of *RtFAD2* were not significantly changed during the cultivations. These phenomena were observed in the TK16 and L1-1 transformants. Accordingly, co-overexpressing *RtFAD1* did not further increase the LA production which was due to the suppression of gene expression or mRNA instability. These results also suggested increased LA content may regulate the *RtFAD1* expression in *R. toruloides*.

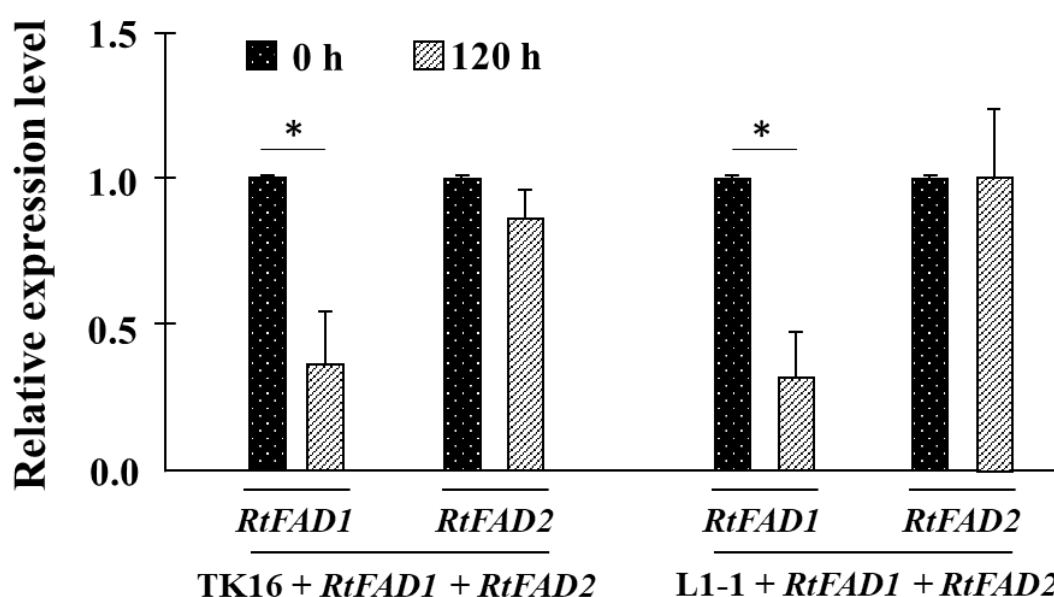


Fig. 4.3.6 Gene expression levels of introduced *RtFAD1* and *RtFAD2* in *RtFAD1+RtFAD2* co-expressing transformants under nitrogen-limited conditions. The gene expression levels of introduced co-expressed *RtFAD1* and *RtFAD2* in TK16 and L1-1 were examined by real-time PCR. The mRNA expression level was normalized with the internal control *RtURA3* gene. The average and SD of each data point was based on three independent measurements. The *p* values were determined by Student's *t*-test. **p*<0.05.

4.4 Discussion

4.4.1 Functions of *RtFad2*

RtFad2 of *R. toruloides* shared high identity and highly conserved $\Delta 12$ -Fad-like protein motifs among yeasts and fungi (Fig. 4.3.1.2). Notably, I also found that *RtFad2* shared 83.2% identity with the characterized *RkFad2* in *R. kratochvilovae* (Cui *et al.*

2016). *RkFad2* in *R. kratochvilovae* was shown to be a bifunctional $\Delta 12/\Delta 15$ Fad and can catalyze the synthesis reactions of LA and ALA. However, according to the results of heterologous expression in *S. cerevisiae* (Fig. 4.3.2), I found only the LA signal and did not observe a corresponding ALA signal. Furthermore, overexpressing the *RtFAD2* did not significantly increase ALA production in our *R. toruloides* strains (Table 4.3.5). As a consequence, my unambiguous results indicated that our target $\Delta 12$ -Fad from the *R. toruloides* NBRC8766 strain possessed the function of synthesizing only LA from the OA precursor.

4.4.2 Intracellular LA content affects the cell growth in *R. toruloides*

Overexpression of *RtFAD2* decreased the growth and changed the cell shapes of my two strains (Fig. 4.3.3.1 and Fig. 4.3.3.3.2). The same growth effects of expressing *RtFAD2* were also observed in different transformants (Fig. 4.3.3.1). Although the growth defect of *RtFAD2* overexpression in *R. toruloides* has not been reported, several studies have demonstrated that $\Delta 12$ -Fads, which controls polyunsaturated fatty acid levels in cells, affected cell growth at low temperature (below 20°C) in *Y. lipolytica* and *Rhodotorula* yeasts (Tezaki *et al.* 2018; He *et al.* 2015; Wang *et al.* 2017). Polyunsaturated fatty acids have been shown to increase the fluidity of the cell membrane and to affect cell integrity (Rodríguez-Vargas *et al.* 2007). Expression of *RtFads* in a recombinant *S. cerevisiae* strain has also been known to have a reduced growth rate (Rodríguez-Vargas *et al.* 2007). Accordingly I surmised that, although LA increased the membrane fluidity contributing to the adaptation to low temperature, the increased membrane fluidity resulted in difficulty maintaining cell shape and growth at room temperature. As Fig. 4.3.3.3.2 shows, in cells cultivated in YPD medium, we observed *RtFAD2* overexpressing TK16 and L1-1 strains displaying an elongated cell shape. To recover the growth of *RtFAD2*-overexpressing strains, *RtFAD1* was co-

overexpressed to lower the LA levels by elevating the OA ratio (Fig. 4.3.3.3.1). Lowering the LA levels by expression of *RtFAD1* slightly recovered the growth and cell shape of *RtFAD2*-overexpressing strains in TK16 and L1-1 (Fig. 4.3.3.3.3 and 4.3.3.3.2). Therefore, the present data implied that increased LA levels in *Rhodotorula* cells may affect cell growth by changing the membrane integrity.

4.4.3 Enzyme activity of *RtFad2*

Interestingly, as the culturing temperature was raised to 37°C, the defective growth in *RtFAD2*overexpressing L1-1 recovered (Fig. 4.3.3.1B). Compared to wild-type TK16, L1-1 can tolerate and grow at temperatures up to 37°C. Esteban *et al.* (2004) revealed that 40°C affected the enzyme activity of *CtFad2* in the plant *C. tinctorius*. Therefore, I considered that the recovery of defective growth in *RtFAD2* expressing L1-1 at 37°C resulted from the suppression of *RtFad2* enzyme activity. In addition, LA was rarely detected in TK16 or L1-1 at 37°C (Table 2.3.8B). These data indicated that 37°C indeed inhibited *RtFad2* activity. The present data may imply that elevated temperatures decreased the enzyme activity of *RtFad2* (Fig. 4.3.3.1B). Cui *et al.* (2016) demonstrated threefold expression levels of *RkFAD2* in *R. kratochvilovae* at 15°C compared to the control group at 28°C, hence the LA content was further increased from 14.7% to 24.5%. Cordova and Alper (2018) showed that expressing *YIFAD2* in *Y. lipolytica* under the control of a high-strength *Y. lipolytica* promoter slightly increased the LA content at 20°C compared to a control group at 28°C. Their results also implied that *YIFad2* probably has higher activity below 30°C. In the present study, *RtFAD2* was driven by constitutive promoter sequence *GPD1* and the transformants were cultivated at 30°C for lipid production. To further enhance LA content in *R. toruloides*, a low-temperature strategy may be implemented in the future.

4.4.4 Enhancement of lipid production by overexpression of C18 fatty acid desaturases

In the present study, overexpression of *RtFAD2* led to an increase in lipid contents and titers in *R. toruloides* strains (Fig. 4.3.4.3 and Fig. 4.3.4.4). A recent study by Yan *et al.* (2020) also discovered that overexpressing *YlFAD2* significantly increased the lipid contents and titers in model oleaginous yeast strain *Y. lipolytica*. I surmised that the overexpressed *RtFad2* further converted the OA precursor into LA, resulting in the enhancement of C18 fatty acid synthesis. Tsai *et al.* (2019) showed the highest lipid titer and content produced in the *RtFAD1*-expressing TK16 transformant were 3.2 g/L and 15%, respectively, but in the present study the *RtFAD2*-overexpressing TK16 transformant produced 5.8 g/L lipid titer and accumulated 27.5% lipid content. Accordingly, our results suggested that overexpressing *RtFAD2* increased lipid production in *R. toruloides* than did the expression of *RtFAD1*. The present study provides a metabolic engineering strategy for enhancing lipid production in *R. toruloides*.

4.4.5 Enhancement of LA production in *R. toruloides*

LAs were considered not only as alternative sources of oleochemical feedstocks for the production of biodegradable products such as lubricants and painting materials instead of petroleum-based products, but also as potential nutraceuticals for food industries (Ménégaud *et al.* 2019; Abdullah *et al.* 2016). However, the conventional sources for LA production from plant platforms are confined by long production cycles (Owuna *et al.* 2020). To satisfy the rising demand for LA, oleaginous yeast *R. toruloides* is perceived as a potentially promising host for competitive LA-rich lipid production from plant-based platforms due to its outstanding lipogenicity and ability to assimilate various cheap industrial by-products (Huang *et al.* 2013; Papanikolaou *et al.* 2017;

Tchakouteu *et al.* 2017). In recent years, several attempts have been made to explore the potential of LA production in *R. toruloides*. Wang *et al.* (2016) successfully enhanced the LA content and titer in the AS 2.1389 strain (27.5% in total lipids, 1.3 g/L) by introducing a heterologous *FvFAD2* from the fungus *F. verticillioides*. Herein, I achieved the elevation of LA contents and titers in two *R. toruloides* strains (TK16 and L1-1) by overexpression of *RtFAD2*. The LA contents of the TK16 and L1-1 strains were enhanced to nearly 2-fold and 1.3-fold (28% and 24% in total lipids), respectively, and the LA titers of TK16 and L1-1 were enhanced to nearly 4-fold and 2-fold (1.7 g/L and 1.6 g/L), respectively (Fig. 4.3.5). Therefore, the expression of native *RtFAD2* can not only increase lipid production but also generate LA-rich lipid. These findings could be applied to the engineering of *R. toruloides* for LA and PUFA production for food industries and other oleochemical industries.

4.4.6 Regulation of C18 fatty acid unsaturation pathway in *R. toruloides*

The highest production levels of lipid and LA were observed in the *RtFAD2*-expressing strains. In the LA synthesis pathway, OA is the precursor to LA production. Hence, we expected that co-overexpressing *RtFAD1* and *RtFAD2* would further enhance the lipid titer and LA production. Yan *et al.* (2020) co-expressed a mammalian *SCD* encoding a $\Delta 9$ -Fad with native *YIFAD2* in *Y. lipolytica* and successfully increased the lipid titer from 25% to 34% compared to the *YIFAD2*-expressing control. Their work showed opposite results to the present data. I suspected that LA negatively regulated the expression of native *RtFAD1*. Bossie and Martin (1989) suggested that LA could serve as a regulator of $\Delta 9$ -FAD (*ScOLE1*) expression levels in *S. cerevisiae*. Gonzalez and Martin (1996) clearly demonstrated that elevated LA content in cells decreased the stability of *ScOLE1* mRNA with a 5'-exoribonuclease encoded by the *XRNI* gene in *S. cerevisiae*. Therefore, the ratio of LA in yeast may be strictly regulated by tuning the

expression of $\Delta 9$ -FAD.

In the real-time PCR results (Fig. 4.3.6), the expression levels of *RtFAD1* were drastically decreased in the *RtFAD1+RtFAD2*-co-expressing strains in TK16 and L1-1 under lipid-accumulating conditions. This implied that LA may trigger the instability or degradation of *RtFAD1* mRNA in *R. toruloides*. Taking the previous and present results together (Fig. 4.3.6), I suggest that *RtFAD1* expression levels may be regulated by the LA content, leading to the suppression of LA production in *R. toruloides*. Yan *et al.* (2020) employed a mammalian $\Delta 9$ -FAD (*SCD*) rather than the native yeast gene, causing a further increase in lipid accumulation from 27.5% to 33.6% in *SCD* and the *Y1A12-FAD*-expressing strain compared to the *Y1FAD2*-expressing strain. Tsai *et al.* (2019) reported that overexpressing *RtFAD1* in the *R. toruloides* NP11 strain only slightly enhanced OA content to 62% in *R. toruloides*. However, my previous study (Wu *et al.* 2018) indicated that OA content of nearly 90% could be achieved in L1-1 at 37°C. So I hypothesized that 37°C could decrease *RtFad2* activity and lead to the reduction of LA content. Therefore, low LA content could not inhibit the expression levels of *RtFAD1* and high OA content could be achieved as described in Chapter 2. Therefore, Fig. 4.3.6 suggests that a cell's LA content may be regulated by decreasing the precursor OA via tuning the *RtFAD2* expression level (Fig. 4.4.5). In conclusion, I suggest that co-overexpressing *RtFAD2* with a heterologous $\Delta 9$ -FAD can probably further expand the limitation of LA production in *R. toruloides*.

Regulation of C18 FA synthesis

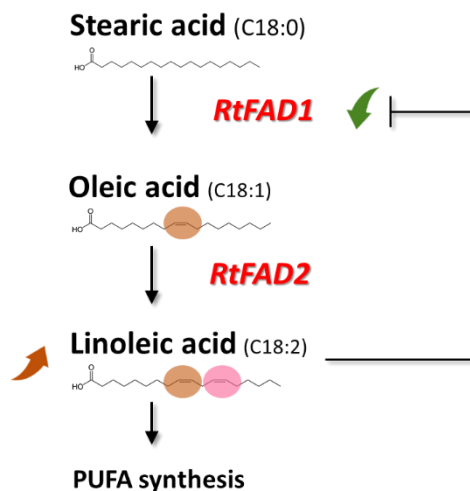


Fig. 4.4.5 Scheme of the putative mechanism of regulation of OA and LA ratio in *R. toruloides*.

4.4.6 Future perspectives

In this chapter, I successfully increased lipid production in two *R. toruloides* strains, TK16 and L1-1, by overexpressing *RtFAD2* and co-expressing *RtFAD1* and *RtFAD2*. Additionally, increased LA contents were also found in the strains overexpressing and co-overexpressing *RtFAD2*. Therefore, I considered that overexpressing *RtFAD2* may also be used to improve lipid production and LA-rich lipid production. Although LA-rich lipids are not ideal feedstocks for biodiesel production because they are prone to oxidation and thus can diminish the performance of biodiesel during long-term storage, LA-rich lipids are considered value-added feedstocks in food industries. Long-chain PUFAs (Lc-PUFAs), such as docosahexaenoic acid (DHA, 22:6, n-3) and eicosapentaenoic acid (EPA, 20:5, n-3), have beneficial effects on human health and are valuable FAs as nutraceuticals. These Lc-PUFAs can be synthesized from ω -3 fatty acids such as ALAs by a series of desaturation and elongation reactions (Patel *et al.* 2020). LA is the indispensable building block for ALA production and Lc-PUFA

synthesis. Fillet *et al.* (2017) successfully produced long-chain monounsaturated fatty acids by introducing plant-derived fatty acid elongases (3-ketoacyl-CoA synthases, KCS) in *R. toruloides*. Therefore, in the future it will be possible to harness *R. toruloides* for Lc-PUFA production by expressing other desaturases and elongases. The present work provides hints for metabolic engineering strategies to enhance LA as an indispensable block for Lc-PUCA production.

4.5 Summary: Overexpression of *RtFAD2* increased lipid production and LA content in thermotolerant L1-1

In this chapter, I sought to explore the lipid production of thermotolerant L1-1 by the overexpression of two genes that encode C18 fatty acid desaturases (*RtFAD1* and *RtFAD2*) from genome-open *R. toruloides* NBRC8766. Although the functions of *RtFAD1* have been identified, those of *RtFAD2* have been barely studied. Therefore, I first performed bioinformatics analysis and identified the functions of the *RtFAD2* gene by heterologous expression in *S. cerevisiae*. By overexpressing *RtFAD2* or co-overexpressing *RtFAD1+RtFAD2*, I increased the lipid production of thermotolerant L1-1. The metabolic engineering strategy of overexpressing *RtFAD2* in the studied strains (TK16 and L1-1) gave the highest lipid titer and lipid content. The real-time PCR results also suggested that enhanced LA amounts in cells might lead to the suppression of *RtFAD1* expression levels and result in the reduction of lipid production.

CHAPTER 5

General conclusions and discussion

The central goal of this dissertation was to establish and explore the utility of novel thermotolerant strain L1-1 of *R. toruloides* to overcome the limitations of lipid production under heat and multi-stress conditions. Additionally, the possibilities for increasing lipid production were further explored by the strategies of stress induction and metabolic engineering.

5.1 Summary of the work

I began by isolating a thermotolerant strain from oleaginous yeast *R. toruloides* DMKU3-TK16 by adaptive breeding at 37°C. In Chapter 2, I successfully isolated stable thermotolerant strain L1-1 from TK16. It was the first report of a thermotolerant *R. toruloides* strain. L1-1 exhibited improved thermotolerance compared to the wild-type strain TK16 at 37°C. The most important discovery is that L1-1 maintained its lipid-producing abilities at 37°C. The lipid titer of L1-1 at 37°C was 4.8-fold higher than that of wild-type TK16. Notably, the lipids produced by L1-1 at 37°C contained 86% OA, which is a preferable fatty acid for biodiesel production. Therefore, the thermotolerant L1-1 is a robust strain with strong potential. To date, the highest OA content was reported in an engineered *Y. lipolytica* that produced 90% OA of total lipid (Tsakraklides *et al.* 2018). Compared to the data of Tsakraklides's group, the natural L1-1 produced OA content (86%) comparable to that of their engineered *Y. lipolytica* strain. Therefore, L1-1 could be a potential platform to produce high-OA lipid for biodiesel production. Recently, a study of *Y. lipolytica* also tried to examine the lipid production of three *Y. lipolytica* strains at 35°C. In that research, the strains accumulated

10% to 25% lipid content in cells (Hackenschmidt *et al.* 2019). However, that study did not assess lipid production at higher temperatures. Therefore, L1-1 is the first reported oleaginous yeast strain that can produce lipid over 35°C.

To further explore the resistances and lipid production of L1-1 under other stresses, L1-1 stress responses and lipid production were examined under thermal (37°C), oxidative (ethanol and H₂O₂), high-osmotic (glucose and sorbitol), and DMSO-induced stress conditions. L1-1 displayed elevated resistances to thermal (37°C), oxidative (ethanol and H₂O₂), osmotic (glucose) and DMSO. By assessing L1-1's stress responses, I found that its abilities to maintain intracellular ROS were linked mainly to its multiple-stress tolerances. Ethanol-induced oxidative stress also increased lipid accumulation in L1-1; the lipid content of L1-1 reached nearly 40% of DCW under ethanol stress. The highest lipid titer in L1-1, 3 g/L, was induced by ethanol combined with H₂O₂. Aside from the elevated lipid production, the dual stresses of ethanol combined with DMSO or glucose stress conditions further induced the OA content in L1-1. In Chapter 3 I identified L1-1 as a multiple-stress-tolerant strain. Ethanol-induced oxidative stresses could trigger lipid accumulation and enhance OA content in L1-1.

In Chapter 4, I aimed to increase the lipid production of L1-1 by expressing two native C18 fatty acid desaturases, *RtFAD1* (encoding Δ 9-fatty acid desaturase) and *RtFAD2* (encoding Δ 12-fatty acid desaturase), from genome-opened strain *R. toruloides* NBRC8766. The functions of *RtFad2* were unknown in *R. toruloides*, so I first identified the encoding gene of *RtFAD2* in the genome database by bioinformatic analysis and its functions by heterologous expression in *S. cerevisiae*. The identified *RtFAD2* generated LA in *S. cerevisiae*. Overexpressing *RtFAD2* in the wild-type TK16 and L1-1 affected growth performance in nutrient medium for both strains, and the enzyme activity in both strains was reduced by raising the temperature to 37°C. Expressing *RtFAD2* in L1-1 had the strongest effect on increasing the lipid content (26.0

$\pm 0.6\%$ of DCW) and titer (6.7 ± 0.7 g/L) compared to the non-engineered L1-1 strain (lipid content: $14.8 \pm 0.8\%$ of DCW; lipid titer: 4.5 ± 0.5 g/L). In addition, the LA content of *RtFAD2* in L1-1 was elevated (2.4 g/L of total lipids) in comparison to the non-engineered L1-1 strain (19% of total lipids). To sum up the results in Chapter 4, the functions of *RtFad2* in *R. toruloides* NBRC8766 were identified and characterized, and its overexpression enhanced lipid production in the thermotolerant L1-1. Aside from lipid production, the enriched LA content in the lipids produced in L1-1 may imply that L1-1 could also produce polyunsaturated fatty acids that are potentially useful in the food and oleochemical industries.

5.2 Suggestions and future works

5.2.1 Revealing the stress-response genes by comparative analysis of genome sequencing, transcriptome and metabolomics in thermotolerant L1-1

The isolated novel L1-1 is the first report of thermotolerant strain in oleaginous yeast *R. toruloides*. Therefore, this strain is an ideal model to elucidate the stress-responses and lipid production under stress conditions. In this work, although the enhanced multi-stress tolerances and lipid production in thermotolerant L1-1 was discussed with the references of model yeast *S. cerevisiae*, the detailed mechanisms of gene-level and metabolomics level largely remained unknown in *R. toruloides*. *R. toruloides* is perceived as a potential strain for lipid production for biofuel and oleochemical industries. However, the basic and detailed studies of stress responses and lipid synthesis are largely lacking in *R. toruloides*. Therefore, it is necessary to further reveal the unknown relationships of stress responses and lipid synthesis to broaden the understanding in this yeast. So I suggest the comparative studies by examining the alteration of genome structure, gene expression and metabolomics in L1-1 should be performed in the future. The future studies may help us to design rational fermentation

strategies such as controlling the fatty acid profile of produced lipids or utilization of inhibitory carbon sources from industrial wastes, and make *R. toruloides* applicable in the practically industrial purposes.

5.2.2 Lipid production with industrial wastes in L1-1

The medium for lipid production by yeast accounts for 60–70% of the total production cost (Díaz *et al.* 2018). To lower the production cost of yeast-derived lipids from *R. toruloides* enough to compete economically with conventional plant oils or even petroleum oil, a large number of attempts have been made to use industrial wastes such as lignocellulosic biomass, crude glycerol, and waste water containing ethanol or acetic acid to produce low-cost lipids in *R. toruloides*. Although it has been proved that *R. toruloides* can use these cheap carbon sources, these industrial wastes were shown to inhibit the growth of *R. toruloides* strains. Consequently, I suggest that the utilization of these industrial wastes in L1-1 should be assessed, especially ethanol-containing wastes such as Sakekasu, which is a waste product from the fermentation of sake, a Japanese liquor. Future studies should strengthen the advantages of the L1-1 strain.

5.2.3 Expression of thermos-stable enzyme in the thermotolerant strain

In Chapter 4, I attempted to increase the lipid producing ability by overexpressing native *R. toruloides* desaturase encoding genes (*RtFAD1* and *RtFAD2*). Although I was considering to produce the lipids in L1-1 at 37°C, the enzyme activity of *RtFad2* were sensitive to elevated temperature at 37°C. As a consequence, the activity features of the expressed target enzyme confined the applications of thermotolerant L1-1 in industries. To explore the L1-1 as a platform used in industry to produce value-added compounds, the temperature ranges of the expressed enzymes in L1-1 should be considered. In the future, thermostable enzymes or enzymes with high activities at high temperatures

would be the promising targets for enhancing lipid producing abilities at high temperatures.

5.3 Future perspectives

Oleaginous yeast *R. toruloides* has been drawing much attention for its outstanding lipid-producing abilities and broad utilization of carbon sources and industrial wastes. Consequently, the lipids produced by *R. toruloides* are considered as alternative and sustainable feedstocks to replace the dominant plant oils and petroleum used in the fuel, food, and oleochemical industries. In this thesis, I isolated a robust and thermotolerant L1-1 strain that showed enhanced tolerances against various stresses and induced lipid production under heat (37°C) and oxidative (ethanol and H₂O₂) stresses. Metabolic engineering strategies were also employed to further increase lipid accumulation in the thermotolerant L1-1 strain. This work also discussed the stress responses of alterations of lipid synthesis in L1-1. The results could be applied to rational designs of fermentation processes. OA (C18 fatty acid) is the dominant fatty acid produced in *R. toruloides*, and it is a preferable feedstock for biodiesel production and a vital component in the synthesis of other valuable substances used in industries. This work also provided clues about the regulatory mechanisms in C18 fatty acid synthesis in *R. toruloides*. The knowledge gained here could be applied to rational designs in metabolic engineering for tailored lipid production in *R. toruloides*. Such efforts based on the present results would be beneficial for the development of green energy and renewable materials for a sustainable world.

6. MATERIALS AND METHODS

6.1 Strains and culture medium

R. toruloides DMKU3-TK16 was derived from the stock culture at the Department of Microbiology, Faculty of Science, Kasetsart University, Thailand (Kraisintu *et al.* 2010). The TK16 derived thermotolerant *R. toruloides* L1-1 was isolated in our lab by adaptive breeding (Wu *et al.* 2018). *R. toruloides* NBRC8766 obtained from the National Bioresource Research Center, NITE (Chiba, Japan) was used for gene isolation. Yeast strains were all freshened in 15% glycerol at -80°C as stocks. The yeast cells were routinely grown on yeast extract/malt extract (YM) agar plates (3 g/L yeast extract, 3 g/L malt extract, 5 g/L peptone, 10g /L dextrose, and 20 g/L agar) or extract/peptone/dextrose (YPD) medium (10 g/L yeast extract, 10 g/L peptone, 20 g/L dextrose) at 30°C for 3 days. The grown cells on plates were kept at 4°C for the following experiments. The *R. toruloides* strains were pre-cultured in YM or YPD medium and transferred into the nitrogen-limited broth (0.75 g/L yeast extract, 0.55 g/L $(\text{NH}_4)_2\text{SO}_4$, 0.4 g/L KH_2PO_4 , 2 g/L $\text{MgSO}_4\cdot 7\text{H}_2\text{O}$ and 70 g/L dextrose) for the experiments of lipid production. YPD agar plates and broth with 150 $\mu\text{g}/\text{mL}$ Zeocin or 100 $\mu\text{g}/\text{mL}$ hygromycin B were employed for transformant selection.

The auxotrophic strain *S. cerevisiae* BY23849 ($\text{MAT}\alpha$, $\text{leu}2\Delta 0$, $\text{ura}3\Delta 0$, $\text{his}3\Delta 1$, $\text{met}15\Delta 0$) strain from the National Bioresource Project-Yeast (NBRP-Yeast) was used for functional identification of *Δ12-FAD* gene from *R. toruloides* NBRC8766 (*RtFAD2*). *S. cerevisiae* transformants carrying pYES2 plasmid (Invitrogen, Massachusetts, USA) were grown on synthetic defined medium (SD) and SD agar plate (2% dextrose, 6.7 g/L yeast nitrogen base w/o amino acids, 3% agar, 20 mg/L histidine, 120 mg/L leucine, 60 mg/L lysine, 20 mg/L arginine, 20 mg/L tryptophan, 20 mg/L tyrosine, 40 mg/L

threonine, 20 mg/L methionine 50 mg/L phenylalanine, 20 mg/L uracil, and 20 mg/L adenine) without uracil supplement (SC-Ura) and selected on SD-Ura agar plates. Resultant transformants were grown in SD medium with 2% raffinose and 0.5% galactose for target protein expression in the heterologous expression experiments. *Escherichia coli* DH5 α was used for all the cloning and plasmid construction experiments.

6.2 Isolation of thermotolerant mutants from *R. toruloides* DMKU3-TK16

The wild-type TK16 was pre-cultured in 5 mL of YM broth at 30°C for 3 days with reciprocal shaking at 170 strokes per minute (spm) until stationary phase. The cultured cells were inoculated into 5 mL of YM broth cell dilution (OD₆₀₀ = 0.5) in a 20 mL-test tube and further cultivated at 37°C for another 3 days with reciprocal shaking at 170 spm as a selection step. The cultures from 37°C were re-inoculated into a fresh 5 mL of YM medium 30°C and grown for 3 days with reciprocal shaking at 170 spm as a recovery step. The repetition of the incubation at 37°C and recovery at 30°C were then repeated to allow the thermotolerant mutants to become dominant in the population. To evaluate the candidate mutants, the cells were serially diluted and spotted on YM plates, then incubated at 37°C for 4–5 days. The cultures that could form colonies on the YM plate at 37°C were considered as thermotolerant candidates. The single colony from the cultures of the candidate thermotolerants were preserved in 15% glycerol and stored at –80°C. The cultures which could not form colonies at 37°C on YM agar plates were diluted and re-inoculated into fresh YM broth and proceeded to the next round of selection until colonies could be observed after selection at 37°C.

6.3 Spot assay

Yeast cells were pre-cultivated in 5 mL of YM broth in a 20 mL test tube at 30°C

for 2 days with reciprocal shaking at 170 spm. Pre-cultured cells at log-phase were diluted and adjusted to OD₆₀₀ values of 1, 10⁻¹, 10⁻², 10⁻³, and 10⁻⁴ with sterilized water. Four microliters of diluted sample was spotted on YM plates containing 30 g/L ethanol, 1.5 mM H₂O₂, 250 g/L glucose, 180 g/L sorbitol, 60 g/L NaCl, or 40 g/L dimethyl sulfoxide (DMSO). The plates were incubated at assessed temperatures for 2–3 days. The YM plates for heat challenge were incubated at 37°C for 4–5 days.

6.4 Cell growth analysis in liquid medium

The cells were pre-cultivated in 5 mL of YPD or YM broth at 30°C for 24 h with reciprocal shaking at 220 spm. Then, the cell dilution [OD₆₀₀ = 0.1] was inoculated into 25 mL of YPD or YM broth in a 100 mL Erlenmeyer flask. The cells were pre-cultured in YM broth and then inoculated in YM broth in Chapter 2 and 3. In Chapter 4, the cells were pre-cultured in YPD broth and then inoculated in YPD broth. Afterward, the cultures were incubated at 30°C for 48 h with reciprocal shaking at 170 spm. The value of OD₆₀₀ was measured at set intervals until the growth reached the maximum OD₆₀₀ value. In Chapter 3, the cell dilution [OD₆₀₀ = 0.1] was inoculated into 5 mL of YM broth with 30 g/L ethanol, 4 mM H₂O₂, 250 g/L dextrose, 180 g/L sorbitol, 60 g/L NaCl, or 40 g/L DMSO in a 20 mL test tube. The cultures were incubated at 30°C for 48 h with orbital shaking at 240 rpm. The 37°C cultivation temperature was applied for the heat challenge samples.

6.5 Measurement of intracellular ROS

The intracellular ROS levels were evaluated by 2',7'-dichlorodihydrofluorescein diacetate (DCFH-DA) (Cayman Chemical, Ann Arbor, MI, USA). The cells cultivated under various stress conditions were collected and washed with distilled water twice. The cells were then suspended in PBS (pH 7.4) with 50 µM of DCFH-DA to an OD₆₀₀

of 1.0 and incubated at 30°C for 1 h. Cells without DCFH-DA treatment were used as background controls. After a 1 h incubation, the DCFH-DA-treated cells were collected and washed with PBS twice. The cells were then suspended in PBS to an OD₆₀₀ of 1.0. A 150 µL aliquot of the cell suspension was loaded onto a 96-well microtitration plate used for absorbance determination at a wavelength of 500 nm (Chen *et al.* 2010). The absorbance values were determined by using an iMark™ Microplate Reader (BioRad, Hercules, CA, USA). The absorbance values of the DCFH-DA-treated cells were subtracted from those of the background controls without DCFH-DA treatment.

6.6 Cell wall lytic enzyme susceptibility

The cell wall rigidity was evaluated by the susceptibility of cells to Uzukizyme (Wako, Osaka, Japan). The log-phase cells cultivated in YM broth at 30°C or 37°C after stress treatments were diluted to an OD₆₀₀ of 1.0. One milliliter of diluted culture was collected and washed with distilled water. The washed cells were then suspended in 1 mL of phosphate-buffered saline (PBS; 137 mM NaCl, 2.7 mM KCl, 10 mM Na₂HPO₄, 1.8 mM KH₂PO₄) (pH 5.0). The same volumes of suspended cells and Uzukizyme (22.7 mg/mL in PBS buffer) were mixed and incubated at 40°C. The cells of control groups without enzyme treatments in each experiment was incubated at 40°C. The value of OD₆₀₀ was measured at 1-h intervals for 4 h. The cell density is shown as the ratio of the OD₆₀₀ to that at time zero.

6.7 Lipid production

For lipid production, cells were firstly cultivated at nutrient medium for increase cell number, the cultivated cells were then transferred into the nitrogen-limited medium for lipid production. The detailed conditions of each experiments used in Chapter 2, 3, 4 were described below.

In Chapter 2, the cells were pre-cultivated into 50 mL of YM broth in a 300-mL flask and cultured at 30°C for 48 h with shaking at 170 rpm. The pre-cultivated cells were harvested and washed once with sterilized water. The washed pellets were transferred into 100 mL of nitrogen-limited medium in a 300-mL flask and incubated at various temperatures with shaking at 150 rpm. In Chapter 3, nitrogen-limited broth containing 30 g/L ethanol, 4 mM H₂O₂, 320 g/L glucose, 180 g/L sorbitol, 60 g/L NaCl, or 40 g/L DMSO was used for lipid production under different stress conditions. Evaluation of the lipid production of cells grown under dual and multiple-stress conditions was conducted in nitrogen-limited broth containing 30 g/L ethanol combined with 4 mM H₂O₂, 320 g/L dextrose, 180 g/L sorbitol, 60 g/L NaCl, or 40 g/L DMSO. The cells for the lipid production evaluation were pre-cultured in 5 mL of YPD broth with shaking at 220 spm for 24 h until the early stationary phase, and then the pre-cultured cells were harvested and resuspended in 5 mL of nitrogen-limited broth. The resuspended cells were cultivated at 30°C or 37°C with shaking at 220 spm for 120 h. In Chapter 4, the *R. toruloides* cells were pre-cultured cultivated in 5 mL of YM broth with shaking at 220 spm for 24 h until the early-stationary phase. All the cells were then transferred to 25 mL of YM medium and incubated at 30°C with agitation at 220 spm for 24 h. The cultured cells were then collected and washed with sterilized water once. Afterward, the washed cells were transferred into 25 mL of nitrogen-limited broth in a 100 mL e-flask at 30°C with reciprocal shaking at 220 spm for 120 h.

After being cultivated in nitrogen-limited medium, the grown cells were then harvested and washed with distilled water twice, and the cell pellets were freeze-dried until a constant weight was obtained. The dry biomass was determined gravimetrically, and cell density was measured by OD₆₀₀. The total lipids were extracted from the freeze-dried samples and quantified by a gas chromatograph equipped with a flame ionization detector (GC-FID).

6.8 Analysis of fatty acid composition

For fatty acid analysis, the freeze-dried cells were firstly rehydrated and suspended in 200 μ L of distilled water, and then 3.75 ml of a chloroform-methanol mixture (1:2 volume) was mixed with suspended cells. 1.25 mL of chloroform with internal standard heptadecanoic acid (C17:0) was then added to the mixture. Lastly, 1.25 mL of chloroform was mixed. The lipids in the chloroform layer were separated by mixing 1.25 mL distilled water and centrifugation. The chloroform was removed by vacuum. Extracted lipids were converted into fatty acid methyl esters by incubation with 1 mL of methanol with 6% (v/v) H₂SO₄ at 80°C for 3 h. The fatty acid methyl esters (FAMES) were extracted by mixing 1 mL of petroleum ether. Lastly, the fatty acid methyl ester samples were obtained by evaporation of the added petroleum ether.

The detailed conditions for FAME analysis are described as follows. In Chapter 2 and 3, the FAME samples were analyzed by a GC-353B gas chromatograph (GL Sciences, Tokyo) equipped with a flame ionization detector and a capillary column (60 m \times 0.25 mm \times 0.25 μ m, TC-70; GL Sciences). The constant pressure of carries gas helium was at 20 kPa. The injection and detection temperature were set to be 250 °C. The column temperature started at 120°C for 2 min and then increased by 20°C/min up to 160°C, where it remained for 2 min. The column temperature was then increased by 6°C/min until it reached 190°C for 1 min. At the last stage, the column temperature was increased to 220°C by 20°C/min, and it remained at 220°C for 2 min. The injector temperature was 250°C and the detector temperature was 250°C. The fatty acids were identified and quantified by comparing their retention times with the fatty acid methyl ester standard mixture. In Chapter 4, the FAME samples were analyzed by using a GC2014 system (Shimadzu, Kyoto, Japan) with a TC-70 capillary column (0.25 mm ID \times 60 m, film thickness 0.25 μ m; GL Sciences). Nitrogen was used as the carrier gas

with the constant pressure at 20 kPa. The column temperature was set to start at 120°C (2 min) then increased by 20°C /min up to 190°C (1 min) and 10°C/min up to 230°C (3 min). The temperature of the injector and the detector was set to be 250°C.

6.9 Lipid staining

The intracellular neutral lipids were stained by Sudan IV (Wako, Osaka, Japan), and the Sudan IV stock solution (2 mg/mL in isopropanol) was prepared for later experiments. The cells collected from the nitrogen-limited medium were washed with phosphate-buffered saline (PBS) (pH 7.4), and resuspended with 200 μ L of Sudan IV staining mixture (Sudan IV stock solution, PBS and DMSO in a ratio of 10:9:1, respectively). The samples were then incubated at 30°C for 40 min. Stained cells were collected and washed twice with 500 μ L of PBS. The washed cell pellets were then resuspended in 10% formaldehyde-PBS solution and incubated at 30°C for 30 min for fixation. The fixed cells were collected and washed with 500 μ L of PBS again and then resuspended in PBS buffer. The fixed cells were placed on a glass slide for further microscopy observation. Microscopy images were obtained with an Axioskop 2 microscope (Zeiss, Oberkochen, Germany).

6.10 Bioinformatics analysis

The amino acid sequences of Δ 9-Fads and Δ 12-Fads were retrieved from GenBank (National Center for Biotechnology Information, Bethesda, MD, USA). The phylogeny was reconstructed with MEGA X software (Kumar *et al.* 2018) by a neighbor-joining algorithm with bootstrap support from 1,000 replicates as a measure of statistical reliability. The retrieved amino acid sequences of various species were compared using multiple sequence alignment web server T-Coffee (<http://tcoffee.org.cat>).

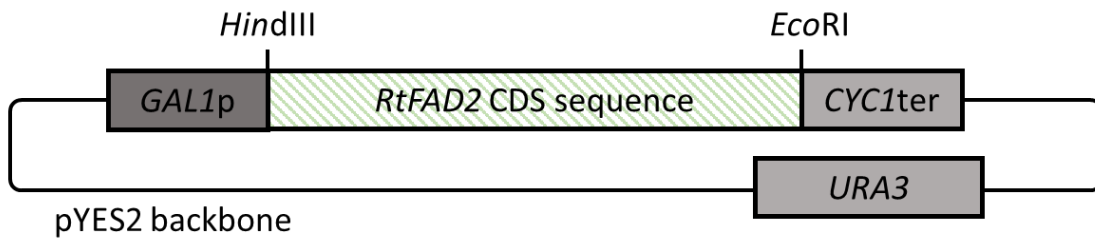
6.11 Plasmid construction

The genomic and gene coding sequence (CDS) of *RtFAD2* from *R. toruloides* NBRC8766 was cloned into pGEM T-Easy vectors from extracted genomic DNA and cDNA samples for the following experiments. The CDS of *RtFAD2* was amplified with the primers (RtFAD2-HindIII-F and RtFAD2-EcoRI-R) (Table 6.17) by PCR using KOD-Plus-NEO DNA polymerase (Toyobo, Osaka, Japan), and cloned into pYES2 vector under the control of *GALI* promoter. The constructed plasmid was then named pYES2-*RtFAD2* for functional identification in *S. cerevisie* (Fig. 6.11A and Table 6.17).

The expression cassette for target gene overexpression in *R. toruloides* strains was obtained from the previous study (Tsai *et al.* 2019). The genomic sequence of *RtFAD2* was prepared by the aforementioned PCR method with the primer pairs (RtFAD2-BglII-F and RtFAD2-NdeI-R) (Table 6.17) and ligated into the overexpression cassette in plasmid after restrictive enzyme digestion. The prepared plasmid was named pPGPD-ShBle-PGPD-genomic *RtFAD2*-TGPD (Table 6.17). For the *RtFAD1* and *RtFAD2* co-expression experiments, the PGPD-ShBle selective marker was replaced with a codon-optimized hygromycin resistant gene (*Hyg*) in a retrieved plasmid with overexpression cassette of genomic *RtFAD1* (pPGPD-ShBle-PGPD-g*RtFAD1*-TGPD). Briefly, the *Hyg* and *GPD1* promoter fragments were amplified by two primer pairs respectively (Hyg-NEB-F and Hyg-NEB-R; RtGPD1-NEB-F and RtGPD1-NEB-R) (Table 6.17), and assembly with a commercial NEBuilder® HiFi DNA Assembly Cloning Kit (NED, Massachusetts, United State). The resultant PGPD- SeHyg fragment was then cloned into pPGPD-ShBle-PGPD-g*RtFAD1*-TGPD to replace the PGPD-ShBle by *EcoRI* site. The resultant plasmid was then named pPGPD-Hyg-PGPD-g*RtFAD1*-TGPD (Table 6.17). The pPGPD-ShBle-PGPD-g*RtFAD1*-TGPD and pPGPD-Hyg-PGPD-g*RtFAD1*-

TGPD were used for preparing overexpression cassettes for target gene expression in *R. toruloides* strains (Fig. 6.11B).

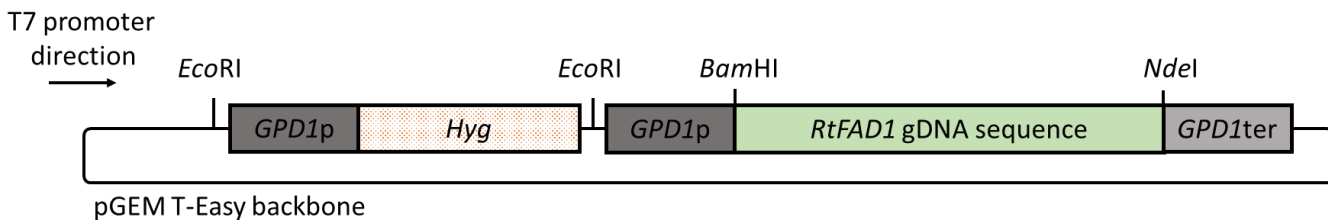
RtFAD2-pYES2 overexpression plasmid



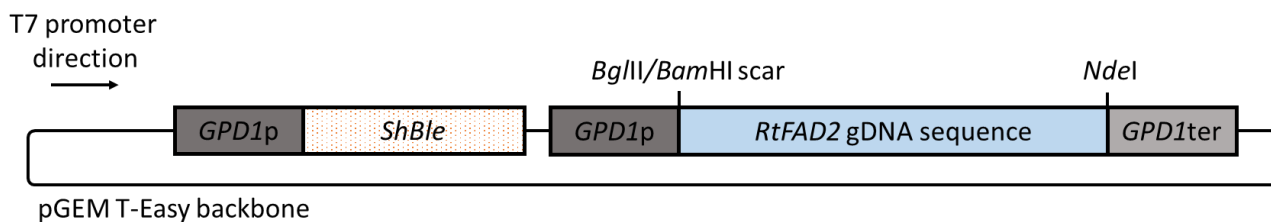
GAL1: *S. cerevisiae* galactokinase 1;
CYC1: *S. cerevisiae* cytochrome b-c1 complex subunit 4;
RtFAD2: *R. toruloides* Δ 12-fatty acid desaturase;
URA3: *S. cerevisiae* orotidine 5'-phosphate decarboxylase

Fig. 6.11A Construction of *RtFAD2* overexpression vector in pYES2 plasmid for heterologous expression in *S. cerevisiae*

RtFAD1 overexpression cassette in pGEM T-Easy plasmid



RtFAD2 overexpression cassette in pGEM T-Easy plasmid



GPD1: *R. toruloides* glycerol-3-phosphate dehydrogenase 1; **RtFAD1:** *R. toruloides* Δ 9-fatty acid desaturase;
ShBle: *S. hindustanus* Bleomycin resistant gene; **RtFAD2:** *R. toruloides* Δ 12-fatty acid desaturase;
Hyg: codon optimized hygromycin B resistant gene;

Fig. 6.11B 11 Constructions of *RtFAD1* and *RtFAD2* overexpression cassettes in pGEM T-easy vector for gene expression in *R. toruloides*.

6.12 Functional expression in *S. cerevisiae*

The *S. cerevisiae* BY23849 was transformed by a lithium acetate method (Kawai *et al.* 2010). Successful transformants were selected on SD-Ura agar plates and verified by PCR with extracted genome. All the resultant transformants were listed in Table 6.17. The yeast transformants were grown in 5 mL SD-Ura liquid medium at 30°C for 24 h with shaking at 170 rpm and then transfer to 5 mL SD-Ura liquid medium containing 20 g/L raffinose and 5 g/L galactose for further 72 h with shaking at 170 rpm at 30°C. The cultured yeast cells were harvested and washed twice using sterilized water. Total lipids of yeast cells were extracted, esterified and analyzed by GC-FID system.

6.13 Yeast transformation

The transformation method of *R. toruloides* strains was performed by a modified lithium acetate method (Tsai *et al.* 2018). Briefly, yeast cells were pre-cultured in 5 mL of YM broth at 30°C for 16 h at 170 rpm, and then the cell dilution [$OD_{600} = 1.0$] was inoculated into 25 mL of YM broth with 50 μ M of hydroxyl urea at 30°C for 3 h at 170 rpm. After 3 h-incubation, 4.5 mL of cultured cells were harvested and washed with Tris-EDTA (TE) buffer (10 mM Tris-HCl, pH 8.0, and 1 mM EDTA) once. The washed cells were then resuspended in 100 μ L of transformation mixture (35% polyethylene glycol-4000, 100 mM lithium acetate, 10 mM Tris-HCl at pH 4.9, and 1 mM EDTA) with a linear DNA fragment and 10% (*v/v*) DMSO. The transformation mixture was incubated without agitation at 30°C for 3 h and treated by heat shock at 37°C for 5 min. The treated mixture was cooled down to room temperature and recovered by the addition of 900 μ L of YPD broth. The recovered cells were cultured at 30°C for 16 h at 170 rpm. The 200 μ L of yeast cells were spread onto YPD agar plates containing 150 μ g/mL of Zeocin or 100 μ g/mL hygromycin B and incubated at 30°C for 2–3 days until the visible colonies appeared. Successful transformants were selected on agar plates with corresponding antibiotics and verified by PCR with extracted genome.

6.14 Real-time PCR analysis

The cells cultivated in nitrogen-limited medium at 30°C with shaking at 220 rpm were collected at 0 and 120 h. The total RNA was extracted by the phenol/chloroform method (Collart *et al.* 1993). cDNA was synthesized from extracted RNA by using a SuperScript IV VILO Master Mix (Invitrogen, Massachusetts, USA). Real-time quantitative PCR (qRT-PCR) was performed using Thunderbird SYBR qPCR Mix (Toyobo, Osaka, Japan) and StepOne™ Real-Time PCR System (Applied Biosystems, California, U.S.A.). All the primers used for qRT-PCR are listed in Table 6.17. Gene

expression data were analyzed using the comparative Ct ($\Delta\Delta\text{Ct}$) method (Livak *et al.* 2001). Gene expression ratios were normalized to internal control *RtURA3* gene using the $2^{-\Delta\Delta\text{Ct}}$ method and determined by the following equations: $\Delta\text{Ct} = \text{Ct}(\text{target gene}) - \text{Ct}(\textit{RtURA3})$.

Table 6.17 Strains for lipid production and primers for plasmid construction and real-time PCR

Strain or primer	Description (genotype/feature) or sequence (5'-3')	Source or feature
Strains		
NBRC8766	<i>R. toulouides</i> NBRC8766 (diploid)	NBRC collection
BY23849	<i>S. cerevisiae</i> BY23849 (<i>MATa, leu2Δ0 ura3Δ0 his3Δ1 met15Δ0</i>)	NBRP-Yeast collection
BY23849 + vector	BY23849/pYES2 empty vector	This study
BY23849 + <i>RtFAD2</i>	BY23849/pYES2- <i>RtFAD2</i>	This study
TK16	<i>R. toulouides</i> DMKU3-TK16	Kraisintu <i>et al.</i> , 2010
TK16 + <i>RtFAD2</i>	TK16/ <i>P_{GPD}-ShBle-P_{GPD}-gRtFAD2-T_{GPD}</i>	This study
TK16 + <i>RtFAD1</i> + <i>RtFAD2</i>	TK16/ <i>P_{GPD}-Hyg-P_{GPD}-gRtFAD1-T_{GPD}/P_{GPD}-ShBle-P_{GPD}-gRtFAD2-T_{GPD}</i>	This study
L1-1	<i>R. toulouides</i> L1-1	Wu <i>et al.</i> , 2018
L1-1 + <i>RtFAD2</i>	L1-1/ <i>P_{GPD}-Ble-P_{GPD}-gRtFAD2-T_{GPD}</i>	This study
L1-1 + <i>RtFAD1</i> + <i>RtFAD2</i>	L1-1/ <i>P_{GPD}-Hyg-P_{GPD}-gRtFAD1-T_{GPD}/P_{GPD}-ShBle-P_{GPD}-gRtFAD2-T_{GPD}</i>	This study
Primers		
<i>RtFAD2-HindIII-F</i>	GTT TTA AGC TTA TGG CCG CCA CCC TCC GCC A	Plasmid construction
<i>RtFAD2-EcoRI-R</i>	GTT TTG AAT TCC TAG AGT CCC TCG ACG CCC GAG	Plasmid construction
<i>RtFAD2-BglII-F</i>	GTT TTA GAT CTA TGG CCG CCA CCC TCC GCC A	Plasmid construction
<i>RtFAD2-NdeI-R</i>	GTT TTC ATA TGC TAG AGT CCC TCG ACG CCC GAG	Plasmid construction
<i>Hyg-NEB-F</i>	CCA GAT CAC TCA CAA ATG AAG AAG CCG GAG CTC	Plasmid construction
<i>Hyg-NEB-R</i>	GAA TTC ACT AGT GAT CTA CTC CTT GGC GCG	Plasmid construction
<i>RtGPD1-NEB-F</i>	ATC ACT AGT GAA TTC GCG GCG	Plasmid construction

<i>RtGPD1-NEB-R</i>	TTG TGA GTG ATC TGG TGT TGT TC	Plasmid construction
<i>RtURA3-qPCR-F</i>	ACG CAA TAA TGC TTG TGC AG	Real-time PCR
<i>RtURA3-qPCR-R</i>	AGC GAT CTC TCT CCC TCT CC	Real-time PCR
<i>RtFAD1-qPCR-F</i>	CCG GTT TCA TCC ACG ATG TCA GC	Real-time PCR
<i>RtFAD1-qPCR-R</i>	CTG AGA CCG CCC AAG AGG TTG GTT TC	Real-time PCR
<i>RtFAD2-qPCR-F</i>	GTC GTT CCG CAA CCC CAA G	Real-time PCR
<i>RtFAD2-qPCR-R</i>	CCA AAG GCG ACG AGG AGG	Real-time PCR

7. REFERENCES

1. **Abdel-Banat BM, Hoshida H, Ano A, Nonklang S, Akada R.** High-temperature fermentation: how can processes for ethanol production at high temperatures become superior to the traditional process using mesophilic yeast? *Appl Microbiol Biotechnol.* 2010;85: 861–7.
2. **Abdullah BM, Zubairi SI, Huri HZ, Hairunisa N, Yousif E, Basu RC.** Polyesters based on linoleic acid for biolubricant basestocks: low-temperature, tribological and rheological properties. *PLoS One.* 2016;11:e0151603.
3. **Adya AK, Canetta E, Walker GM.** Atomic force microscopic study of the influence of physical stresses on *Saccharomyces cerevisiae* and *Schizosaccharomyces pombe*. *FEMS Yeast Res.* 2006;6:120–8.
4. **Alishah AH, Rafiei N, Garcia-Granados R, Alemzadeh A, Morones-Ramírez JR.** Biomass and lipid induction strategies in microalgae for biofuel production and other applications. *Microb Cell Fact.* 2019;18:178.
5. **Anness BJ.** The reduction of dimethyl sulphoxide to dimethyl sulphide during fermentation. *J Inst Brew.* 1980;86:134–7.
6. **Anderson PJ, McNeil K, Watson K.** High-efficiency carbohydrate fermentation to ethanol at temperatures above 40°C by *Kluyveromyces marxianus* var. *marxianus* isolated from sugar mills. *Appl Environ Microbiol.* 1986;51:1314–20.
7. **Arous F, Jaouani A, Mechichi T.** Microbial wastewater treatment. *Elsevier Inc.* 2019;Chapter 8:153–174.
8. **Athenaki M, Gardeli C, Diamantopoulou P, Tchakouteu SS, Sarris D, Philippoussis A, Papanikolaou S.** Lipids from yeasts and fungi: physiology, production and analytical considerations. *J Appl Microbiol.* 2018;124:336–67.
9. **Auesukaree C.** Molecular mechanisms of the yeast adaptive response and tolerance to stresses encountered during ethanol fermentation. *J Biosci Bioeng.* 2017;124:133–42.
10. **Bai S, Wallis JG, Denolf P, Browse J.** Directed evolution increases desaturation of a cyanobacterial fatty acid desaturase in eukaryotic expression systems. *Biotechnol Bioeng.* 2016;113:1522–30.
11. **Banat IM, Nigram P, Marchant R.** Isolation of thermotolerant, fermentative yeasts growing at 52°C and producing ethanol at 45°C and 50°C. *World J Microbiol Biotechnol.* 1992;8:259–63.
12. **Bellou S, Triantaphyllidou IE, Aggeli D, Elazzazy AM, Baeshen MN, Aggelis**

- G.** Microbial oils as food additives: recent approaches for improving microbial oil production and its polyunsaturated fatty acid content. *Curr Opin Biotechnol.* 2016;37:24–35.
13. **Beney L, Gervais P.** Influence of the fluidity of the membrane on the response of microorganisms to environmental stresses. *Appl Microbiol Biotechnol.* 2001;57:34–42.
 14. **Bhatia SC.** Advanced Renewable Energy Systems. *Woodhead Publishing India.* 2014.
 15. **Bloom M, Evans E, Mouritsen OG.** Physical properties of the fluid lipid-bilayer component of cell membranes: a perspective. *Q Rev Biophys.* 1991;24:293–397.
 16. **Bossie MA, Martin CE.** Nutritional regulation of yeast Δ^9 -fatty acid desaturase activity. *J Bacteriol.* 1989;171:6409–13.
 17. **BP Statistical Review of World Energy.** BP statistical review of world energy 2019 (68th edition). British Petroleum Company, London. 2019.
 18. **Bravim F, de Freitas JM, Fernandes AA, Fernandes PM.** High hydrostatic pressure and the cell membrane: stress response of *Saccharomyces cerevisiae*. *Ann N Y Acad Sci.* 2010;1189:127–32.
 19. **Caspeta L, Nielsen J.** Thermotolerant yeast strains adapted by laboratory evolution show trade-off at ancestral temperatures and preadaptation to other stresses. *MBio.* 2015;6:e00431–15.
 20. **Cakar ZP, Seker UO, Tamerler C, Sonderegger M, Sauer U.** Evolutionary engineering of multiple-stress resistant *Saccharomyces cerevisiae*. *FEMS Yeast Res.* 2005;5:569–78.
 21. **Chen HH, Jiang JG.** Lipid accumulation mechanisms in auto- and heterotrophic microalgae. *J Agric Food Chem.* 2017;65:8099–110.
 22. **Christophe G, Kumar V, Nouaille R, Gaudet G, Fontanille P, Pandey A, Soccol CR, Larroche C.** Recent developments in microbial oils production: a possible alternative to vegetable oils for biodiesel without competition with human food? *Braz Arch Biol Technol.* 2012;55:29–46.
 23. **Cordova LT, Alper HS.** Production of α -linolenic acid in *Yarrowia lipolytica* using low-temperature fermentation. *Appl Microbiol Biot.* 2018;102:8809–16.
 24. **Cui J, He S, Ji X, Lin L, Wei Y, Zhang Q.** Identification and characterization of a novel bifunctional Δ^{12}/Δ^{15} -fatty acid desaturase gene from *Rhodospiridium kratochvilovae*. *Biotechnol Lett.* 2016;38:1155–64.
 25. **De Freitas JM, Bravim F, Buss DS, Lemos EM, Fernandes AA, Fernandes PM.** Influence of cellular fatty acid composition on the response of *Saccharomyces cerevisiae* to hydrostatic pressure stress. *FEMS Yeast Res.* 2012;12:871–8.

26. **Díaz ML, Cuppari S, Soresi D, Carrera A.** In silico analysis of fatty acid desaturase genes and proteins in grasses. *Appl Biochem Biotechnol.* 2018;184:484–99.
27. **Díaz T, Fillet S, Campoy S, Vázquez R, Viña J, Murillo J, Adrio JL.** Combining evolutionary and metabolic engineering in *Rhodospiridium toruloides* for lipid production with non-detoxified wheat straw hydrolysates. *Appl Microbiol Biotechnol.* 2018;102:3287–300.
28. **Dinh HV, Suthers PF, Chan SHJ, Shen Y, Xiao T, Deewan A, Jagtap SS, Zhao H, Rao CV, Rabinowitz JD, Maranas CD.** A comprehensive genome-scale model for *Rhodospiridium toruloides* IFO0880 accounting for functional genomics and phenotypic data. *Metab Eng Commun.* 2019;9:e00101.
29. **Dong T, Knoshaug EP, Pienkos PT, Laurens LML.** Lipid recovery from wet oleaginous microbial biomass for biofuel production: a critical review. *Appl. Energy.* 2016;177: 879–5.
30. **Dulermo T, Nicaud JM.** Involvement of the G3P shuttle and β -oxidation pathway in the control of TAG synthesis and lipid accumulation in *Yarrowia lipolytica*. *Metab Eng.* 2011;13:482–91.
31. **Esteban, AB, Sicardo MD, Mancha M, Martínez-Rivas JM.** Growth temperature control of the linoleic acid content in safflower (*Carthamus tinctorius*) seed oil. *J Agric Food Chem.* 2004;52:332–6.
32. **Fei Q, O'Brien M, Nelson R, Chen X, Lowell A, Dowe N.** Enhanced lipid production by *Rhodospiridium toruloides* using different fed-batch feeding strategies with lignocellulosic hydrolysate as the sole carbon source. *Biotechnol Biofuels.* 2016;9:130.
33. **Fickers P, Le Dall MT, Gaillardin C, Thonart P, Nicaud JM.** New disruption cassettes for rapid gene disruption and marker rescue in the yeast *Yarrowia lipolytica*. *J Microbiol Methods.* 2003;55:727–37.
34. **Fillet S, Ronchel C, Callejo C, Fajardo MJ, Moralejo H, Adrio J.** Engineering *Rhodospiridium toruloides* for the production of very long-chain monounsaturated fatty acid-rich oils. *Appl Microbiol Biotechnol.* 2017;101:7271–80.
35. **Gibson BR, Lawrence SJ, Leclaire JP, Powell CD, Smart KA.** Yeast responses to stresses associated with industrial brewery handling. *FEMS Microbiol Rev.* 2007;31:535e569.
36. **Gonzalez CI, Martin, CE.** Fatty acid-responsive control of mRNA stability. *J Biol Chem.* 1996;271:25801–09.

37. **Griel AE, Cao Y, Bagshaw DD, Cifelli AM, Holub B, Kris-Etherton PM.** A macadamia nut-rich diet reduces total and LDL-cholesterol in mildly hypercholesterolemic men and women. *J Nutr.* 2008;138:761–7.
38. **Guan N, Li J, Shin HD, Du G, Chen J, Liu L.** Microbial response to environmental stresses: from fundamental mechanisms to practical applications. *Appl Microbiol Biotechnol.* 2017;101:3991–4008.
39. **Guo M, Cheng S, Chen G, Chen J.** Improvement of lipid production in oleaginous yeast *Rhodospiridium toruloides* by ultraviolet mutagenesis. *Eng Life Sci.* 2019;9:548–56.
40. **Hackenschmidt S, Bracharz F, Daniel R, Thürmer A, Bruder S, Kabisch J.** Effects of a high-cultivation temperature on the physiology of three different *Yarrowia lipolytica* strains. *FEMS Yeast Res.* 2019;19:foz068.
41. **Hassan MH, Kalam MA.** An overview of biofuel as a renewable energy source: development and challenges. *Procedia Eng.* 2013;56:39–53.
42. **He J, Yang Z, Hu B, Ji X, Wei Y, Lin L, Zhang Q.** Correlation of polyunsaturated fatty acids with the cold adaptation of *Rhodotorula glutinis*. *Yeast.* 2015;32:683–90.
43. **Herrero E, Ros J, Bellí G, Cabisco E.** Redox control and oxidative stress in yeast cells. *Biochim Biophys Acta.* 2008;1780:1217–35.
44. **Hohmann S.** Osmotic stress signaling and osmoadaptation in yeasts. *Microbiol Mol Biol Rev.* 2002;66:300–72.
45. **Hu C, Zhao X, Zhao J.** Effects of biomass hydrolysis by-products on oleaginous yeast *Rhodospiridium toruloides*. *Bioresour Technol.* 2009;100:4843–7.
46. **Huang Q, Wang Q, Gong Z, Jin G, Shen H, Xiao S, Xie H, Ye S, Wang J, Zhao ZK.** Effects of selected ionic liquids on lipid production by the oleaginous yeast *Rhodospiridium toruloides*. *Bioresour Technol.* 2013;130:339–44.
47. **Huang XF, Liu JN, Lu LJ, Peng KM, Yang GX, Liu J.** Culture strategies for lipid production using acetic acid as sole carbon source by *Rhodospiridium toruloides*. *Bioresour Technol.* 2016;206:141–9.
48. **Indest KJ, Eberly JO, Hancock DE, Jung CM, Carr MR, Blakeney GA.** *Rhodococcus jostii* RHA1 TadA-homolog deletion mutants accumulate less polyhydroxyalkanoates (PHAs) than the parental strain. *J Gen Appl Microbiol.* 2016;62:213–16.
49. **Joshi RM, Pegg MJ.** Flow properties of biodiesel fuel blends at low temperatures. *Fuel.* 2007;86:143–51.
50. **Kamineni A, Shaw J.** Engineering triacylglycerol production from sugars in oleaginous yeasts. *Curr Opin Biotech.* 2020;62:239–47.
51. **Karamerou EE, Webb C.** Cultivation modes for microbial oil production using

- oleaginous yeasts – A review. *Biochem Eng J.* 2019;151:107322.
52. **Kitichantaropas Y, Boonchird C, Sugiyama M, Kaneko Y, Harashima S, Auesukaree C.** Cellular mechanisms contributing to multiple stress tolerance in *Saccharomyces cerevisiae* strains with potential use in high-temperature ethanol fermentation. *AMB Express.* 2016;6:1–14.
 53. **Klis FM, Boorsma A, De Groot PW.** Cell wall construction in *Saccharomyces cerevisiae*. *Yeast* 2006;23:185–202.
 54. **Knothe G.** Dependence of biodiesel fuel properties on the structure of fatty acid alkyl esters. *Fuel Process Technol.* 2005;86:1059–70.
 55. **Kraisintu P, Yongmanitchai W, Limtong S.** Selection and optimization for lipid production of a newly isolated oleaginous yeast, *Rhodospiridium toruloides* DMKU3-TK16. *Kasetsart J.* 2010;44:436–45.
 56. **Kumar S, Kushwaha H, Bachhawat AK, Raghava GP, Ganesan K.** Genome sequence of the oleaginous red yeast *Rhodospiridium toruloides* MTCC 457. *Genome Announc.* 2012;11:8.
 57. **Lahtvee PJ, Kumar R, Hallström BM, Nielsen J.** Adaptation to different types of stress converge on mitochondrial metabolism. *Mol Biol Cell.* 2016;27:2505–14.
 58. **Lamers D, van Biezen N, Martens D, Peters L, van de Zilver E, Jacobs-van Dreumel N, Wijffels RH, Lokman C.** Selection of oleaginous yeasts for fatty acid production. *BMC Biotechnol.* 2016;16:45.
 59. **Lapuerta M, Armas O, Rodríguez-Fernández J.** Effect of biodiesel fuels on diesel engine emissions. *Prog Energ Combust.* 2008;34:198–223.
 60. **Ledesma-Amaro R, Nicaud JM.** *Yarrowia lipolytica* as a biotechnological chassis to produce usual and unusual fatty acids. *Prog Lipid Res.* 2015;61:40–50.
 61. **Levin DE.** Regulation of cell wall biogenesis in *Saccharomyces cerevisiae*: the cell wall integrity signaling pathway. *Genetics.* 2011;189:1145–75.
 62. **Li Y, Zhao ZK, Bai F.** High-density cultivation of oleaginous yeast *Rhodospiridium toruloides* Y4 in fed-batch culture. *Enzyme Microb Technol.* 2007;41:312–7.
 63. **Liu Y, Koh CMJ, Ji L.** Bioconversion of crude glycerol to glycolipids in *Ustilago maydis*. *Bioresour Technol.* 2011;102:3927–33.
 64. **Liu Z, Feist AM, Dragone G, Mussatto SI.** Lipid and carotenoid production from wheat straw hydrolysates by different oleaginous yeasts. *J Clean Prod.* 2020;249:119308.
 65. **Los DA, Murata N.** Membrane fluidity and its roles in the perception of environmental signals. *Biochim Biophys Acta.* 2004;1666:142–57.
 66. **Ma Y, Liu Y.** Biofuels: Alternative feedstocks and conversion processes for the production of liquid and gaseous biofuels (2nd Edition). *Elsevier Inc.* 2019;Chapter

21:503–22.

67. **Mahan KM, Le RK, Yuan J, Ragauskas AJ.** A review on the bioconversion of lignin to microbial lipid with oleaginous *Rhodococcus opacus*. *J Biotechnol Biomater.* 2017;7:2.
68. **Makareviciene V, Sendzikiene E, Gumbyte M.** Application of simultaneous oil extraction and transesterification in biodiesel fuel synthesis: a review. *Energies.* 2020;13:2204.
69. **Maresca B, Kobayashi G.** Changes in membrane fluidity modulate heat shock gene expression and produced attenuated strains in the dimorphic fungus *Histoplasma capsulatum*. *Arch Med Res.* 1993;24:247–9.
70. **Ménégaud L, Jalil A, Thomas C, Masson D.** Macrophage fatty acid metabolism and atherosclerosis: the rise of PUFAs. *Atherosclerosis.* 2019;291:52–61.
71. **Navarro-Tapia E, Querol A, Pérez-Torrado R.** Membrane fluidification by ethanol stress activates unfolded protein response in yeasts. *Microb Biotechnol.* 2018;11:465–75.
72. **Owuna FJ, Dabai MU, Sokoto MA, Dangoggo SM, Bagudo BU, Birnin-Yauri UA, Hassan LG, Sada I, Abubakar AL, Jibrin MS.** Chemical modification of vegetable oils for the production of biolubricants using trimethylolpropane: a review. *Egypt J Pet.* 2020;25:75–82.
73. **Papanikolaou S, Aggelis G.** Lipids of oleaginous yeasts. Part I: Biochemistry of single cell oil production. *Eur J Lipid Sci Technol.* 2011;113:1031–51.
74. **Papanikolaou S, Kampisopoulou E, Blanchard F, Rondags E, Gardeli C, Koutinas AA, Chevalot I, Aggelis G.** Production of secondary metabolites through glycerol fermentation under carbon-excess conditions by the yeasts *Yarrowia lipolytica* and *Rhodospiridium toruloides*. *Eur J Lipid Sci Technol.* 2017;119:1600507.
75. **Park YK, Nicaud JM, Ledesma-Amaro R.** The engineering potential of *Rhodospiridium toruloides* as a workhorse for biotechnological applications. *Trends Biotechnol.* 2018;36:304–17.
76. **Pastor MM, Proft M, Pascual-Ahuir A.** Mitochondrial function is an inducible determinant of osmotic stress adaptation in yeast. *J Biol Chem.* 2009;284: 30307–17.
77. **Patel A, Karageorgou D, Rova E, Katapodis P, Rova U, Christakopoulos P, Matsakas L.** An Overview of potential oleaginous microorganisms and their role in biodiesel and omega-3 fatty acid-based industries. *Microorganisms.* 2020;8:434.
78. **Paul D, Magbanua Z, Arick M 2nd, French T, Bridges SM, Burgess SC, Lawrence ML.** Genome sequence of the oleaginous yeast *Rhodotorula glutinis* ATCC 204091. *Genome Announc.* 2014;13:e00046-14.

79. **Pedroso N, Matias AC, Cyrne L, Antunes F, Borges C, Malhó R, de Almeida RFM, Herrero E, Marinho HS.** Modulation of plasma membrane lipid profile and microdomains by H₂O₂ in *Saccharomyces cerevisiae*. *Free Radic Biol Med.* 2009;46:289–98.
80. **Pérez-Gallardo RV, Briones LS, Díaz-Pérez AL, Gutiérrez S, Rodríguez-Zavala JS, Campos-García J.** Reactive oxygen species production induced by ethanol in *Saccharomyces cerevisiae* increases because of a dysfunctional mitochondrial iron–sulfur cluster assembly system. *FEMS Yeast Res.* 2013;13:804–19.
81. **Pina C, Santos C, Couto JA, Hogg Tim.** Ethanol tolerance of five non-*Saccharomyces* wine yeasts in comparison with a strain of *Saccharomyces cerevisiae*—influence of different culture conditions. *Food Microbiol.* 2004;21:439–47.
82. **Polburee P, Limtong S.** Economical lipid production from crude glycerol using *Rhodospiridiobolus fluvialis* DMKU-RK253 in a two-stage cultivation under non-sterile conditions. *Biomass Bioenerg.* 2020;138:105597.
83. **Qazizada ME.** Design of a batch stirred fermenter for ethanol production. *Procedia Eng.* 2016;149:389–401.
84. **Qi F, Kitahara Y, Wang Z, Zhao X.** Novel mutant strains of *Rhodospiridium toruloides* by plasma mutagenesis approach and their tolerance for inhibitors in lignocellulosic hydrolysate. *J Chem Technol Biotechnol.* 2014;89:735–42.
85. **Qi F, Sun L, Zhang ML, Jiang XZ, Cao X, Huang JZ.** Alpha-linolenic acid production by the mutant *Rhodospiridium toruloides*. *Int J Food Eng.* 2016; 2:140–6.
86. **Quinn PJ, Joo F, Vigh L.** The role of unsaturated lipids in membrane structure and stability. *Prog Biophys Mol Biol.* 1989;53:71–103.
87. **Ralser M, Wamelink MMC, Latkolik S, Jansen EEW, Lehrach H, Jakobs C.** Metabolic reconfiguration precedes transcriptional regulation in the antioxidant response. *Nat Biotechnol.* 2009;27:604–5.
88. **Rizwanul-Fattah IM, Masjuki HH, Kalam MA, Hazrat MA, Masum BM, Imtenan S, Ashraful AM.** Effect of antioxidants on oxidation stability of biodiesel derived from vegetable and animal based feedstocks. *Renew Sust Energ Rev.* 2014;30:356–70.
89. **Rizwanul-Fattah IM, Masjuki HH, Kalam MA, Hazrat MA, Masum BM, Imtenan S, Ashraful AM.** Effect of antioxidants on oxidation stability of biodiesel derived from vegetable and animal based feedstocks. *Renew Sust Energ Rev.* 2014;30:356–70.

90. **Rodríguez-Vargas S, Sánchez-García A, Martínez-Rivas JM, Prieto JA, Randez-Gil F.** Fluidization of membrane lipids enhances the tolerance of *Saccharomyces cerevisiae* to freezing and salt stress. *Appl Environ Microbiol.* 2007;73:110–6.
91. **Sadowska-Bartosz I, Pączka A, Moloń M, Bartosz G.** Dimethyl sulfoxide induces oxidative stress in the yeast *Saccharomyces cerevisiae*. *FEMS Yeast Res.* 2013;13:820–30.
92. **Satomura A, Katsuyama Y, Miura N, Kuroda K, Tomio A, Bamba T, Fukusaki E, Ueda M.** Acquisition of thermotolerant yeast *Saccharomyces cerevisiae* by breeding via stepwise adaptation. *Biotechnol Prog.* 2013;29:1116–23.
93. **Schulze U, Lidén G, Nielsen J, Villadsen J.** Physiological effects of nitrogen starvation in an anaerobic batch culture of *Saccharomyces cerevisiae*. *Microbiology.* 1996;142:2299–310.
94. **Selvaraj R, Praveenkumar R, Moorthy IG.** A comprehensive review of biodiesel production methods from various feedstocks. *Biofuels.* 2019;10:325–33.
95. **Semchyshyn HM, Lozinska LM.** Fructose protects baker's yeast against peroxide stress: potential role of catalase and superoxide dismutase. *FEMS Yeast Res.* 2012;12:761–73.
96. **Shi K, Gao Z, Shi TQ, Song P, Ren LJ, Huang H, Ji XJ.** Reactive oxygen species-mediated cellular stress response and lipid accumulation in oleaginous microorganisms: the state of the art and future perspectives. *Front Microbiol.* 2017;8:793.
97. **Shomal R, Hisham H, Mlhem A, Hassan R, Al-Zuhair S.** Simultaneous extraction–reaction process for biodiesel production from microalgae. *Energy Rep.* 2019;5:37–40.
98. **Soccol CR, Neto CJD, Soccol VT, Sydney EB, da Costa ESF, Medeiros ABP, de Souza Vandenberghe LP.** Pilot scale biodiesel production from microbial oil of *Rhodospiridium toruloides* DEBB 5533 using sugarcane juice: Performance in diesel engine and preliminary economic study. *Bioresour Technol.* 2017;223:259–68.
99. **Spagnuolo M, Yaguchi A, Blenner M.** Oleaginous yeast for biofuel and oleochemical production. *Curr Opin Ciotech.* 2019;57:73–81.
100. **Sreeharsha RV, Mohan SV.** Obscure yet promising oleaginous yeasts for fuel and chemical production. *Trends Biotechnol.* 2020;in press.
101. **Stanley D, Bandara A, Fraser S, Chambers PJ, Stanley GA.** The ethanol stress response and ethanol tolerance of *Saccharomyces cerevisiae*. *J Appl Microbiol.* 2010;109:13–24.

102. **Stukey JE, McDonough VM, Martin CE.** The *OLE1* gene of *Saccharomyces cerevisiae* encodes the delta 9 fatty acid desaturase and can be functionally replaced by the rat stearoyl-CoA desaturase gene. *J Biol Chem.*1990;265:20144–9.
103. **Swan TM, Watson K.** Stress tolerance in a yeast lipid mutant: membrane lipids influence tolerance to heat and ethanol independently of heat shock proteins and trehalose. *Can J Microbiol.* 1999;45:472–9.
104. **Tan SX, Lim S, Ong HC, Pang YL.** State of the art review on development of ultrasound-assisted catalytic transesterification process for biodiesel production. *Fuel.* 2019;235:886–907.
105. **Tchakouteu SS, Kopsahelis N, Chatzifragkou A.** *Rhodospiridium toruloides* cultivated in NaCl-enriched glucose-based media: Adaptation dynamics and lipid production. *Eng Life Sci.* 2017;17:237–48.
106. **Tezaki S, Iwama R, Kobayashi S, Shiwa Yuh.** Δ 12-fatty acid desaturase is involved in growth at low temperature in yeast *Yarrowia lipolytica*. *Biochem Biophys Res Commun.* 2017;488:165–170.
107. **Thapa R, Carrero-Colon M, Crowe M, Gaskin E, Hudson K.** Novel *FAD2*–1A alleles confer an elevated oleic acid phenotype in soybean seeds. *Crop Sci.* 2016;56:226–31.
108. **Tsai YY, Ohashi T, Wu CC, Bataa D, Misaki R, Savitree L, Fujiyama K.** Delta-9 fatty acid desaturase overexpression enhanced lipid production and oleic acid content in *Rhodospiridium toruloides* for preferable yeast lipid production. *J Biosci Bioeng.* 2019;127:430–40.
109. **Tsakraklides V, Kamineni A, Consiglio AL, MacEwen K, Friedlander J, Blitzblau HG, Hamilton MA, Crabtree DV, Su A, Afshar J, Sullivan JE, LaTouf WG, South CR, Greenhagen EH, Shaw AJ, Brevnova EE.** High-oleate yeast oil without polyunsaturated fatty acids. *Biotechnol Biofuels.* 2018;11:131.
110. **Uprety BK, Dalli SS, Rakshit SK.** Bioconversion of crude glycerol to microbial lipid using a robust oleaginous yeast *Rhodospiridium toruloides* ATCC 10788 capable of growing in the presence of impurities. *Energ Convers Manage.* 2017; 135:117–28.
111. **Vasconcelos B, Teixeira JC, Dragone G, Teixeira JA.** Oleaginous yeasts for sustainable lipid production—from biodiesel to surf boards, a wide range of “green” applications. *Appl Microbiol Biotechnol.* 2019;103:3651–67.
112. **Vázquez J, Grillitsch K, Daum G, Mas A, Beltran G, Torija MJ.** The role of the membrane lipid composition in the oxidative stress tolerance of different wine yeasts. *Food Microbiol.* 2019;78:143–54.
113. **Verma P, Sharma MP, Dwivedi G.** Evaluation and enhancement of cold flow

- properties of palm oil and its biodiesel. *Energy Reports*. 2006;2:8–13.
114. **Vicente G, L. Bautista F, Rodríguez R, Javier Gutiérrez F.** Biodiesel production from biomass of an oleaginous fungus. *Biochem Eng J*. 2009;48:22–7.
 115. **Wallace-Salinas V, Gorwa-Grauslund MF.** Adaptive evolution of an industrial strain of *Saccharomyces cerevisiae* for combined tolerance to inhibitors and temperature. *Biotechnol Biofuels*. 2013;6:151.
 116. **Wang F, Gao B, Huang L, Su M, Dai C, Zhang C.** Evaluation of oleaginous eustigmatophycean microalgae as potential biorefinery feedstock for the production of palmitoleic acid and biodiesel. *Bioresour Technol*. 2018;270:30–7.
 117. **Wang J, Chen W, Nian H, Ji X, Lin L, Wei Y, Zhang Q.** Inhibition of polyunsaturated fatty acids synthesis decreases growth rate and membrane fluidity of *Rhodospiridium kratochvilovae* at low temperature. *Lipids*. 2017;52:729–35.
 118. **Wang Y, Zhang S, Pötter M, Sun W, Li L, Yang X, Jiao X, Zhao ZK.** Overexpression of $\Delta 12$ -fatty acid desaturase in the oleaginous yeast *Rhodospiridium toruloides* for production of linoleic acid-rich lipids. *Appl Biochem Biotechnol*. 2016;180:1497–507.
 119. **Welters HJ, Diakogiannaki E, Mordue JM, Tadayyon M, Smith SA, Morgan NG.** Differential protective effects of palmitoleic acid and cAMP on caspase activation and cell viability in pancreatic beta-cells exposed to palmitate. *Apoptosis*. 2006;11:1231–38.
 120. **Wiebe MG, Koivuranta K, Penttilä M, Ruohonen L.** Lipid production in batch and fed-batch cultures of *Rhodospiridium toruloides* from 5 and 6 carbon carbohydrates. *BMC Biotechnol*. 2012;12:26.
 121. **Wong L, Holdridge B, Engel J, Xu P.** Genetic tools for streamlined and accelerated pathway engineering in *Yarrowia lipolytica*. *Methods Mol Biol*. 2019;1927:155–77.
 122. **Wu CC, Ohashi T, Tsai YY, Misaki R, Savitree L, Fujiyama K.** Isolation of a thermotolerant *Rhodospiridium toruloides* DMKU3-TK16 mutant and its fatty acid profile at high temperature. *FEMS Microbiol Lett*. 2018;365:fny203.
 123. **Wu S, Hu C, Jin G, Zhao X, Zhao ZK.** Phosphate-limitation mediated lipid production by *Rhodospiridium toruloides*. *Bioresour Technol*. 2010;101:6124–9.
 124. **Wu S, Zhao X, Shen H, Wang Q, Zhao ZK.** Microbial lipid production by *Rhodospiridium toruloides* under sulfate-limited conditions. *Bioresour Technol*. 2011;102:1803–7.
 125. **Yan FX, Dong GR, Qiang S, Niu YJ, Hu CY, Meng YH.** Overexpression of $\Delta 12$, $\Delta 15$ -Desaturases for enhanced lipids synthesis in *Yarrowia lipolytica*. *Front Microbiol*. 2020;11:289.
 126. **Zhang M, Shi J, Jiang L.** Modulation of mitochondrial membrane integrity and

- ROS formation by high temperature in *Saccharomyces cerevisiae*. *Electron J Biotechnol*. 2015;18:202–9.
127. **Zhang S, Ito M, Skerker JM, Arkin AP, Rao CV.** Metabolic engineering of the oleaginous yeast *Rhodospiridium toruloides* IFO0880 for lipid overproduction during high-density fermentation. *Biomass Bioenerg*. 2016;100:9393–405.
128. **Zhang S, Skerker JM, Rutter CD, Maurer MJ, Arkin AP, Rao CV.** Engineering *Rhodospiridium toruloides* for increased lipid production. *Biotechnol Bioeng*. 2016;113:1056–66.
129. **Zhang X, Liu M, Zhang X, Tan T.** Microbial lipid production and organic matters removal from cellulosic ethanol wastewater through coupling oleaginous yeasts and activated sludge biological method. *Bioresour Technol*. 2018;267:395–400.
130. **Zhao X, Hu C, Wu S, Shen H, Zhao ZK.** Lipid production by *Rhodospiridium toruloides* Y4 using different substrate feeding strategies. *J Ind Microbiol Biotechnol*. 2011;38:627–32.
131. **Zhao X, Wu S, Hu C, Wang Q, Hua Y, Zhao ZK.** Lipid production from Jerusalem artichoke by *Rhodospiridium toruloides* Y4. *J Ind Microbiol Biotechnol*. 2010;37:581–5.
132. **Zhou W, Wang H, Chen L, Cheng W, Liu T.** Heterotrophy of filamentous oleaginous microalgae *Tribonema minus* for potential production of lipid and palmitoleic acid. *Bioresour Technol*. 2017;239:250–7.
133. **Zhu Z, Zhang S, Liu H, Shen H, Lin X, Yang F, Zhou YJ, Jin G, Ye M, Zou H, Zhao ZK.** A multi-omic map of the lipid-producing yeast *Rhodospiridium toruloides*. *Nat Commun*. 2012;3:1112.

8. ACKNOWLEDGEMENTS

I would like to express my deep gratitude to Prof. Fujiyama, my research supervisor and mentor, for his continuous guidance, enthusiastic encouragement, constructive critiques of my research work and endless supports throughout my life in Osaka. Without his sincere help, I may not go so far to this moment.

Next, I would present my grateful appreciation to Prof. Honda and Prof. Matsuda for being my committee members. Without their critical comments and constructive suggestions on my thesis, I could not see the weak points in my thesis and improve it so much. I would also like to thank Dr. Ohashi, for his tireless advice and selfless assistance in keeping my progress on schedule. I learned a lots precious attitudes from him in scientific writing and presentation skills.

My grateful thanks are also extended to Dr. Kajiura and Dr. Misaki for their helpful support in my experiments and constructive suggestions on my research work. I would also like to extend my appreciation to all the members of Fujiyama laboratory for offering their valuable help and giving me unforgettable memories in my life. Herein, I would like to present my appreciation to Prof. Savitree as well for her kind and constructive suggestions on my publications. I also want to thank Prof. Honda and Dr. Saito for their generosity of offering me experimental machines and experimental information. Also, I would like to thank Japan-Taiwan Exchange Association (公益財団法人日本台湾交流協会) and Japan Student Services Organization (独立行政法人日本学生支援機構) for their financial support.

Lastly, the special thanks would definitely go to my family who always support me and being my emotional anchor even we are apart from each other.

To those that see this: Thanks for reading my thesis!

9. RESEARCH ACHIEVEMENTS

9.1 Publications:

Present studies

1. **Wu CC, Ohashi T, Tsai YY *et al.*** Isolation of a thermotolerant *Rhodospiridium toruloides* DMKU3-TK16 mutant and its fatty acid profile at high temperature. *FEMS Microbiol Lett.* 2018;365:fny203.
2. **Wu CC, Ohashi T, Misaki R, *et al.*** Ethanol and H₂O₂ stresses enhance lipid production in an oleaginous *Rhodotorula toruloides* thermotolerant mutant L1-1. *FEMS Yeast Res.* 2020;20:foaa030.
3. **Wu CC, Ohashi T, Kajiura H *et al.*** Functional characterization and overexpression of Δ 12-desaturase in the oleaginous yeast *Rhodotorula toruloides* for production of linoleic acid-rich lipids. *J Biosci Bioeng.* 2021(in press).

Related study

1. **Tsai YY, Ohashi T, Wu CC *et al.*** Delta-9 fatty acid desaturase overexpression enhanced oleic acid content in *Rhodospiridium toruloides* for preferable yeast lipid production. *J Biosci Bioeng.* 2019;127:430–40.

9.2 Conferences:

1. **Wu CC, Ohashi T, Tsai YY *et al.*** Characterization of fatty acid profile and gene expression of fatty acid desaturases at high temperature in thermotolerant isolated from *Rhodospiridium toruloides* DMKU3-TK16. JSBBA Annual Meeting, Setagaya, Tokyo, Japan (2019 Mar.). (Oral presentation)
2. **Wu CC, Ohashi T, Tsai YY *et al.*** Production of high oleic acid containing oil in

- a multi-stress tolerant mutant isolated from oleaginous yeast *Rhodospiridium toruloides* DMKU3-TK16. Biotechnology and Chemistry for Green Growth. Awajishima, Hyogo, Japan (2018 Sep.). (Poster presentation)
3. **Wu CC, Ohashi T, Tsai YY *et al.*** Enhanced production of unsaturated fatty acid of isolated thermotolerant mutant in *Rhodospiridium toruloides* DMKU3-TK16. Biotechnology and Chemistry for Green Growth. Awajishima, Hyogo, Japan (2018 Mar.). (Poster presentation)
 4. **Wu CC.** Production of oleic acid rich-oil in a multi-stress tolerant mutant isolated from oleaginous yeast *Rhodospiridium toruloides* DMKU3-TK16. 13th KAIST-OSAKA U Symposium 2018, Suita, Osaka, Japan (2018 Oct.). (Oral presentation)
 5. **Wu CC, Ohashi T, Tsai YY *et al.*** Multiple stress tolerances in a thermotolerant L1-1 isolated from oleaginous yeast *Rhodospiridium toruloides* DMKU3-TK16. 70th SBJ Annual Meeting, Senriyama, Osaka, Japan (2018 Sep.). (Oral presentation)
 6. **Wu CC, Ohashi T, Tsai YY *et al.*** Characterization of fatty acid profile and gene expression of fatty acid desaturases at high temperature in thermotolerant isolated from *Rhodospiridium toruloides* DMKU3-TK16. JSBBA Annual Meeting, Nagoya, Aichi, Japan (2018 Mar.). (Oral presentation)
 7. **Wu CC, Ohashi T, Tsai YY *et al.*** Isolation of thermotolerant mutants and characterization of fatty acid profile in *Rhodospiridium toruloides* DMKU3-TK16. 69th SBJ Annual Meeting, Shinjuku-ku, Tokyo, Japan (2017 Sep.). (Oral and poster presentation)